MIAMI UNIVERSITY
The Graduate School

Certificate for Approving the Dissertation

We hereby approve the Dissertation of

William Frank Penwell

Candidate for the Degree:
Doctor of Philosophy

_____

Dr. Luis A. Actis, Mentor

_____

Dr. Mitchell F. Balish, Reader

_____

Dr. Joseph M. Carlin, Reader

_____

Dr. Annette Bollmann

_____

Dr. Jack C. Vaughn

Graduate School Representative

ABSTRACT

Iron acquisition in *Acinetobacter baumannii*

by William Frank Penwell

Acinetobacter baumannii is a clinically important Gram-negative opportunistic nosocomial pathogen partly because of the advent of pan-drug resistant clinical isolates. This pathogen persists and grows under harsh conditions including iron limitation imposed by the environment and the human host. The ability of *A. baumannii* ATCC 19606^T to grow under iron-limiting conditions requires the production of the siderophore, acinetobactin, which was also demonstrated to be essential for this strain to cause a successful infection. Initial studies have examined components involved in synthesis and uptake of acinetobactin; however, other components of this siderophore-mediated system have yet to be identified or characterized. The acinetobactin chromosomal gene cluster harbors all the traits needed for biosynthesis, export, and transport of this siderophore with the exception of an *entA* ortholog, which is needed for the production of acinetobactin precursor, 2,3-dihydroxybenzoic acid. Accordingly, the *entA* ortholog in ATCC 19606^T was identified using genetic complementation and found located in a different genomic region next to genes coding for iron acquisition functions. Analysis of the nucleotide sequence of this ortholog with other *A. baumannii* sequenced genomes revealed that while most of the strains code for an active *entA* gene, the clinical isolate AYE has a natural *entA* mutation and does not produce acinetobactin. Despite not being able to produce acinetobactin, AYE is still able to grow under iron-limiting conditions, a phenotype that is in accordance with the fact that this strain produces an uncharacterized hydroxamate siderophore, which we called baumannoferrin. Comparison of the siderophore-mediated system between ATCC 19606^T and AYE underline the ability of different *A. baumannii* isolates to acquire iron using different systems. The ATCC 19606^T acinetobactin gene cluster also includes two genes coding for ABC-type efflux transport functions predicted to be involved in acinetobactin secretion. Accordingly, we demonstrated that *A. baumannii* requires BarA and BarB for efficient secretion of acinetobactin although additional transport systems could be involved in the secretion of this siderophore. Taken together, the results from this study furthered our understanding of the acinetobactin-mediated siderophore system while concurrently demonstrating the diversity of

iron-acquisition functions this pathogen expresses to persist and cause infection under restricted conditions, such as those found in medical settings and the human host.

Iron acquisition in *Acinetobacter baumannii*

A Dissertation

Submitted to the Faculty of
Miami University in partial
fulfillment of the requirements
for the degree of
Doctor of Philosophy
Department of Microbiology

by

William Frank Penwell
Miami University
Oxford, Ohio
2013

Dissertation Director: Luis A. Actis, Ph.D.

Table of Contents

List of Tables

List of Figures

Dedication

To Mary, Mom, Frank, Brad, and Alexandra

This could not have been done without your support and encouragement

Acknowledgements

It goes without saying that graduate school has been one of the most trying times of my life and it was made possible with help from some of the most astonishing people that I have ever known. I want to first thank my wife, Mary, for her unending support, comfort, and especially her understanding for all the times work trumped our time together. I am excited to travel down the unknown road with you and to start our family together. I want to thank my parents for their constant support, love, prayers, encouragement and determination to do my best and to never give up. To Brad and Alexandra for providing a constant source of humor, stories, and much needed distraction from all the science and making the distance from home seem a little less. My family has always stood by me and dealt with my absence from family events with a smile and profound sense of pride.

I owe my deepest gratitude to my advisor, Dr. Luis Actis, for letting me join his lab and giving me the opportunity to learn from him, which has not only made me a better scientist, writer, and teacher, but a better person. His incalculable contributions of expertise has made it possible to complete this work and I can only hope that one day I will become as good as advisor to my students as Lu has been to me. I will always remember our many "coke breaks" where we had many scientific and non-scientific conversations. You have given me the knowledge, experience, and determination to be the best researcher that I can be and for that I will always treasure our friendship.

I also want to acknowledge my committee members, who helped advanced and mold my scientific development. I want to thank them all for being my friends who were willing to discuss anything whether it was scientific, baseball, the NCAA brackets, or careers. A special thanks goes to Dr. Mitch Balish and Dr. Joseph Carlin for being my readers and giving me constructive criticism on my dissertation. I would also like to thank Dr. Gary Janssen and Dr. Andor Kiss for bestowing a love of collecting vinyl records, for which my wife really appreciates. I need to thank Dr. John Hawes, who is sadly no longer with us. He helped tremendously by teaching me HPLC and who unfortunately passed away before he could see the product of his guidance.

I consider it an honor to have worked with so many great people in my time in the Actis lab. I owe much to MaQ, Sheri, and Jen Gaddy who provided initial instruction and guidance when I first joined the lab. They provided a friendly, welcoming environment for a new grad

student that felt overwhelmed and out-of-place. For that, I will never forget you and will always remember the kindness you showed me. Dan, thank you for always being there to bounce ideas off of and providing a different outlook on my research. We have had some good memories together such as “Blood agar”, the inappropriate adventures with Brad and Chris O. and the night “we” decided to throw the cat in the pool. You were a good friend and I wish you the best in the future. Emily, I wish you the best of luck with your remaining time here at Miami. Use it wisely because before you know it, you will be writing your dissertation and wondering where all the time went. Amber B., even though your time here was short, you have made a huge impact on the lab and accomplished so much. Since you arrived there has never been a dull moment. Steve F., I can never thank you enough for teaching me so much in your short time here, you have provided endless insight to my research and gave great advice for my future as a Post-doc. Thank you for allowing me to help with your research. Brock, your endless thought provoking ideas and questions always kept me on my toes. I will never forget the contributions you have made to me research and my development as a scientist. To the many undergrads that I have worked with in the lab (especially Ashley R., Thomas P., and George C.) thank you for making it fun to come to work every day. I thank you all and wish you all the best.

Thanks to Barb Stahl and Darlene Davidson for all of your help throughout the years. To all of my fellow graduate students in the Department of Microbiology at Miami, I wish you the best of luck and I deeply thank you for all that you have done for me. I would like to thank Ryan Relich and his wife Amanda, Racheal Desmone, Dominika Jurkovic, Jason Clark, Dipendra Gautman, John Neary, Chika Nwugo, Chris Sedlacek, Tzvia Cuperman, Liz French, Rachel Prichard, Nick Ketchum, Heather Beck, Steven Distelhorst, Ryann Brzoska, Tyler Garretson, Jenna Dolhi, Anand Prakash, and the other current and past graduate students for your friendship and support. My thanks to Tony Neal, Morgan Towles, Darius Scott, Joe Valent, Sean Leventen, Pat Walsh, Jim Walter, Tristan Pursley, Casey Connell, and the rest of my friends from the MUWC thank you so very much for being there for me, providing a stress release and for the memories. Lastly, to Snickers, who always provided a constant distraction and for always wanting “to help” me read or write during all these years that he has been part of my life.

Chapter 1

Introduction

Taxonomy and characteristics of *Acinetobacter* species

Acinetobacter species are bacteria that belong to the family Moraxellaceae and are strictly aerobic, gram-negative, glucose non-fermenting, catalase-producing, non-spore forming coccobacilli. To date, the genus contains 27 named species and 9 DNA-DNA hybridization groups (1). Members of this species are considered to be metabolically versatile and ubiquitous in the environment (2). They have been isolated from many diverse environmental niches including meat products, cheese, milk, vegetables, fruits, soil, drinking water, human normal flora, and health care settings (3-6).

Some *Acinetobacter* species have the capability of being opportunistic human pathogens, usually causing infections in individuals with serious underlying conditions (2, 7, 8). The species that have been implicated in human infections are *A. lwoffii, A. johnsonii, A. calcoaceticus, A. radioresistens, A. haemolyticus, A. junii, A. pittii, A. nosocomialis,* and *A. baumannii* (1, 2). *A. baumannii* is the most clinically important species with numerous reports of hospital outbreaks, particularly in the intensive care unit (ICU). Multidrug resistance by *A. baumannii* is also a growing problem, with reports of clinical isolates being resistant to many different classes of antibiotics (1, 2, 9).

Clinical importance of *A. baumannii*

In the last decade, *A. baumannii* has emerged globally as an important pathogen that is associated with hospital and community-acquired infections (10-12). This nosocomial pathogen typically affects immunocompromised patients and causes a multitude of diseases including pneumonia, bacteremia, urinary tract infections (UTI), meningitis, and wound-associated infections (1, 2, 7, 8). Ventilator-associated pneumonia (VAP) is the most frequently reported condition associated with infections by *A. baumannii* (5-10% of cases in ICU), and the mortality rate of VAP ranges from 25% to 75% (2, 13-15). One case study observed that multidrug resistant (MDR) *A. baumannii* was isolated with the highest frequency (80.05%) of all MDR pathogens associated with VAP, which could correlate with the poor prognosis that is seen with *A. baumannii* VAP infections (16). Bacteremia is another clinical manifestation of *A. baumannii* that causes high mortality among infected individuals (2). *A. baumannii* ranks tenth among the

most frequently isolated organisms from bloodstream infections in U.S. hospitals (2). Respiratory infections, burns and trauma are all predisposing factors that can lead to bacteremia (8). The mortality rate of bloodstream infections caused by *A. baumannii* seems to depend on the condition of the patient: those in general wards have a mortality rate of 5% compared to the 50% mortality rate of those located in the intensive care units (ICUs) (8, 17).

UTI are regularly seen in patients with permanent indwelling catheters and elderly patients (8). *A. baumannii* infrequently causes secondary meningitis in patients who have undergone neurosurgical procedures (8, 18). One case study has shown that *A. baumannii* is only responsible for 4.5% of meningitis in post-surgical patients, with mortality rates ranging from 15% to 34% (18). Another recently reported, rare infection associated with this pathogen is necrotizing fasciitis (19, 20). Most patients who develop necrotizing fasciitis have underlying conditions such as systemic lupus, Human Immunodeficiency Virus (HIV) infections, diabetes, and wounds associated with war trauma (19-21).

One of the chief reasons for the emergent interest in *A. baumannii* is the significant increase in the incidence of wound infections over the past decade due to military personnel sustaining traumatic injuries during Operation Enduring Freedom in Afghanistan and Operation Iraqi Freedom in Iraq (22, 23). From January 2002 to August 2004, 102 U.S. soldiers injured during conflict were diagnosed with bloodstream *A. baumannii* infections. Almost all (97%) of these soldiers sustained combat-related traumatic injuries before infection (23). Numerous investigations have been undertaken to try to identify the source of *A. baumannii* infections in the military setting. One hypothesis was that soldiers were coming into contact with *A. baumannii* found in the soil after being injured; however, no clinically relevant *A. baumannii* strain has been isolated from the soil (24). Several case studies have found a strong correlation between *A. baumannii* infections in wounded soldiers and the census of "host-nation" patients who are also being treated in the same medical facility where US soldiers were treated after sustaining combat-related injuries (25, 26). Griffith *et al*. (25) reported that prolonged hospitalization in combat healthcare systems increased the chances of *A. baumannii* infections and that decreasing either the number of "host-nation" patients or length of time spent in the hospital had correlated positively with the incidence of *A. baumannii* infections in wounded soldiers.

Several risk factors have been linked to the transmission of *A. baumannii* throughout the hospital setting (8). Colonized healthcare workers are a major source of transmission (6, 27-29). Reports have shown that the hand carriage rate among hospital staff members for *A. baumannii* ranges from 3% to 23% (6, 8). Transmission of bacteria through healthcare worker hands was linked to an outbreak of bacteremia in a neonatal ICU. (6, 28). Another risk factor is extended ICU care, where patients require prolonged respiratory treatment and the possible aid of a ventilator, which could lead to ventilator-associated pneumonia (8, 30).

A. baumannii has become a successful nosocomial pathogen largely due to its ability to persist in the hospital environment (7, 8). Major factors contributing to this persistence are its ability to tolerate desiccation and to resist disinfectants and many antibiotics (7, 10, 31). The ability of *A. baumannii* to resist disinfectants allows for spread of the pathogen from contaminated surfaces and increased person-to-person contact (32). Experimental data have demonstrated that *A. baumannii* can survive desiccation better than other *Acinetobacter* spp. (33). This ability was linked to an outbreak of *A. baumannii* infections throughout an ICU, where bed rails functioned as the reservoir source (33, 34). The ability to develop resistance to all currently available antibiotics is paramount to the success of this species as a pathogen, making it one of the most difficult microorganisms to treat and control (35, 36).

The ability of *A. baumannii* to acquire antimicrobial resistance genes at a rapid rate and the resistance of clinical strains to all known antibiotics have led to this pathogen being deemed a "red alert" pathogen that needs to be targeted for the development of new antibiotics by 2020 (7, 10, 37). Antimicrobial resistance by *A. baumannii* is mediated by all major resistance mechanisms, which include active efflux pumps, enzymatic inactivation, and modification of target sites (31). Some resistance mechanisms have been found in several isolates and these mechanisms may have been acquired by horizontal gene transfer from unrelated sources (31). Many *A. baumannii* outbreaks caused by MDR strains can be traced to international clones I, II or III (10, 38). A study performed by Higgins *et al*. (39) determined that out of 492 imipenem-resistant *A. baumannii* isolates from around the world, nearly half of them clustered with isolates from international clone II. This study also observed that some *A. baumannii* isolates recovered from wounded American soldiers fighting in Iraq were related to international clones I and II (39). Treatment with antibiotics has led to selective pressure favoring the persistence of certain isolates in the hospital environment and allowing these isolates to become more prevalent in

causing nosocomial outbreaks (10, 38). Since *A. baumannii* is highly resistant to many different classes of antibiotics, this pathogen has become a serious burden on the healthcare system (10).

Antibiotic resistance is the most widely studied virulence factor associated with *A. baumannii* pathogenesis, but less is known about other factors linked to the virulence of this organism. One such factor is the ability of *A. baumannii* to form biofilms, allowing this pathogen to prosper in the medical setting by attaching to inanimate surfaces found throughout the hospital like linens, bed rails, and plastics such as polystyrene (34, 40-43). The *csuA/BABCDE* operon, which encodes a chaperone-usher pili assembly system, is necessary for *A. baumannii* ATCC 19606^{T} to form biofilms on plastic surfaces like polystyrene (41, 44). A CsuE deficient strain, which does not form CsuA/BABCDE pili, does not adhere to plastic as strongly as the parental strain; however, this mutant still adheres to biotic surfaces, such as *Candida albicans* and human bronchial epithelial cells (44, 45). Furthermore, microscopic examination of a CsuE mutant grown on a blood agar plate exhibited thinner pili on the cell surface, which were CsuA/BABCDE-independent (45). These results indicate that other uncharacterized pili can be produced by *A. baumannii*, and they are involved in adherence to biotic surfaces such as human epithelial cells.

The ability of *A. baumannii* to form biofilm on polystyrene correlates positively with its ability to adhere to a human bronchial epithelial cell line (46). Outer membrane protein A (OmpA) is one protein that has been found not only to play a role in biofilm formation on plastics but also to be important for *A. baumannii* adherence and invasion of bronchial and laryngeal epithelial cells (44, 47). As compared with the parental strain, an OmpA-deficient strain was attenuated for virulence in a murine pneumonia model (47). OmpA has also been linked to the induction of apoptosis in host cells, and is important in bacterial resistance to host complement (48, 49). Proteins involved in K1 capsule production, which were recently identified, are also an important virulence factor for *A. baumannii* in causing successful infections (50). It was demonstrated that capsule-negative mutants could not survive in a rat soft tissue model and that clearance of the capsule-negative mutants occurs within 24 h of inoculation (50). The capsule is also important for resistance of *A. baumannii* to complement when grown in human serum (50).

Another virulence factor that has been studied in detail is the ability of *A. baumannii* to survive in an iron-limited environment, like the human host. In response to low iron,

A. baumannii produces the siderophore acinetobactin to acquire this essential micronutrient (51-53). A better understanding of the acinetobactin system could lead to the development of new antimicrobial drugs to help treat infections caused by MDR *A. baumannii* infections.

Importance of iron

Iron is the fourth most abundant transition metal in the Earth's crust and is an important growth factor for almost all bacteria, with the exception of the causative agent of Lyme disease, *Borrelia burgdorferi,* and lactic acid bacteria, such as *Lactobacillus acidophilus* (54-56). This essential nutrient is involved in numerous biological processes including electron transport, photosynthesis, tricarboxylic acid cycle-mediated metabolic process, deoxynucleotide biosynthesis, and protection from free radicals (57-59). Iron exists in one of two interconvertible states, a reduced ferrous (Fe^{2+}) form and an oxidized ferric (Fe^{3+}) form. The chemical properties of iron make it an extremely versatile prosthetic component for use in biological processes. Even though this micronutrient is abundant, its bioavailability is limited. In aerobic environments at neutral pH, iron occurs in the insoluble, oxidized, ferric form, which limits the availability of iron to approximately 10^{-18} M, well below the 10^{-6} M required by bacteria for optimal growth (55, 59-62).

Similar constraints are present in the human host, where iron is sequestered by high-affinity iron-binding proteins, making it unavailable for pathogens to utilize (63-66). Controlling the amount of free iron prevents reactive oxygen species from forming by the Fenton reaction [$Fe^{+2} + H_2O_2 \rightarrow Fe^{+3} + OH^{\cdot} + OH^{-}$], limiting the damage to host macromolecules (57, 67). Sequestering of iron by the host is known as nutritional immunity and is considered one of the first lines of defense against bacterial infections (66). Proteins involved in iron sequestration include transferrin, lactoferrin, and the intracellular storage protein ferritin (57, 63, 66, 68). Another innate immune host protein involved in limiting the amount of available iron is hepcidin, a peptide hormone which controls extracellular iron concentrations. Expression of hepcidin is activated by inflammatory cytokine interleukin-6 (63, 68-71). Hepcidin controls extracellular iron concentrations by binding to the transport protein ferroportin. This binding causes ferroportin to be degraded, preventing the release of iron from cellular stores (69, 70). To overcome host nutritional immunity, bacteria have adapted high-affinity iron acquisition systems to obtain this essential micronutrient, which are depicted in Fig. 1.

Figure 1. Iron acquisition systems used by bacteria. **A.** Receptor-mediated uptake of transferrin. **B**. Receptor-mediated uptake of lactoferrin. **C**. Receptor-mediated uptake of hemoproteins. **D.** Hemophore-mediated uptake of heme from host proteins like hemoglobin and hemopexin. **E.** Siderophore-mediated uptake of ferric iron from host proteins like transferrin, lactoferrin and ferritin.

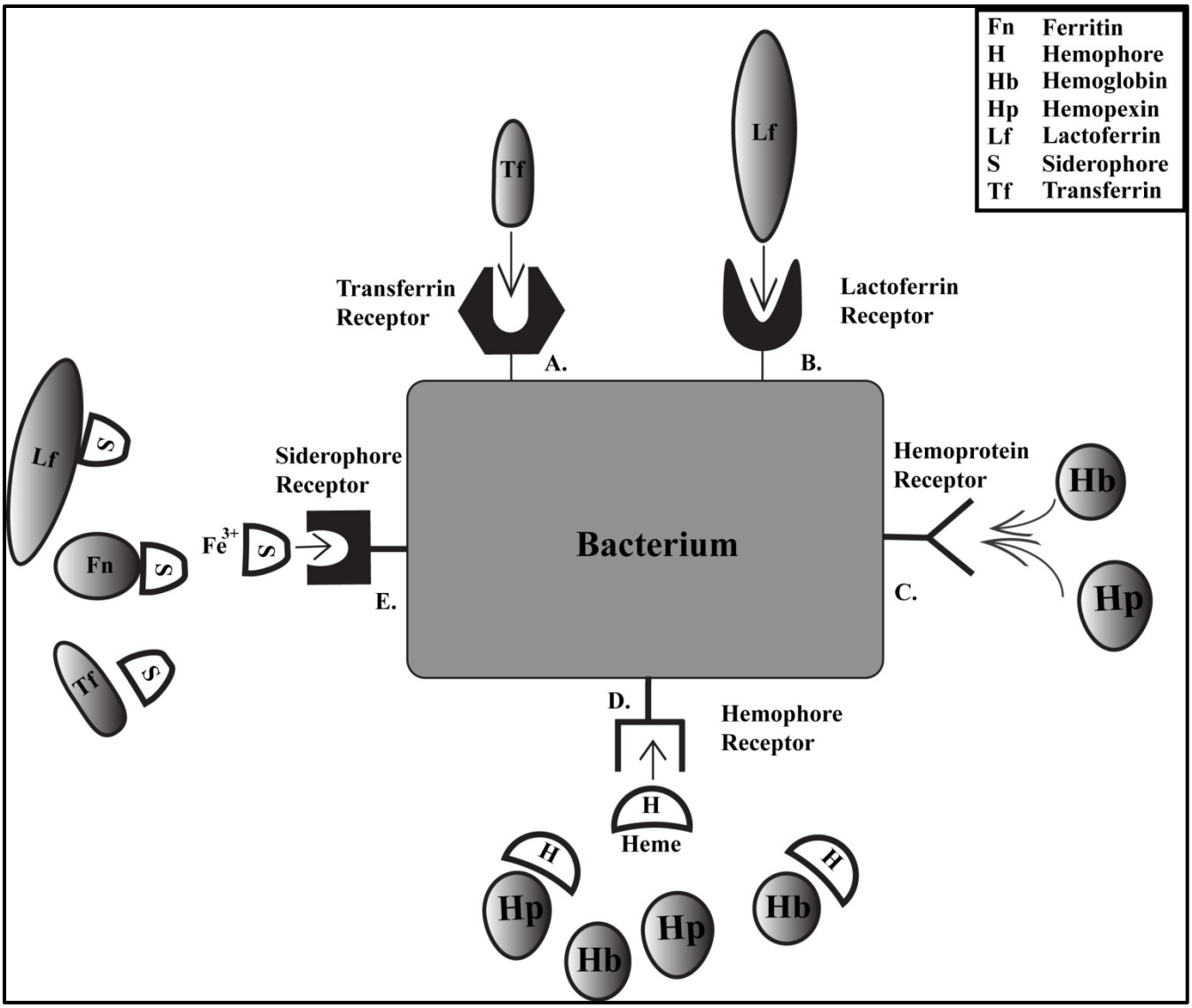
Fn Ferritin
H Hemophore
Hb Hemoglobin
Hp Hemopexin
Lf Lactoferrin
S Siderophore
Tf Transferrin
Tf
Lf
Transferrin Receptor
Lactoferrin Receptor
A.
B.
Lf
S
Fn
S
Tf
S
Siderophore Receptor
Fe3+
S
E.
Bacterium
Hemoprotein Receptor
Hb
Hp
C.
D.
Hemophore Receptor
H
Heme
H
Hp
Hb
Hp
H
Hb

One iron acquisition system that bacteria employ involves a direct interaction of iron-binding proteins, such as transferrin and lactoferrin, with specific outer membrane receptors. After these iron-bound host proteins bind to the specific receptor, iron is stripped from the host proteins, which are then released from the receptors and the iron is transported into the cell (57, 64, 66). This type of system has been described in pathogens such as *Neisseria gonorrhoeae* (72), *Neisseria meningitidis* (73) , and *Haemophilus influenzae* (74).

A second high-affinity system utilized by bacteria is the uptake of heme, an abundant iron source in vertebrate hosts. Heme acquisition systems involve either surface receptors that recognize hemoproteins or the use of a secreted hemophore (66, 75). Hemoproteins, like hemoglobin or hemopexin, are recognized by specific outer membrane receptors that bind these proteins (76). Once binding occurs, heme is removed from hemoproteins and transported into the cell (76). Some bacterial pathogens can also use a hemophore to remove heme from host proteins (66, 75, 76). After the hemophore has bound heme, it enters the cell through a specific outer membrane receptor, and once inside the bacteria, iron is released from heme by either a heme oxygenase or reverse ferrochelatase activity (76, 77). Examples of pathogens that use heme as an iron source include *H. influenzae* (78), *Vibrio cholerae* (79), *Serratia marcescens* (80), and *Yersinia pestis* (81).

Low molecular weight ferric chelators, known as siderophores, constitute another high-affinity system used by bacteria to acquire iron (66, 68, 82). Siderophores sequester iron from host proteins and once a ferric-siderophore complex has formed, it is transported back into the cell by a specific receptor. The iron is released from the siderophore, transported into the cytosol and then used for cellular processes. Because this dissertation focuses on siderophore-dependent iron acquisition by *A. baumannii*, the next section will detail the biosynthesis, secretion and uptake of siderophores.

Siderophore-mediated iron acquisition

General

Siderophores are produced by a variety of bacteria, fungi and plants to help overcome iron limitations in the environment (58, 68). Siderophores are defined as low-molecular weight compounds that have high affinity and specificity for ferric iron. The affinity constant with which siderophores bind ferric iron lies between $10^{12}\,M^{-1}$ to $10^{52}\,M^{-1}$; ferrous iron binds with a

lower affinity (58, 66, 83, 84). The difference in siderophore affinity between ferric and ferrous iron is directly related to the difference in their Lewis acid characteristics (84, 85). Ferrous iron is considered to have a "soft" metal center that has a higher affinity towards nitrogen donor groups and differs from the "hard" metal center of ferric iron, which, as a strong Lewis acid, prefers to bind to "hard" donor groups like oxygen (84, 85). Even though siderophores are structurally diverse, they all have an oxygen atom as the donor group (58). This "hard" donor group allows a stable ligand to form due to the interactions between the negatively charged oxygen atom and the positively charged iron center (58).

More than 500 siderophores have been identified, all differing in their structure. Nonetheless, they can be grouped into three main classes based on the moiety that provides the oxygen ligand for ferric iron binding (58, 68, 84, 85). The three classes of siderophores are catecholates (phenolates), hydroxamates, and hydroxycarboxylates. Some siderophores are described as having a mixed catechol-hydroxamate structure, including anguibactin and acinetobactin, which are produced by *Vibrio anguillarum* 775 and *A. baumannii* ATCC 19606^{T}, respectively (51). All siderophores must be first synthesized, then secreted from the cell, and finally brought back into the cell by a specific outer membrane receptor.

Siderophore Biosynthesis

When in an iron-limited environment, bacteria up-regulate genes involved in siderophore-dependent iron acquisition, which includes genes needed for biosynthesis of the siderophore. Interest in siderophore biosynthesis has grown over the past decade largely due to the role of siderophores as virulence factors for pathogens and as potential targets for antimicrobial therapies (55, 86). Although siderophores can be classified into the three main structural classes described above, they can also be broadly classified into two groups based on the enzymatic machinery involved in biosynthesis: those that depend on non-ribosomal peptide synthetase (NRPS) multimodular enzymes for synthesis, and those that are produced by an NRPS-independent pathway (82, 86, 87).

The NRPS pathway is used for the synthesis of secondary metabolites, including antibiotics, toxins, pigments and siderophores (82, 88). This pathway is comprised of multimodular enzymes that assemble amino acids into peptides by forming peptide bonds without requiring RNA as a template for assembly (82). Since no RNA template is needed, the

sequence in which amino acids are added to the peptide is determined by the order of NRPS domains (82). Three types of functional domains are required for peptide growth. These domains are the adenylation (A), peptidyl carrier protein (PCP), and condensation (C) domains (58, 82). These domains are physically tethered to each other in repeats to form a module of A-PCP-C domains and each module is responsible for the incorporation of one amino acid into the growing peptide (Fig. 2) (58). These modules are responsible for carrying out four kinds of catalytic operations (82).

The A domain selects and activates amino acids that will be incorporated into the peptide (Fig. 2A) (58, 82). The A domain activates amino acids as aminoacyl adenylates in an ATP-dependent manner and this activation forms an aminoacyl-AMP that is then transferred to the peptidyl-carrier domain (or aryl-carrier domain when using aryl acids) (58, 82). Before this transfer occurs, the PCP domain must first be converted from the apo form to the holo form, which has a phosphopantetheinyl arm (82). This post-translational modification of the PCP domain is carried out by phosphopantetheinyl transferase (PPTase) enzymes, which are normally encoded by a gene in the siderophore biosynthetic gene cluster (82, 89). The phosphopantetheinyl arm covalently binds the aminoacyl-AMP and acts as a tether for elongation (58, 82). The C domain catalyzes peptide bond formation between activated amino acids, which results in transfer of the growing peptide to the PCP domain of the downstream module (Fig. 2B) (58). The final step is chain termination and release of the siderophore. The siderophore is still covalently linked to the most downstream PCP domain in the assembly line and must be chemically cleaved from the phosphopantetheinyl arm (58, 82). The final module of the assembly line has a thioesterase (TE) domain in place of the C domain (58, 82). This domain will transfer the fully grown peptide or siderophore to a water molecule, releasing it from the PCP domain (Fig. 2C) (58, 82). There are also examples in which a nucleophile from the peptide itself is used instead of water, with a cyclic product being released (58).

Diversity of siderophores that are assembled by the NRPS pathway can be attributed to auxiliary domains in a module that allow for modification of an amino acid in a particular way. The auxiliary domains include methyltransferase (MT), epimerase (E), cyclization (Cy) and reductase (Red) domains. The MT domain methylates the amino acids using S-adenosylmethionine as a methyl donor (58). The E domain converts L-amino acids into D-

amino acids (58). The Cy domain forms five-member heterocyclic rings (58). The Red domain changes the redox state of an amino acid (58).

Siderophores that are assembled by the NRPS-independent biosynthetic pathways have not been as intensively studied as those produced by NRPS pathways, and a more comprehensive understanding of the molecular mechanism by which these siderophores are assembled is needed (87). Siderophores that are produced by this pathway are not polypeptides but are assembled using alternating dicarboxylic acids and diamine or amino alcohol moieties as building blocks for siderophore biosynthesis (86, 87). These building blocks are linked together by amide or ester bonds (86, 87). Aerobactin, a hydroxamate siderophore produced by *Escherichia coli*, is the best studied siderophore assembled by the NRPS-independent biosynthetic pathways. Aerobactin production utilizes two siderophore synthetase enzymes, IucA and IucC, which are used to catalyze the formation of key amide bonds that link dicarboxylic acids and diamine units together to form the siderophore (87)

.

Figure 2. NRPS modules used in siderophore synthesis. (A) An amino acid is activated by the adenylation (A) domain with ATP and then transferred to the phosphopantetheine (wavy line) on the peptidyl carrier protein (PCP) domain. (B) The condensation (C) domain catalyzes the formation of the peptide bond between two activated amino acids, which results in a growing peptide chain. (C) The fully grown peptide is transferred off the final PCP domain by the thioesterase (TE) domain, which releases the peptide through hydrolysis. Modified from Crosa *et al*., 2004 (58).

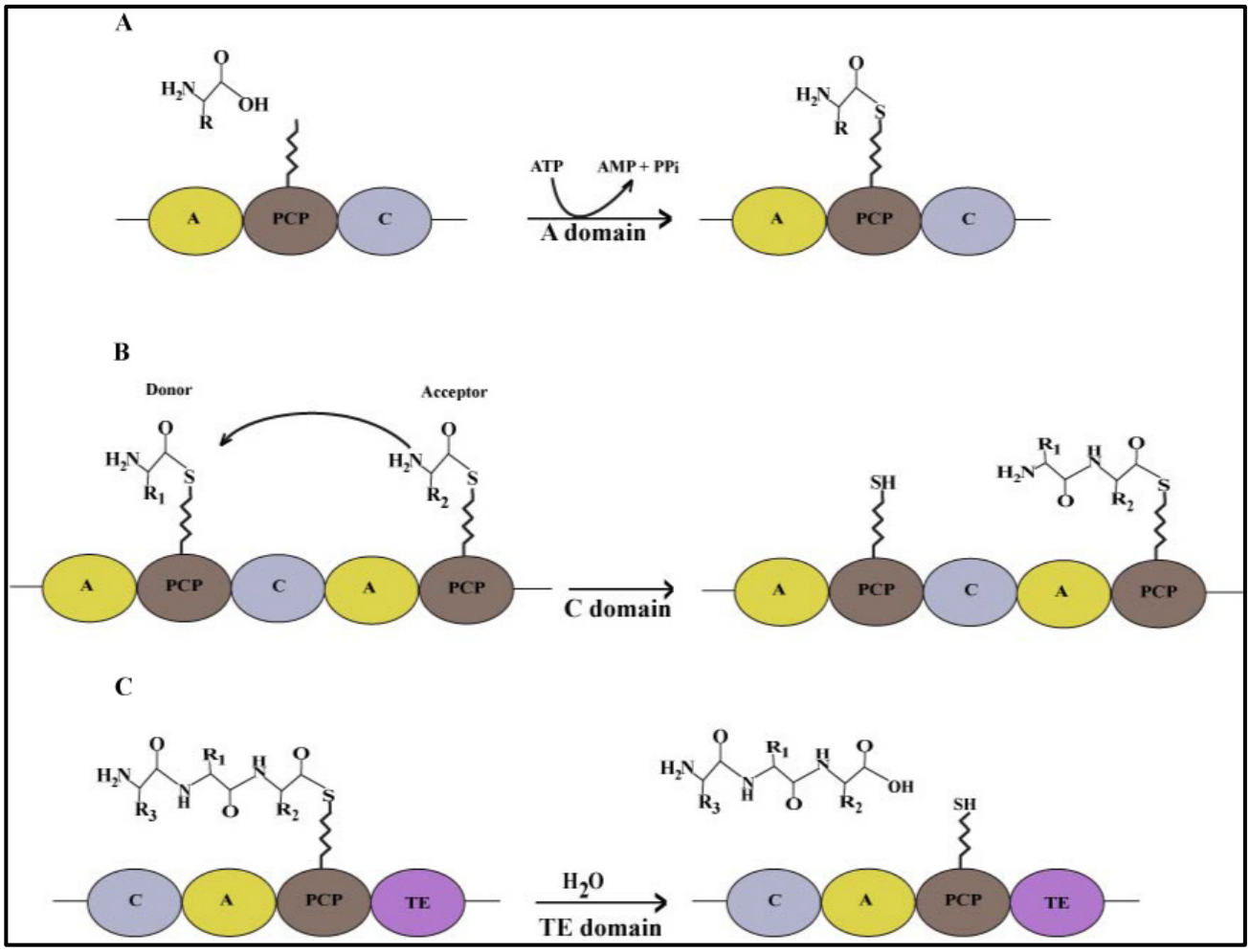
A
ATP
AMP + PPi
A domain
A
PCP
C
B
Donor
Acceptor
C domain
SH
C
H2O
TE domain
TE

Siderophore secretion

Once biosynthesis of the siderophore has occurred, it must be secreted from the cell into the extracellular milieu. Since siderophores are charged hydrophobic molecules and therefore cannot passively diffuse across the membrane, an active secretion mechanism is necessary. Only a few siderophore secretion systems have been identified thus far. The exporters that have been investigated or suggested to be involved in secretion are efflux pumps from the major facilitator superfamily (MFS) or ATP-binding cassette (ABC) superfamily proteins.

The MFS is the largest group of membrane transporters and has been shown to transport a variety of compounds, including antibiotics, primary metabolites, and sugars (90, 91). MFS pumps possess 12, 14, or 24 transmembrane domains and all identified pumps can be classified into one of 58 distinct families based on the solute that is transported (92). Even though numerous MFS exporters have been studied, only a few have been identified in export of siderophores. A few examples of MFS exporters involved in siderophore secretion include EntS in *E. coli*, CsbX in *Azotobacter vinelandii* and PvsC in *V. parahaemolyticus* (93-95).

Enterobactin in *E. coli* is secreted by the Fur-regulated EntS protein. The *entS* gene is found within the *ent-fep* cluster, which contains the genes needed for enterobactin utilization (93). A mutation in *entS* resulted in a reduction in the amount of secreted enterobactin and an increase in the amount of enterobactin breakdown products (93). The breakdown products can be attributed to ester cleavage of enterobactin by the Fes protein (96). Enterobactin secretion is not exclusively mediated by EntS due to the fact that a mutation in the TolC protein of *E. coli* completely abolished secretion of enterobactin (97). This led to the hypothesis that multiple exporters are involved in the secretion of enterobactin, with EntS involved in export across the cytoplasmic membrane but another exporter being responsible for secretion from the periplasmic space as part of a two-step secretion process (97).

The other proteins involved in siderophore secretion belong to the ABC transport family, which consists of both uptake and efflux transport systems (98). ABC transporters are comprised of a transmembrane domain (TMD) and a cytoplasmic nucleotide binding domain (NBD) (98). Two TMDs and two NBDs make up the typical structure of an ABC transporter (98). ABC importers achieve this architecture with a total of four individual polypeptides (two TMD and two NBD) that combine to form the functional transporter as seen with the BtuCD and Nik systems both from *E. coli* (98-101). ABC exporters are generally less complex than ABC

importers (98). In general the functional complex is either a homodimer or a heterodimer of a TMD fused with NBD as seen with two *E. coli* exporters, CydCD and MsbA (98, 102-104). Only a few ABC exporters have been identified as being involved in siderophore secretion. A few examples include PvdE from *Pseudomonas aeruginosa,* IroC from *Salmonella enterica* serovar Typhimurium, ORF14 and ORF15 from *V. anguillarum,* and ExiT from *Mycobacterium smegmatis* (105-108).

One of the more recently described siderophore efflux systems is PvdE, an ABC exporter involved in secreting pyoverdine in *P. aeruginosa* (105, 109). Yeterian *et al.* (105) demonstrated that a mutation in *pvdE* prevented the pyoverdine precursor (pyoverdine without the fluorescent chromophore) from being secreted from the inner membrane to the periplasmic space. The fact that PvdE secretes the pyoverdine precursor only to the periplasmic space strengthens to the hypothesis that multiple export systems are involved in secreting certain siderophores from the cytoplasm to the extracellular milieu in a two-step process. The secretion system comprised of PvdRT-OmpQ has been proposed to be involved in the secretion of pyoverdine from the periplasmic space, and a mutation in any of the PvdRT-OmpQ components leads to the accumulation of pyoverdine in the periplasmic space (110). The involvement of PvdRT-OmpQ in efflux from the periplasmic space has been debated (111).

Ferric-siderophore uptake

Despite the advances that have occurred in the last decade, the understanding of siderophore secretion is lagging as compared with the understanding of siderophore biosynthesis and the import of the ferric-siderophore complex. Once secreted into the extracellular milieu, the siderophore acquires ferric iron to form a ferric-siderophore complex that must be transported into the cell. The process by which ferric-siderophore complexes are transported into the cell has been intensely studied and characterized (88). Ferric-siderophore complexes exceed the molecular weight limit of porins and therefore require their own dedicated outer membrane receptor for import into the cell (57, 68). Numerous such receptors have been identified and several x-ray crystal structures have been elucidated (57). The crystal structures have been determined for the FhuA aerobactin (112) and the FepA enterobactin (113) receptors from *E. coli* and for the FpvA pyoverdine (114) and the FptA pyochelin (115) receptors from *P. aeruginosa.*

All outer membrane receptors that are involved in siderophore import have an overall similar three-dimensional structure, with a transmembrane domain and a plug domain. The transmembrane domain, which is formed by residues of the C-terminal region, consists of 22 β-barrel strands that extend into the periplasmic space and through the outer membrane (57, 68, 88, 116). The residues of the N-terminal region form a plug domain that folds inside the barrel, blocking the opening and preventing the ferric-siderophore complex from directly entering the periplasmic space (57, 68, 88, 116). Both domains are involved in binding of ferric-siderophore complexes to the receptor (88, 114).

The binding site for the ferric-siderophore complex is located within the cavity formed by the extracellular loops of the β-barrel and the plug domain (58, 88, 116). Details of how the ferric-siderophore interacts with the extracellular loops and plug domain have been determined for FhuA, FepA and FecA (Fig. 3) (116-118). Binding of the ferric-siderophore complex causes two separate conformational changes to occur in the plug domain (88, 118). The first conformational change that occurs is unwinding of a specific region on the plug domain known as the switch domain, and this change allows for the interaction between TonB and the TonB-box located in the plug domain of the receptor (57, 119, 120). TonB is a membrane anchored, periplasmic spanning protein that interacts with the outer membrane receptor through the C-terminal domain (120). The N-terminal domain of TonB interacts with two other membrane embedded proteins, ExbB and ExbD, which together transduce energy from the cytoplasmic membrane to the outer membrane receptor to allow for the second conformational change to occur (57, 58, 120). The second conformational change allows the formation of a transient channel through which the ferric-siderophore complex passes to enter the periplasmic space (57). How this transient channel forms is still unknown (120). The channel is formed either by the removal of the plug domain from the β-barrel or by conformational changes within the plug domain itself (57, 58, 120).

Once inside the periplasmic space, a periplasmic siderophore-binding protein binds the ferric-siderophore complex and delivers it to a cognate ABC transporter for import into the cytoplasm (57, 68, 121). Once the ferric-siderophore complex enters the cytoplasm, the ferric iron molecule has to be dissociated from the siderophore for use by the bacterium for cellular processes. Iron dissociation can occur by one of two mechanisms (88). One mechanism is through the use of a reductase that reduces ferric iron to ferrous iron, which in turn triggers the

release of the ferrous iron molecule from the siderophore (88). The reductases that are involved have broad substrate specificity are not considered to be specialized enzymes, unlike those which mediate the second mechanism for the release of ferric iron (122). This mechanism employs specialized enzymes to remove the ferric iron molecule by ester cleavage of the ferric-siderophore complex. This mechanism results in degradation of the siderophore, preventing it from being recycled (88). This is in contrast to the first mechanism, in which the siderophore can be reused after reduction of the ferric iron molecule (96). Only a few esterases that are involved in the release of iron from ferric-siderophore complexes have been identified. The first esterase that was studied was Fes from *E. coli*, which is responsible for the ester cleavage of ferric-enterobactin (96). Additional esterases include IroD and IroE which are found in both *Salmonella* species and uropathogenic *E. coli*, and release ferric iron by ester cleavage of ferric-salmochelin (123, 124). In *Bacillus* spp. the esterase BesA is responsible for ester cleavage of the enterobactin-like siderophore bacillibactin (125).

Figure 3. Crystal structures of siderophore outer membrane receptors. (A) The crystal structures of FpvA with bound pyoverdine. The β-barrel and the plug domains are colored green and red, respectively. Pyoverdine is shown as a space-fill model. (B) The crystal structure of FecA with bound ferric-citrate. The β-barrel domain is colored blue. The plug domain is colored green, orange, purple and yellow. Ferric citrate is shown as a bond model and is interacting with β-barrel loop 7 and 8, colored red, and the switch helix in the plug domain, colored orange. Panel A was adapted from Cobessi *et al*., 2005 (114) and Panel B from Ferguson *et al.,* 2002 (116).

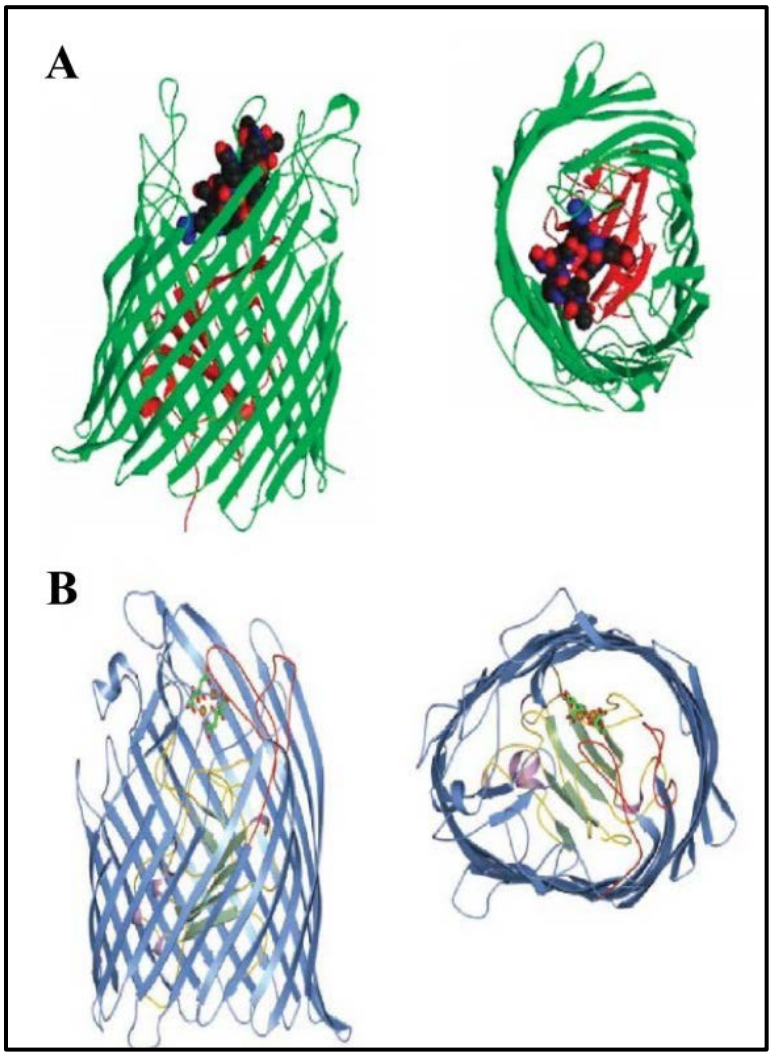
A
B

Regulation of siderophore-dependent iron acquisition

Siderophore biosynthesis, secretion, and uptake are all tightly controlled by bacteria not only to conserve energy and precursors but also to prevent an excess of iron, which can lead to damage of macromolecules through its involvement in the Fenton reaction. Bacteria have evolved mechanisms to regulate expression of iron acquisition genes. The regulatory mechanisms that have been identified include extracytoplasmic function (ECF) sigma factors like FecI (126, 127), AraC-type regulators (128, 129), and post-transcriptional regulation by antisense RNA like RyhB (126-130).

Fur is another important regulator of gene expression in bacteria that responds to intracellular iron concentrations (131-134). During iron-replete conditions, ferrous iron is a cofactor of Fur, which binds a specific sequence located in promoters known as a Fur box (135, 136). Once bound to the Fur box, this 17-kDa protein prevents transcription of iron-regulated genes, including those involved in the acquisition of this metal (131, 132). Two Fur dimers recognize and bind the Fur box in order to act as a transcriptional repressor (137). In iron-depleted conditions, the concentration of ferrous iron drops in the cell, causing the Fur protein to dissociate from the Fur box, allowing expression of iron-regulated genes, including those coding for iron uptake functions (137, 138).

Fur and the consensus sequence of the Fur box have been best characterized in *E. coli*, in which this regulator has been shown to control about 90 genes at the transcriptional level (139). It has also been demonstrated over the past decade that Fur controls transcription of genes involved not only in iron acquisition but also in oxidative stress, iron storage, metabolism, virulence, and acid tolerance (132, 140).

Siderophores and antimicrobial compounds

Over the past decade, a need for new antimicrobial compounds has arisen with the advent of MDR bacteria, such as *A. baumannii*, plaguing our healthcare systems. Since iron is essential for pathogenic bacteria to cause a successful infection, siderophore-mediated iron acquisition systems have been exploited as potential therapeutic targets. One strategy utilizes the siderophore uptake machinery to deliver an antibiotic conjugated to the siderophore, whereas the other strategy uses drugs designed to inhibit siderophore biosynthesis activities to block production of the siderophore.

The first strategy, known as the "Trojan Horse strategy", uses synthetically designed siderophores conjugated to an antibiotic molecule to grant the antibiotic entry into the cell through an active transport through bacterial outer membrane siderophore receptors (141). This strategy tricks the bacteria into utilizing the biomimetic siderophore to bypass the permeability barrier that is presented by the outer membrane, an important resistance factor of pathogenic bacteria (83, 141). This approach has been adapted from naturally occurring antibiotic conjugated siderophores, known as sideromycins (83). These biomimetic siderophores have been shown to be active against *M. tuberculosis* and *P. aeruginosa* (141-143).

The second strategy uses inhibitor drugs that block siderophore synthesis enzymes, preventing the production of siderophores by pathogens. This strategy is of interest since these enzymes have little homology to mammalian enzymes, allowing bacterial processes to be selectively targeted. In the 1970s, it was reported that the small compound, p-aminosalicylate (PAS), could inhibit production of mycobactin in *M. smegmatis* and *M. bovis* (144). With the improved understanding of the NRPS siderophore biosynthesis pathway, new drugs have been developed against biosynthesis enzymes that have similar activity in a plethora of bacteria (88). One such example is the aryl acid-adenylating enzymes that are responsible for the incorporation of an aryl-capping group in catecholic siderophore (88, 145, 146). Reports have shown that by using an aryl acid adenylate analogue, the growth of *M. tuberculosis* and *Y. pestis* can be inhibited in an iron-dependent manner (147). The major caveat of this second strategy is that drug development thus far is only for enzymes that are part of the NRPS-dependent pathway. Siderophores produced by the NRPS-independent pathway will not be inhibited by drugs targeting the enzymes in this biosynthesis pathway. Therefore, treating pathogenic bacteria that produce siderophores synthesized by NRPS-independent pathway could become problematic. With more research on siderophore biosynthesis, it may possible to develop inhibitors against siderophores produced by both pathways.

Iron acquisition in *A. baumannii*

Expression of siderophore-mediated iron acquisition systems in different A. baumannii clinical isolates

To successfully infect and persist in the host, pathogenic bacteria such as *A. baumannii* require iron for cellular processes. One virulence factor that has been examined in *A. baumannii* is its ability to acquire iron from the host. Dorsey *et al.* (148) tested a collection of clinical isolates to determine if they could grow in M9 minimal medium that was supplemented with the synthetic iron chelator ethylenediamine-di-(o-hydroxyphenyl) acetic acid (EDDHA). The results indicated that all clinical isolates examined survive under iron-limiting conditions, but there were also variations in the expression of elements involved in iron acquisition among these clinical isolates, including both siderophore receptors and the ability to secrete the precursor histamine (148). These variations among different clinical isolates showed that different *A. baumannii* strains can express unrelated iron uptake systems to survive iron-limiting conditions. To date, four different siderophore uptake systems in *A. baumannii* have been described (Fig. 4) (51-53, 149-151).

One siderophore cluster that has been characterized is found in the clinical isolate 8399 (Fig. 4A) (149). Described by Dorsey *et al.* in 2003(149), this isolate seems to produce and secrete 2,3-dihydroxybenzoic acid (DHBA) in addition to a high-affinity catechol siderophore. This cluster contains genes coding for proteins involved in synthesis of DHBA (DhbBCA) as well as proteins involved in siderophore assembly (DhbF and DhbE) (149). This cluster also contains genes encoding putative proteins involved in siderophore utilization (OM73 and Fes) and proteins that could be involved in siderophore secretion (P45 and P114) (149).

Another siderophore system that has been described is found in the *A. baumannii* clinical isolate 17978, which was isolated from a fatal case of meningitis (152). This clinical isolate was source of the first sequenced genome to be reported for *A. baumannii* (153). Genome analysis of *A. baumannii* 17978 revealed a 26-kbp cluster that contains genes coding for biosynthesis, secretion and utilization of fimsbactin, which is a catechol-hydroxamate siderophore (Fig. 4B) (53, 154). This cluster is flanked by 14-base pair repeats and contains two putative transposase genes, which suggests that this cluster was obtained by horizontal gene transfer (53, 154). This is supported by a bioinformatics examination of genomes from 50 clinical isolates by Antunes *et al.* (151), who found that this siderophore cluster is unique to 17978.

The research by Antunes *et al.* (151) also described a third siderophore cluster present in all examined 50 clinical isolates, with the exception of *A. baumannii* SDF, which does not contain any siderophore systems (Fig. 4C). This third cluster contains eight genes that have a putative function in the biosynthesis of an uncharacterized hydroxamate siderophore (150, 151). This cluster also contains genes coding for the secretion and utilization of this hydroxamate siderophore (150, 151). Microarray analysis of *A. baumannii* 17978 showed that several genes from this cluster exhibited more than a 100-fold increase in expression under iron-limiting conditions, demonstrating the relevance of this cluster for iron acquisition in *A. baumannii* isolates (150).

Like the hydroxamate cluster, the acinetobactin cluster, the fourth group of genes associated with siderophore-mediated iron acquisition, is also present in the majority of clinical isolates examined by Antunes *et al*. (151). Of all the siderophore clusters identified in *A. baumannii*, the acinetobactin cluster is the most extensively studied, with the majority of the research being performed on the type strain ATCC 19606^{T} (Fig. 4D).

Figure 4. Schematic representation of siderophore gene clusters found in *A. baumannii*. (A) The catechol siderophore gene cluster found in the *A. baumannii* clinical isolate 8399 was adapted from Dorsey *et al*., 2003 (149). (B) The fimsbactin gene cluster coding for a siderophore found in *A. baumannii* clinical isolate, ATCC 17978 (154). (C) The uncharacterized hydroxamate siderophore gene cluster identified by Antunes *et al.* (151, 155). (D) The acinetobactin gene cluster (52). The arrows and their direction indicate the location and direction of transcription of the predicted genes. The numbers underneath the arrows correspond to the predicted protein functions, which are indicated in the table below each gene cluster. Those genes predicted to be involved in biosynthesis, uptake and export of siderophores are colored blue, red, and orange, respectively. Hypothetical genes are represented by black arrows. Panel A was adapted from Dorsey *et al.,* 2003 (149); panel B was adapted from Proschak *et al*., 2013 (156); panel C was adapted from Antunes *et al*., 2011 (151); panel D was adapted from Mihara *et al*., 2004 (52).

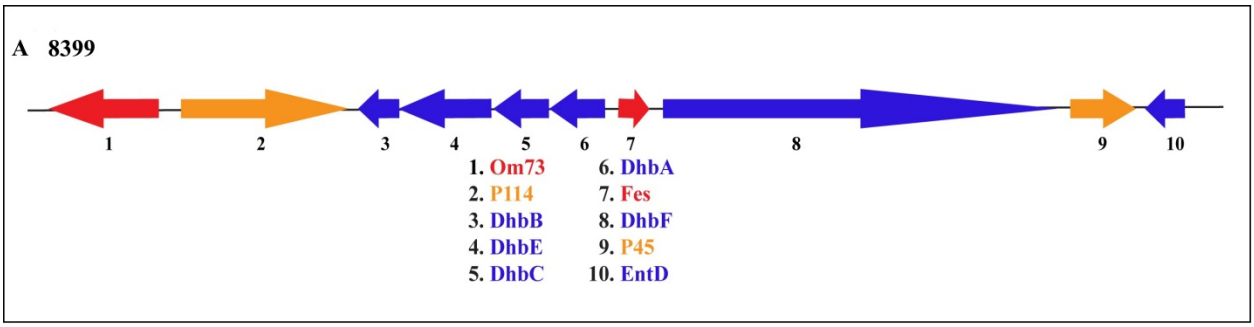
A 8399
1 2 3 4 5 6 7 8 9 10
1. Om73
2. P114
3. DhbB
4. DhbE
5. DhbC
6. DhbA
7. Fes
8. DhbF
9. P45
10. EntD

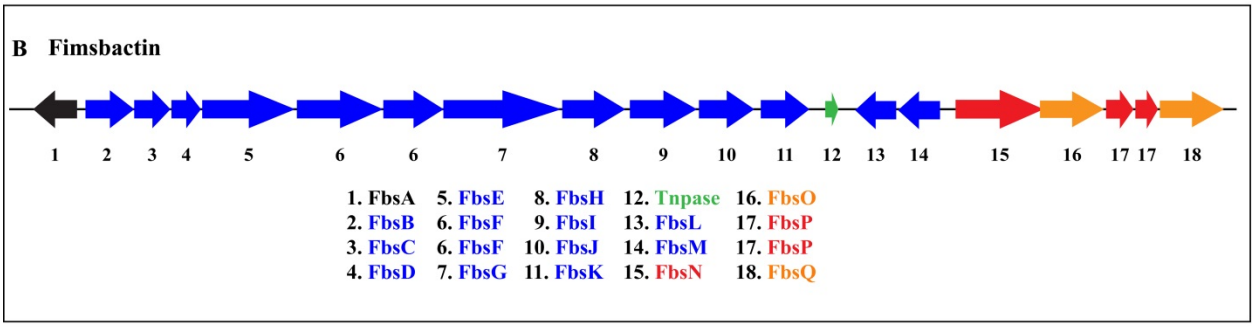
B Fimsbactin
1 2 3 4 5 6 6 7 8 9 10 11 12 13 14 15 16 17 17 18
1. FbsA
2. FbsB
3. FbsC
4. FbsD
5. FbsE
6. FbsF
6. FbsF
7. FbsG
8. FbsH
9. FbsI
10. FbsJ
11. FbsK
12. Tnpase
13. FbsL
14. FbsM
15. FbsN
16. FbsO
17. FbsP
17. FbsP
18. FbsQ

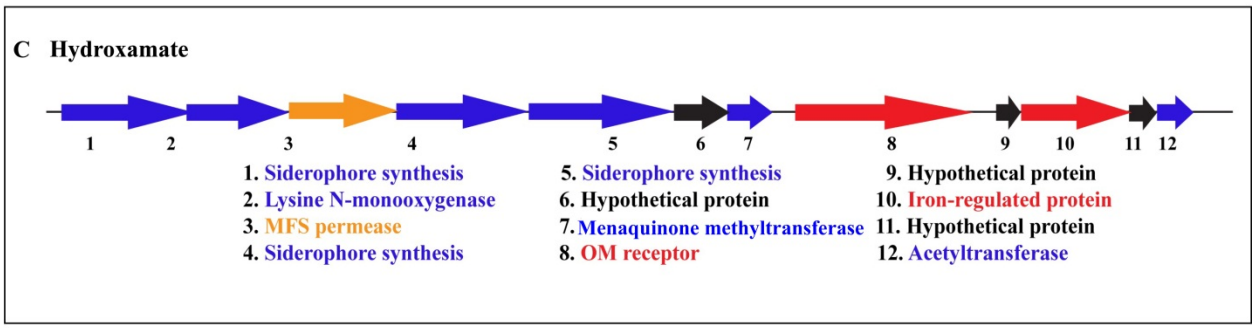
C Hydroxamate
1 2 3 4 5 6 7 8 9 10 11 12
1. Siderophore synthesis
2. Lysine N-monooxygenase
3. MFS permease
4. Siderophore synthesis
5. Siderophore synthesis
6. Hypothetical protein
7. Menaquinone methyltransferase
8. OM receptor
9. Hypothetical protein
10. Iron-regulated protein
11. Hypothetical protein
12. Acetyltransferase

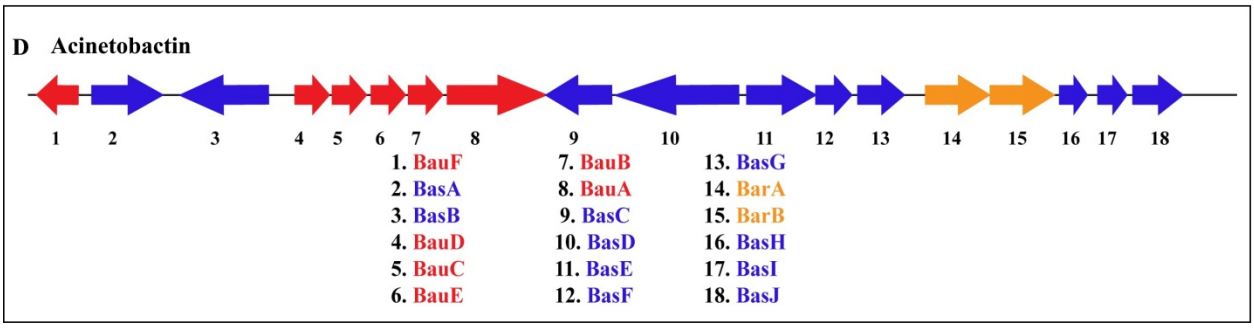
D Acinetobactin
1 2 3 4 5 6 7 8 9 10 11 12 13 14 15 16 17 18
1. BauF
2. BasA
3. BasB
4. BauD
5. BauC
6. BauE
7. BauB
8. BauA
9. BasC
10. BasD
11. BasE
12. BasF
13. BasG
14. BarA
15. BarB
16. BasH
17. BasI
18. BasJ

The acinetobactin cluster in A. baumannii ATCC 19606^T

Under iron-limiting conditions, the *A. baumannii* ATCC 19606^T type strain produces the siderophore acinetobactin, which contains both a catechol and a hydroxamate functional group. Yamamoto *et al*. (157) showed that acinetobactin is composed of *N*-hydroxyhistamine, L-threonine, and 2,3-dihydroxybenzoic acid (DHBA). Structurally, acinetobactin is related to anguibactin, a plasmid-encoded siderophore produced by the fish pathogen *V. anguillarum* (158), the only difference being that acinetobactin possesses an oxazoline ring instead of a thiazoline ring (51, 52). The fact that both organisms can use either siderophore strengthens the argument that the two siderophores are structurally and functionally related (51).

Dorsey *et al*. (51) and Mihara *et al*. (52) independently identified the acinetobactin locus, which contains 18 genes involved in the production, secretion and utilization of this siderophore. Ten of these genes, *basABCDEFGHIJ,* are involved in the biosynthesis of acinetobactin in a process that resembles an NRPS pathway (52). The *basF* and *basJ* genes are homologous to *E. coli entB* and *entC*, respectively, which are used for the biosynthesis of the precursor moiety DHBA from chorismic acid (52, 159). Another gene, *basC*, might be used to produce the other precursor moiety, *N*-hydroxyhistamine, by oxidizing histamine (52). Sequence analysis performed by Mihara *et al*. (52) showed that the predicted proteins coded for by the *basE*, *basF*, *basH* and *basI* genes are similar to other proteins involved in early stages of siderophore biosynthesis in other bacteria. Therefore, these genes could all play roles in early stages of acinetobactin biosynthesis (52).

The amino acid sequences of BasA, BasB, and BasD can all be aligned to various parts of VibF, a well-characterized NRPS protein that has multi-catalytic domains (52, 88, 160). The adenylation (A) domain, the condensation (C) domain, the peptidyl carrier protein (PCP) domain and the cyclization (Cy) domain are present within BasA, BasB and BasD; together, they assemble acinetobactin from three precursors; DHBA, L-threonine, and *N*-hydroxyhistamine (52). The role of *basD* in acinetobactin biosynthesis was tested by Dorsey *et al*. (51), who found that a *basD* mutant failed to grow under iron-limiting conditions. Biochemical analysis also showed that this mutant was negative for the presence of a siderophore, indicating that this mutant was unable to produce a fully functional siderophore (51). These results showed that acinetobactin is the only high-affinity siderophore produced by the ATCC 19606^T strain (51). All genes need to produce fully functional acinetobactin are present in this locus, except for a

homolog of the *entA* gene, which is needed for the production of the essential DHBA moiety (52). This gene could be located in a second genetic cluster that may contain other genes involved in siderophore-mediated iron acquisition.

Random transposition mutagenesis performed by Dorsey *et al*. (51) also identified mutants that failed to grow in iron-limiting conditions, despite producing acinetobactin. DNA sequence investigation of these mutants identified a five-gene polycistronic locus, *bauDCEBA*, involved in ferric acinetobactin uptake (51). The first two genes of this operon are *bauD* and *bauC*, which code for predicted inner membrane proteins that are related to permeases (51, 52). The *bauE* product has sequence similarity with cytoplasmic ferric-siderophore transport ATP-binding proteins (52). Together these three proteins could comprise an ABC importer that is responsible for transporting the ferric-acinetobactin from the periplasmic space into the cytoplasm. Sequence analysis of *bauB*, the fourth gene in the locus, shows similarities with FatB, an anguibactin transporter that is a lipoprotein anchored in the inner membrane, with the iron transport active site exposed to the periplasmic space (51). The last gene of the locus, *bauA*, codes for a protein that is related to FatA, the ferric-anguibactin outer membrane receptor in *V. anguillarum* 775 (51, 52). Phenotypic analysis of an *A. baumannii* ATCC 19606^T BauA deficient isogenic derivative confirmed that BauA is the ferric-acinetobactin outer membrane receptor (51, 52).

BauA is essential for uptake of acinetobactin, but it is not the only siderophore receptor that has been identified in *A. baumannii* ATCC 19606^T. Recent proteomic research done on *A. baumannii* ATCC 19606^T by Nwugo *et al.* (161) showed that several proteins were up-regulated in iron-limiting conditions that represented potential ferric-siderophore receptors other than BauA. This finding leads to the possibility that *A. baumannii* can use xenosiderophores, which are exogenously produced by other bacteria and could be used to compete with other microorganisms for available iron in the environment or in the host when co-existing as a member of the human microbiota (161, 162). Funahasi *et al*. (163) also identified the FhuE protein, as an outer membrane receptor that could utilize xenosiderophores. They demonstrated that in iron-limiting conditions, the growth of an acinetobactin-deficient ATCC 19606^T isogenic mutant could be recovered with the addition of xenosiderophores like desferrioxamine B and desferricoprogen, and that a disruption in FhuE abolished the utilization of these xenosiderophores (163).

Mihara *et al*. (52) also described three other genes that are involved in iron acquisition. These genes are *bauF*, *barA* and *barB*. The gene coding for BauF is predicted to be an esterase and has sequence similarity to ViuB, which is an esterase that releases iron from vibriobactin (52, 164). The other two genes, *barA* and *barB*, possibly encode ABC transporters involved in siderophore secretion (52).

The necessity of the acinetobactin-mediated iron acquisition system for *A. baumannii* ATCC 19606^T in causing a successful infection in the host was determined with various infection models (165). Using an *ex vivo* model, Gaddy *et al*. (165) showed that mutants deficient in acinetobactin production or utilization failed to persist within A549 human alveolar epithelial cells. Similar results were obtained with an *in vivo* infection assay using the greater wax moth *Galleria mellonella*, which were also confirmed with a mouse sepsis model (165). The results showed that acinetobactin production or utilization mutants failed to kill as efficiently as the wild-type, but this impairment could be restored to wild-type level if iron was added to the infection inocula (165). In conclusion, the results show that the acinetobactin-mediated iron acquisition system is crucial for *A. baumannii* ATCC 19606^T to cause a successful infection *in vivo* and that antibacterial drugs targeting this system might provide future treatment options against this pathogen.

Project summary

The objective of this project is the characterization of components of the acinetobactin-mediated siderophore system that have not yet been examined or identified in *A. baumannii*. Through this effort, we describe the role of *barA* and *barB*, which code for ABC transporters and are needed for efficient secretion of acinetobactin. Characterization of these two genes not only expands information on the acinetobactin system but also further our knowledge concerning the export machinery involved in siderophore secretion. Using genetic complementation, we identified the location of the *entA* ortholog, which, though found outside the acinetobactin genetic cluster, is nonetheless essential for siderophore production and virulence in *ex vivo* and *in vivo* models. Furthermore, to determine if the acinetobactin-mediated siderophore system is essential in other *A. baumannii* clinical isolates, we examined the capability of the clinical isolate AYE to acquire iron in an acinetobactin-independent manner through the use of an uncharacterized hydroxamate siderophore. Taken together, the results from this study not only further our understanding of the acinetobactin-mediated siderophore system, but also demonstrate how different *A. baumannii* clinical isolates acquire iron using different siderophore-mediated systems that are required for the virulence of this pathogen.

Chapter 2

The role of BarA and BarB in acinetobactin secretion and virulence in *Acinetobacter baumannii* ATCC 19606^{T}

William F. Penwell, Amber C. Beckett, Daniel L. Zimbler, Brock A. Arivett and Luis A. Actis

Abstract

Acinetobacter baumannii is a human pathogen that must overcome iron-limiting conditions imposed by the human host to cause a successful infection. To acquire this essential micronutrient, *A. baumannii* expresses the high-affinity acinetobactin-mediated iron acquisition system. The genome of the type strain ATCC 19606^T harbors a cluster of genes coding for acinetobactin biosynthesis and uptake of ferric-acinetobactin complexes. This cluster also includes two genes, *barA* and *barB*, which code for a putative metal ABC transporter that potentially could be involved in the secretion of acinetobactin. To test this hypothesis, the ATCC 19606^T *barA/B* region was disrupted by allelic exchange to generate the *barA/B*::Gm^R derivative, 3213. In iron-chelated conditions, the *barA/B* mutant showed a reduced growth phenotype when compared to the parental strain, which could be restored with the addition of iron. HPLC analysis revealed that the BarA/B deficient strain secreted a reduced level of acinetobactin after 24 h of growth in M9 minimal medium. BarA/B played a role not only in siderophore secretion but also in virulence of *A. baumannii* ATCC 19606^T. Experimental infections using *ex vivo* and *in vivo* models provided evidence supporting the role of BarA/B in virulence, although to a greater degree than in an acinetobactin-deficient strain. Taken together, these results show that inactivation of the *barA/B* genes reduced but did not abolish acinetobactin secretion, leading to the possibility that an alternative secretion pathway exists for acinetobactin secretion in *A. baumannii.*

Introduction

Over the last decade *Acinetobacter baumannii* has been recognized as an important pathogen that causes severe infections in immunocompromised patients (7, 166). *A. baumannii* has been linked to a wide range of infections including pneumonia, urinary tract infections, septicemia, and more recently necrotizing fasciitis (20, 167). This pathogen has also been reported as the etiological agent in a significant number of severe infections in wounded military personnel injured during Operation Enduring Freedom in Afghanistan and Operation Iraqi Freedom in Iraq (23). *A. baumannii* has also become a major concern in the healthcare setting (7, 10). This is due in part, to the ability of this pathogen to persist in the hospital environment and to resist a wide range of antibiotics, making treatment of infected individuals problematic. Despite the fact that *A. baumannii* is a successful nosocomial pathogen, very little is known about the virulence factors that allow this bacterium to be an effective pathogen. Virulence phenotypes that have been examined in *A. baumannii* include the ability to form biofilms on plastic surfaces, to adhere to human epithelial cells, and to thrive under iron-limiting conditions such as those found in the host.

In the human host, iron is sequestered by host glycoproteins such as transferrin and lactoferrin, making iron unavailable to bacteria (55, 64, 168). However, iron is an essential micronutrient for almost all bacteria and is needed as a cofactor or as a prosthetic group for enzymes that are required for cellular functions and metabolic pathways (55). To overcome this host nutritional immunity, bacteria produce and secrete low-molecular weight compounds, termed siderophores, which sequester iron from host proteins by forming ferric-siderophore complexes, and are transported back into the cell by specific outer membrane receptors (55, 64). The mechanisms by which siderophores are secreted from the cell have been less thoroughly investigated than the proteins involved in biosynthesis and ferric-siderophore uptake. Investigations conducted on the proteins involved in siderophore secretion have identified export machinery belonging to two types of transporters, the major facilitator superfamily (MFS) and the ATP-binding cassette (ABC) transporter family. The ABC transporter family includes the proteins ExiT in *Mycobacterium smegmatis* (108), IroC in *Salmonella enterica* serovar Typhimurium (106), IrtA in *M. tuberculosis* (169), PvdE in *Pseudomonas aeruginosa* (105) and ORF14 and ORF15 in *Vibrio anguillarum* (107, 170), which are used for the secretion of exochelin, salmochelin, carboxymycobactin, pyoverdine, and anguibactin, respectively.

In iron-limiting conditions, *A. baumannii* produces acinetobactin to sequester iron from host iron-binding proteins (51). This catechol-hydroxamate siderophore is a non-cyclic derivative of 2,3-dihydroxybenzoic acid (DHBA) linked to threonine and *N*-hydroxyhistamine (171). Dorsey *et al*. (51) and Mihara *et al*. (52) independently identified the acinetobactin cluster in the *A. baumannii* type strain ATCC 19606^T, which was experimentally demonstrated to be the only functional siderophore produced by this strain (51). Almost all genes needed for the biosynthesis of this siderophore are located within this 26.5-kb cluster (51, 52), with the exception of the *entA* gene (see Chapter 2). The acinetobactin cluster also contains the genes coding for the uptake of ferric-acinetobactin complexes, which include the acinetobactin outer membrane receptor, BauA (51). Previous research has described genes involved in production and uptake of this siderophore and revealed that mutants in both acinetobactin biosynthesis and uptake not only have a decreased growth phenotype under *in vitro* iron-limiting conditions, but also display a decreased virulence phenotype as compared to the parental strain (51, 165).

Also located within the acinetobactin cluster are two genes, *barA* and *barB*, which code for proteins that have sequence similarity to putative ABC export systems that are involved in siderophore secretion, most notably ORF14 and ORF15 from *V. anguillarum* 775. Since these two genes reside within the acinetobactin cluster and code for an ABC transport system, it was hypothesized that *barA* and *barB* are involved in acinetobactin secretion. In this study, we present experimental evidence demonstrating that BarA and BarB (BarA/BarB) are needed by *A. baumannii* ATCC 19606^T for optimal growth under iron-chelated conditions and also for efficient secretion of acinetobactin. BarA/B was also determined to be needed for full virulence of ATCC 19606^T when tested in *ex vivo* and *in vivo* models. However, a BarA/B deficient strain showed only reduction in the amount of acinetobactin secreted, not a complete abrogation of acinetobactin secretion, suggesting that other export systems may also play roles in acinetobactin secretion.

Materials and Methods

Bacterial strains, plasmids, and culture conditions

Bacterial strains and plasmids used in this work are shown in Table 1. Strains were routinely cultured in Luria Bertani (LB) broth or agar (172) at 37ºC in the presence of

Table 1. Bacterial strains and plasmids used in this study

Strain/plasmid	Relevant characteristics[a]	Source/reference
Strains		
A. baumannii		
ATCC 19606^T	Nosocomial isolate	ATCC
ATCC 19606^T s1	ATCC 19606^T *basD* mutant, Km^R	(51)
ATCC 19606^T 3213	ATCC 19606^T *barA/barB* mutant, Gm^R	This work
E. coli		
Top10	Used for recombinant DNA methods	Invitrogen
DH5α	Used for recombinant DNA methods	Gibco-BRL
Plasmids		
pCR-Blunt-II-Topo	PCR cloning vector, Km^R, Zeo^R	Invitrogen
pEX100T	Mobilizable suicide plasmid in ATCC 19606^T, Amp^R	ATCC
pPS856	Source of FRT-Gm^R-FRT cassette Amp^R, Gm^R	(173)
pRK2073	Used as helper in plasmid conjugation Tp^R	(174)
pMU671	pCR-Blunt-II-Topo harboring the ATCC 19606^T *barA* and *barB* genes, Km^R, Zeo^R	This work
pMU981	pMU671 derivative with ATCC 19606^T *barA/barB*::*gent* insertion, Km^R, Zeo^R and Gm^R	This work
pMU984	3.4 kb *Pvu*II fragment from pMU981 cloned into pEX100T	This work

[a]Amp, ampicillin; Km, kanamycin; Tet, tetracycline; Gm, gentamicin; Zeo, zeocin; Tp, trimethoprim; R, resistance/resistant.

appropriate antibiotics. M9 minimal medium was used for growth under chemically defined conditions (175). Iron-rich and iron-limiting conditions were achieved by the addition of $FeCl_3$ dissolved in 0.01M HCl and 2,2' dipyridyl (DIP), respectively, to LB or M9 minimal medium.

General DNA procedures

Total DNA was isolated either by ultracentrifugation in CsCl density gradients (176) or by using a mini-scale method (177). Plasmid DNA was isolated using commercial kits (Qiagen). Restriction endonucleases were purchased from New England Biolabs and used according to the manufacturer's specifications. DNA was size-fractionated by agarose gel electrophoresis (172).

***In silico* analyses of BarA/B**

The HHMTOP serve (http://www.enzim.hu/hmmtop/) along with the TMHMM program (www.cbs.dtu.dk/services/TMHMM-2.0/) were used for predicting transmembrane domains and topology of the proteins (178, 179). Transmembrane data was visualized using the TMRPres2D program (http://biophysics.biol.uoa.gr/) (180). ScanProsite, Pfam, and the Conserved Domain Database were used for motif and domain scans (181-183). NCBI BLASTP was used for comparative genome analyses (184).

Site-directed insertional mutagenesis of *barA/B*

The *barA* and *barB* genes were PCR-amplified using Pfu DNA polymerase (Stratagene) from *A. baumannii* ATCC 19606^T total DNA using primers 2979 (5'-TTATCTGGCAACCTGTGG-3') and 2984 (5'-GGGTGTGTCTGAGTAAGC-3') (Fig. 5A). The 3.8-kb amplicon was cloned into pCR-Blunt-II-Topo (Invitrogen) to generate plasmid pMU671. An internal 1751-bp fragment, located 667 bp upstream of the 3'end of *barA* and 1084 bp downstream of the 5' end of *barB*, was deleted by *Sca*I digestion (Fig. 5A). The 1.3-kb Gm^R-Flp recombinase target (FRT) cassette from pPS856 was excised using *Sma*I and then ligated into the *Sca*I-digested pMU671 to form pMU981. To facilitate the allelic exchange of the disrupted *barA* and *barB* genes into *A. baumannii* ATCC 19606^T chromosome, the entire 3.4-kbp *barA/B::gent* was excised from pMU981 using a *Pvu*II digestion and then subcloned into the *Sma*I site of pEX100T to form pMU984.

Figure 5. The genetic and domain organization of *barA* and *barB*. (A) The *basE-basI* polycistronic operon, from the *A. baumannii* ATCC 19606^{T} acinetobactin gene cluster that contains the *barA and barB* genes. The horizontal arrows and their direction indicate the predicted location of coding regions and their direction of transcription, respectively. The Gent-FRT cassette, which codes for gentamicin resistance, was inserted into the fragment deleted by *Sca*I (S) digestion. Numbers on top of the horizontal line indicate DNA sizes in bp. Primers used to amplify *barA/B* are shown in red. The horizontal lines indicate the chromosomal regions either cloned or used to confirm recombinant derivatives by PCR. Primer numbers used for amplification are shown in red. The numbers next to each bar indicate the location of primers used in PCR amplification. Membrane topology and domains present in BarA (B) and BarB (C). The underlined sequences for both proteins indicate transmembrane-spanning segments with the cytoplasmic and periplasmic regions of the TMD colored green and blue, respectively. The Walker A and Walker B motifs and the signature sequence motif are colored orange, red, and purple, respectively.

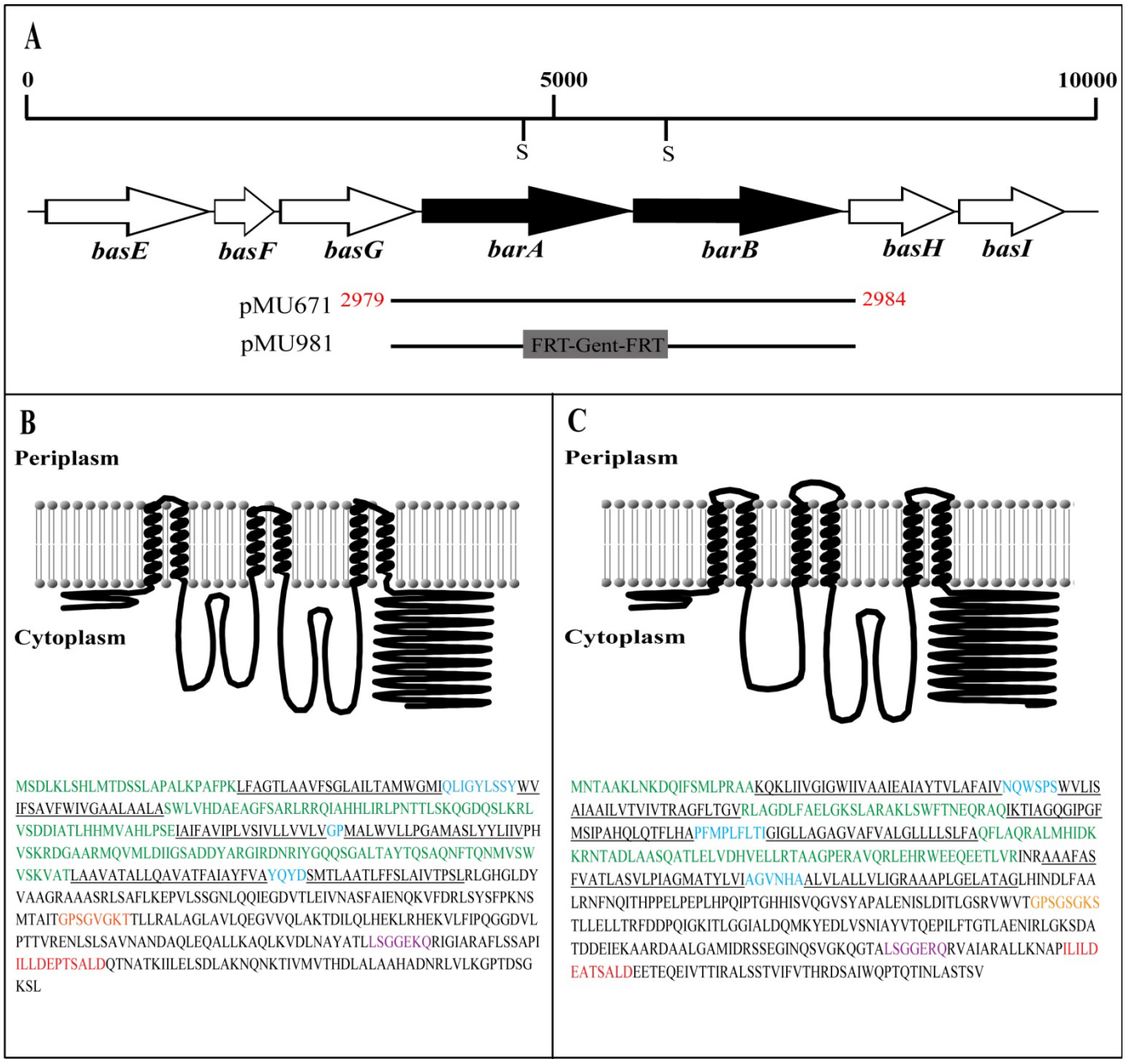
A
0
5000
10000
S
S
basE
basF
basG
barA
barB
basH
basI
pMU671
2979
2984
pMU981
FRT-Gent-FRT
B
Periplasm
Cytoplasm
MSDLKLSHLMTDSSLAPALKPAFPKLFAGTLAAVFSGLAILTAMWGMIQLIGYLSSYWV
IFSAVFWIVGAALAALASWLVHDAEAGFSARLRRQIAHHLIRLPNTTLSKQGDQSLKRL
VSDDIATLHHMVAHLPSEIAIFAVIPLVSIVLLVVLVGPMALWVLLPGAMASLYYLIIVPH
VSKRDGAARMQVMLDIIGSADDYARGIRDNRIYGQQSGALTAYTQSAQNFTQNMVSW
VSKVATLAAVATALLQAVATFAIAYFVAYQYDSMTLAATLFFSLAIVTPSLRLGHGLDY
VAAGRAAASRLSAFLKEPVLSSGNLQQIEGDVTLEIVNASFAIENQKVFDRLSYSFPKNS
MTAITGPSGVGKTTLLRALAGLAVLQEGVVQLAKTDILQLHEKLRHEKVLFIPQGGDVL
PTTVRENLSLSAVNANDAQLEQALLKAQLKVDLNAYATLLSGGEKQRIGIARAFLSSAPI
ILLDEPTSALDQTNATKIILELSDLAKNQNKTIVMVTHDLALAAHADNRLVLKGPTDSG
KSL
C
Periplasm
Cytoplasm
MNTAAKLNKDQIFSMLPRAAKQKLIIVGIGWIIVAAIEAIAYTVLAFAIVNQWSPSWVLIS
AIAAILVTVIVTRAGFLTGVRLAGDLFAELGKSLARAKLSWFTNEQRAQIKTIAGQGIPGF
MSIPAHQLQTFLHAPFMPLFLTIGIGLLAGAGVAFVALGLLLLSLFAQFLAQRALMHIDK
KRNTADLAASQATLELVDHVELLRTAAGPERAVQRLEHRWEEQEETLVRINRAAAFAS
FVATLASVLPIAGMATYLVIAGVNHAALVLALLVLIGRAAAPLGELATAGLHINDLFAA
LRNFNQITHPPELPEPLHPQIPTGHHISVQGVSYAPALENISLDITLGSRVWVTGPSGSGKS
TLLELLTRFDDPQIGKITLGGIALDQMKYEDLVSNIAYVTQEPILFTGTLAENIRLGKSDA
TDDEIEKAARDAALGAMIDRSSEGINQSVGKQGTALSGGERQRVAIARALLKNAPILILD
EATSALDEETEQEIVTTIRALSSTVIFVTHRDSAIWQPTQTINLASTSV

E. coli Top10 cells harboring pMU984, *E. coli* DH5α cells harboring pRK2073, and *A. baumannii* ATCC 19606^T cells were used as the donor, helper, and recipient strains, respectively, in a triparental mating. Transconjugants were selected on LB agar plates containing 100 µg/ml of gentamicin and confirmed to be *A. baumannii* by growth on Simmons' citrate agar plates. Disruption of the *barA/B* genes in *A. baumannii* ATCC 19606^T-3213 derivative was confirmed by PCR using primers 2986 (5'-ATTGCGATTTTTGCTGTA-3') and 2897 (5'-TTCACCACCAGACAATGC-3') (Fig. 5A) and observing a molecular mass shift consistent with deletion of the *Sca*I fragment and insertion of the Gm^R-FRT cassette.

Determination of *barA/B* mutant growth phenotype and acinetobactin secretion

The minimal inhibitory concentration of the iron chelator DIP was determined in LB broth or M9 minimal medium containing increasing concentrations of this chelator. Cell growth was determined spectrophotometrically at 600 nm after overnight incubation at 37°C in a shaking incubator set at 200 rpm.

Triplicate bacterial cultures for each strain were grown in 1 ml of M9 minimal medium for 24 h and then cultures were combined and adjusted to the equivalent $OD_{600.}$ Cell-free culture supernatants were collected by centrifugation at 10,000 rpm for 3 min. The amount of acinetobactin secretion was assessed by Arnow's test (185) and high-performance liquid chromatography (HPLC). For the Arnow's test, 1 volume of reagent A (0.5 N HCl), reagent B (10% $NaNO_3$, $NaMoO_4$) and reagent C (1 N NaOH) were successively added to 1 volume of culture supernatant. The amount of catechol present was measured by determining the OD_{510} after 10 min incubation at room temperature. HPLC analysis was performed with an Agilent 1100 LC instrument as previously described (186). Briefly, M9 minimal medium culture supernatants were filtered through 0.45 µm cellulose acetate filter units (Spin-x centrifuge filter units, Costar, Cambridge, MA). Supernatants were then fractionated over a Vydac C-8, 5 µm, 250 mm x 4.6 mm reversed-phase column (Grace Davison Discovery Science, Deerfield, IL). Water and acetonitrile were used as mobile phases and detection was at 317 nm with a flow rate of 0.5 ml/min.

The amount of acinetobactin and DHBA secreted was determined using the values obtained from the HPLC profiles for each set of pooled samples (n=3). The percent reduction in the amount of secreted acinetobactin and DHBA was determined by using the formula (A-

B)/A)*100, where A is the HPLC values for ATCC 19606^T and B is the HPLC value for the 3213 *barA/B* mutant.

Siderophore utilization assay

The production of acinetobactin was tested with a siderophore utilization assay in which the *A. baumannii* ATCC 19606^T acinetobactin-deficient s1 strain was used as a reporter strain (51). $FeCl_3$, distilled water, or M9 culture supernatants from ATCC 19606^T or the 3213 *barA/B* mutant were spotted onto 7-mm filter disks and deposited on L agar plates containing 225 uM DIP. Growth halos were measured after 30 h incubation at 37^{o}C.

A549 infection assays

A549 human alveolar epithelial cells (187), which were provided by Dr. E. Lafontaine (College of Veterinary Medicine, University of Georgia, USA), were cultured and maintained in DMEM supplemented with 10% heat-inactivated fetal bovine serum at 37°C in the presence of 5% CO_2 as previously described (44). A549 monolayers maintained in modified Hanks balanced salt solution (mHBSS, same as HBSS but without glucose) for 24 h at 37°C in 5% CO_2 without infection remained viable as determined by trypan blue exclusion assays. Twenty-four-well tissue culture plates were seeded with approximately 10^4 epithelial cells per well and then incubated for 16 h at 37°C in 5% CO_2. Bacterial cells were grown 24 h in LB broth at 37ºC with shaking at 200 rpm, collected by centrifugation at 15,000 rpm for 10 min, washed, resuspended, and diluted in mHBSS. The A549 monolayers were singly infected with 10^3 cells of the ATCC 19606^T parental strain, the S1 (*basD*$^-$) or 3213 (*barA/B*$^-$) isogenic derivative. Inocula were estimated spectrophotometrically at OD_{600} and confirmed by plate count. Infected monolayers were incubated 24 h in mHBSS at 37°C in 5% CO_2. Incubation of ATCC 19606^T in mHBSS for 24 h at 37^{o}C does not result in significant bacterial growth (188). The tissue culture supernatants were collected, the A549 monolayers were lysed with sterile, distilled H_2O, and lysates were added to the cognate tissue culture supernatants. Bacteria were collected from the resulting suspensions by centrifugation, resuspended in 1 ml sterile, distilled H_2O, serially diluted, and then plated on nutrient agar. After overnight incubation at 37ºC, the colony forming units (CFUs) were counted and CFU/ml values for each sample were calculated and recorded. Counts were compared using the Mann-Whitney U test; P values ≤ 0.05 were considered significant.

Experiments were done three times in triplicate using fresh biological samples each time. To determine bacterial relative fitness, the recovered CFUs were divided by the CFUs of the inoculum used to infect monolayers.

Galleria mellonella killing assays

Bacteria grown in LB broth were collected by centrifugation and suspended in sterile phosphate-buffered saline solution (PBS). The number of bacteria was estimated spectrophotometrically at OD_{600} and diluted in PBS to appropriate concentrations. All bacterial inocula were confirmed by plating serial dilutions on LB agar and determining colony counts after overnight incubation at 37°C. Ten freshly received final-instar *G. mellonella* larvae (Grubco, Fairfield, OH) weighing 250-350 mg were randomly selected and used in killing assays as described previously (189). Briefly, the hemocoel at the last left proleg was injected with 5-µl inocula containing 1 x 10^4 bacteria ± 0.25 log of each tested strain using a syringe pump (New Era Pump Systems, Inc., Wantagh, NY) with a 26 G½ needle. Each test series included control groups of non-injected larvae or larvae injected with sterile PBS. The test groups included larvae infected with the parental strain ATCC 19606^T, the s1 *basD* mutant, or the 3213 *barA/B* insertion derivative. Injected larvae were incubated at 37°C in darkness, assessing death at 24 h intervals over 6 d. Larvae were considered dead and were removed if they did not respond to probing. Results were not considered if more than two deaths occurred in the control groups. Experiments were repeated three times using 10 larvae per experimental group and the survival curves were plotted using the Kaplan-Meier method (190). *P* values ≤ 0.05 were considered statistically significant for the log-rank test of survival curves (SAS Institute Inc., Cary, NC).

Results

In silico analyses of BarA/B

The acinetobactin cluster contains two genes, *barA* and *barB*, that have been proposed to be involved in acinetobactin secretion from the cell into the extracellular milieu (52). The *barA* and *barB* genes encode proteins of 536 and 531 amino acids, respectively, and are located within a polycistronic operon with the siderophore assembly genes *basE*, *basF*, *basH,* and *basI* (Fig. 5A) (52). The promoter that for this operon was determined to be located upstream of the *basE* gene and that this sequence includes a putative Fur box, which was experimentally proven to be up-regulated under iron-limiting conditions (52). A sequence homology search performed with BLASTP revealed that BarA and BarB are related to ORF14 (46.8% identity, 65.3% similarity) and ORF15 (49.6 % identity, 67.4% similarity), respectively, from *V. anguillarum* 775. Located within the anguibactin cluster on the plasmid pJM1, ORF14 and ORF15 code for putative proteins that are related to ABC transporters (107). A disruption in ORF14, the BarA homolog, not only abolished growth under iron-chelated conditions but also abolished anguibactin production in *V. anguillarum* 775 (107, 170).

The predicted domain architecture of the proteins coded by *barA*/*B* suggests an ABC transporter with a fused ATPase and permease components, which are typical of bacterial ABC exporters (191). Both BarA/B have N-terminal sequences that include transmembrane-spanning domains (TMD) and a nucleotide-binding domain (NBD) located in the C-terminal regions. The HMMTOP transmembrane topology prediction server determined that both proteins contain six transmembrane-spanning segments (Fig. 5B and 5C) with the NBD located in the cytoplasm (178). Motif scanning of both NBD showed characteristic motifs shared by proteins of the ABC transport family, which include Walker A (WA) boxes, Walker B (WB) boxes, and the ABC signature motif (SM) (181-183, 191, 192). BarA has conserved sequences of WA ^{361}GPSGVGKT^{368}, WB ^{475}ILLDEPTSALD^{485} and SM ^{454}LSGGEKQ^{460} whereas BarB has WA ^{354}GPSGSGKS^{361}, WB ^{478}ILILDEATSALD^{489} and SM ^{458}LSGGERQ^{464} sequences (Fig. 5B and 5C) (192). Taken together, the *in silico* analyses are consistent with BarA and BarB being a heterodimer that constitutes a fully functional ABC exporter involved in siderophore secretion; however, the exact interaction that these proteins have with each other remains to be determined.

BarA/B are required for growth in iron-limited conditions

To confirm the role of BarA/B in acinetobactin secretion, the isogenic derivative 3213 was generated by allelic exchange using the construct pMU984 (Table 1). This construct was produced by the deletion of 1751 bp from the 3'end of *barA* and the 5'end of *barB* and then inserting the gentamicin resistance cassette within *barA* and *barB*. PCR was used to confirm the correct genetic arrangements of the wild-type and the isogenic derivative (data not shown). The 3213 *barA/B* mutant displayed no growth defects and reached a similar cell density to that of ATCC 19606^T after 24 h incubation in M9 minimal medium (Fig. 6A), as well as LB (data not shown), without the addition of antibiotics.

ATCC 19606^T, 3213, and the ATCC 19606^T s1 mutant, which is impaired in BasD-mediated acinetobactin biosynthesis, were grown in M9 minimal medium with increasing concentrations of DIP to examine the ability of the isogenic derivatives to grow under iron-limiting conditions. Fig. 6B shows that the 3213 *barA/B* isogenic derivative had a significant growth defect at 100 μM DIP ($P = 0.002$). The growth defect of *barA/B* mutant was not as pronounced as the ATCC 19606^T s1 mutant ($P = 0.0003$), which was used as a control; however, at 150 μM DIP both mutants had almost no growth. The iron utilization deficient phenotype of the 3213 and s1 mutants was corrected to wild type levels when the M9 cultures containing 100 μM or 150 μM DIP were each supplemented with 50 μM $FeCl_3$ (Fig. 6C). These results indicate that BarA/B are needed but not essential by *A. baumannii* ATCC 19606^T for growth under iron-limiting conditions and function in iron acquisition.

Figure 6. The iron acquisition phenotype of the *barA/barB* mutant under iron-chelated conditions. (A) Growth curves of the ATCC 19606^T parental strain (blue circles) and the 3213 isogenic *barA/B* mutant (red triangles) in M9 minimal medium. (B) Growth of the ATCC 19606^T parental strain (blue), the *barA/B* 3213 isogenic derivative (red) and the s1 mutant (yellow) in M9 minimal medium with increasing concentrations of DIP. (C) Growth of ATCC 19606^T (blue), the *barA/B* isogenic derivative (red) and the s1 mutant (yellow) in M9 minimal medium with and without the addition or supplemented with 50 μM $FeCl_3$ plus either 100 μM or 150 μM DIP.

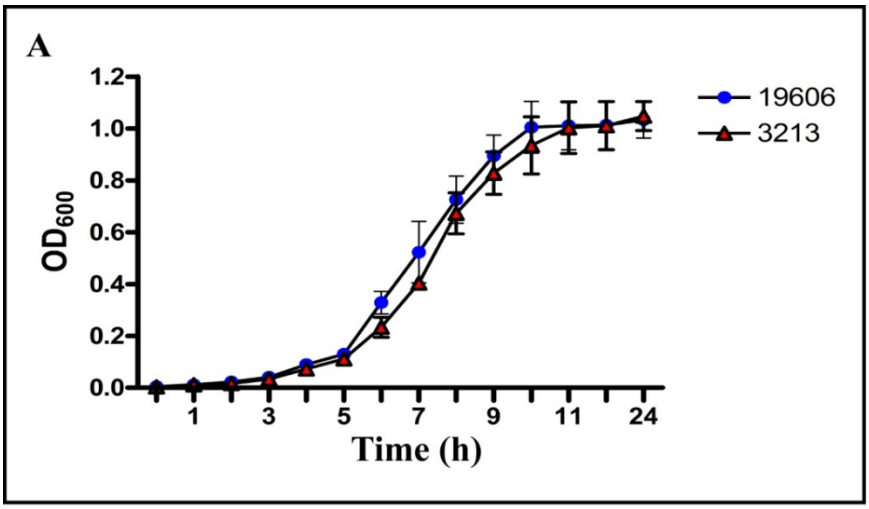
A
1.2
1.0
0.8
0.6
0.4
0.2
0.0
OD600
1
3
5
7
9
11
24
Time (h)
19606
3213

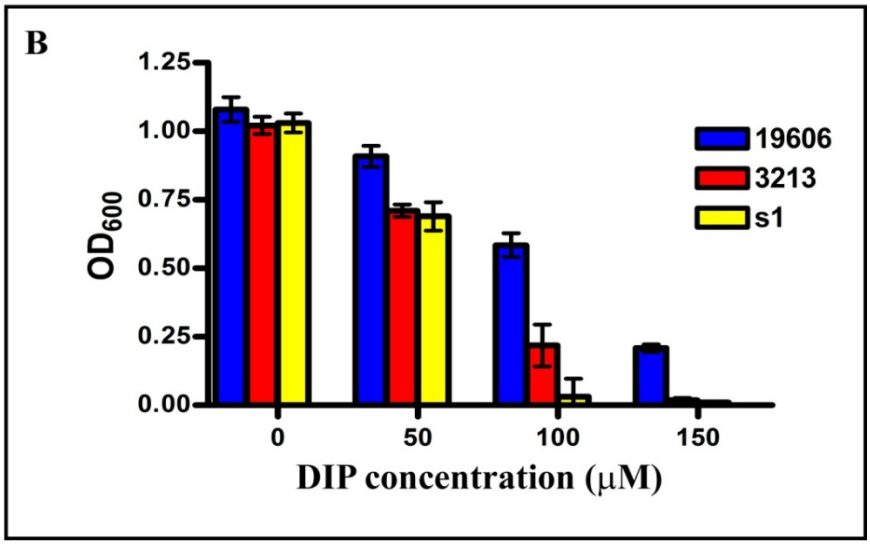
B
1.25
1.00
0.75
0.50
0.25
0.00
OD600
0
50
100
150
DIP concentration (μM)
19606
3213
s1

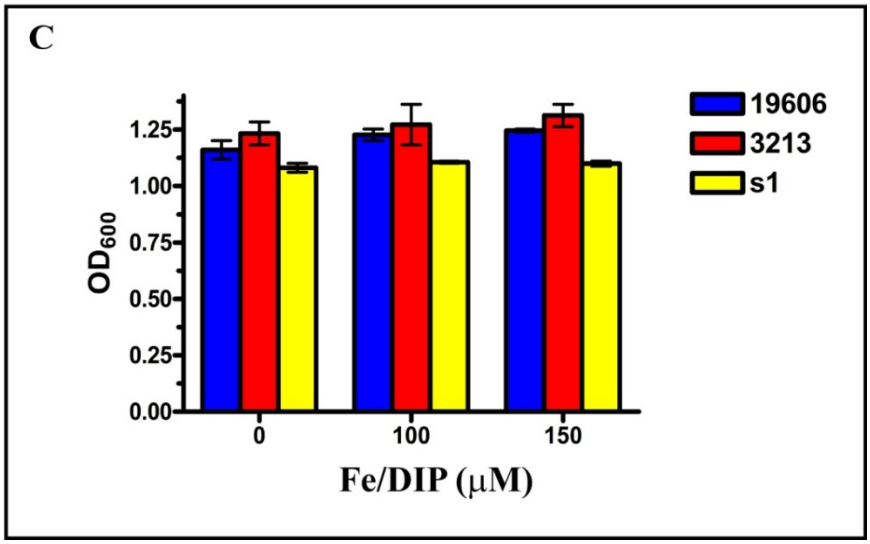
C
1.25
1.00
0.75
0.50
0.25
0.00
OD600
0
100
150
Fe/DIP (μM)
19606
3213
s1

BarA/B involvement in acinetobactin export

The production and utilization of acinetobactin is required by *A. baumannii* ATCC 19606^T for optimal growth under iron-limiting conditions. Since the *barA/B* isogenic derivative displayed a decreased growth phenotype under iron-liming conditions, it was hypothesized that *barA* and *barB* might be required for efficient secretion of acinetobactin. In order to confirm that BarA/B are involved in secretion, the strains ATCC 19606^T and 3213 were cultured for 24 h in M9 minimal medium and normalized to the lowest OD_{600}, and secretion of acinetobactin into cell-free culture supernatants was examined by the Arnow's colorimetric assay (185), which detects the presence of catechols, like the DHBA moiety present in acinetobactin, and also quantitatively by HPLC.

The 3213 derivative showed a 35% decrease (P = 0.0011) in the amount of catechol present in the culture supernatant when compared to the wild-type ATCC 19606^T (Fig. 7A). Since this assay only detects the total amount of catechol present in the supernatant and cannot distinguish acinetobactin from its catechol precursor, HPLC was used for quantitative assessment of the release of acinetobactin from these two strains. HPLC analysis of culture supernatants of bacteria grown in M9 minimal medium indicated the presence of two peaks with elution times of ~9.0 and ~10.5 min, corresponding to acinetobactin and the DHBA precursor, respectively (Fig. 7B, Table 2). The 3213 isogenic derivative had a 40% reduction in the amount of acinetobactin secreted when compared to the wild-type (P = 0.0003) after 24 h of growth in M9 minimal medium (Fig. 7B, Table 2). However, there was not a significant reduction (P = 0.07) in the amount of secreted DHBA in the culture supernatant of the 3213 derivative when compared to the wild-type (Fig. 7B, Table 2). These results collectively suggest that BarA/B are involved in acinetobactin secretion but the BarA/B-deficient strain has a reduction in, rather than a complete loss of acinetobactin secretion.

As previously stated, *barA/B* are two genes located in a seven-gene polycistronic operon, in which the other five genes code for proteins involved in acinetobactin biosynthesis (Fig. 5A). The deletion/insertion method used to generate the isogenic derivative 3213 could have caused polar effects on the two downstream genes, *basH and basI,* which encode a putative thioesterase and a phosphopantetheinyl transferase, respectively (52). To assess whether downstream polar effects occurred, a siderophore utilization assay was employed using the ATCC 19606^T s1 derivative, which does not produce acinetobactin but expresses all functions needed for its

Figure 7. The role of BarA/B in acinetobactin secretion. (A) Arnow's reaction of M9 cultures supernatants of ATCC 19606^T (blue) or the 3213 *barA/B* isogenic derivative (red). (B) HPLC profiles of sterile M9 medium or culture supernatants from ATCC 19606^T or *barA/B* mutant 3213. Acinetobactin (Ab) and DHBA peaks are labeled in the chromatogram of the 3213 *barA/B* mutant. The values corresponding to the amount (mAU) of the detected peaks from each sample are shown in Table 2.

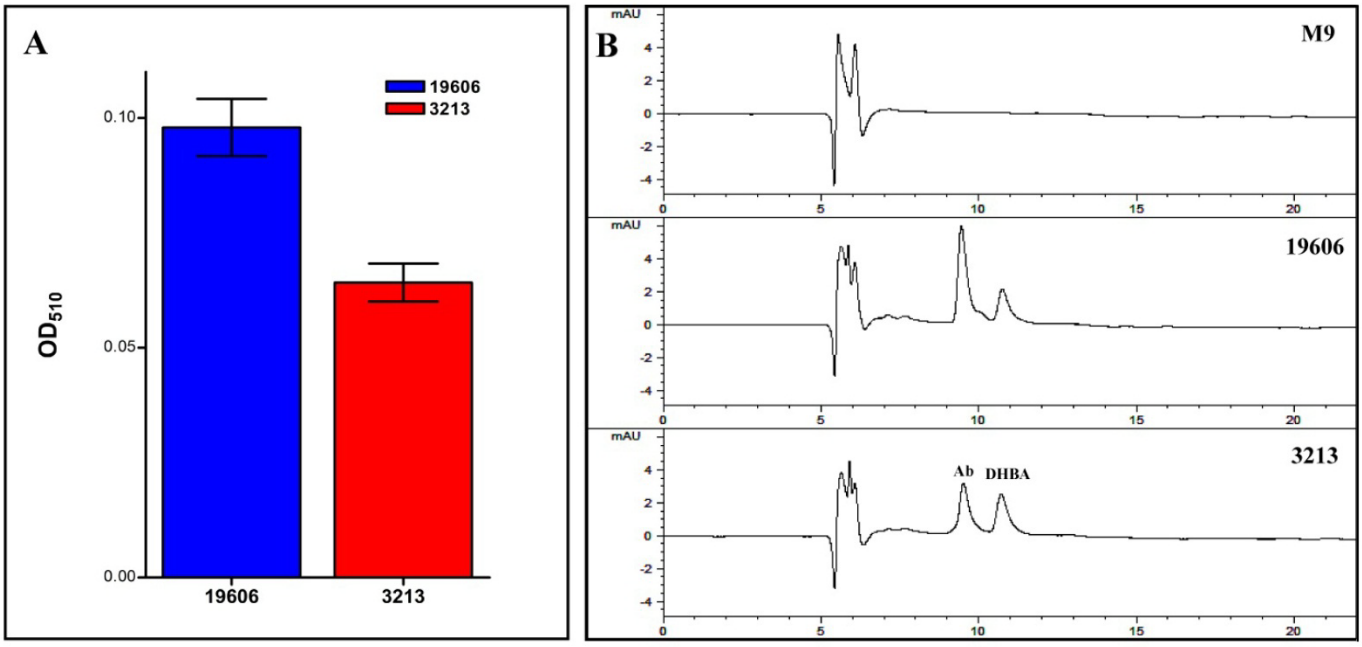
A
19606
3213
0.10
0.05
0.00
OD510
19606
3213
B
M9
19606
3213
mAU
Ab
DHBA

Table 2. The amount (mAU) of acinetobactin and DHBA detected in the chromatograms of ATCC 19606^T and the 3213 *barA/B* mutant. This table also indicates the percent reduction in the secretion by the 3213 isogenic derivative compared to the wild-type.

Samples	Acinetobactin (mAU)	DHBA (mAU)
19606^T	6.18±.24	2.36±.03
3213	3.71±.02	2.0±.12
Reduction	40.0%	14.9%

utilization, as an indicator strain (51). The data from the bioassay (Table 3) indicated that culture supernatants from the ATCC 19606^T and the 3213 isogenic derivative were able to recover the growth of the ATCC 19606^T s1 derivative, demonstrating that the parental strain and the isogenic mutant both secrete fully functional acinetobactin that can be utilized by the s1 derivative. Therefore the method used to generate the isogenic derivative 3213 does not cause a downstream polar effect, and the reduction in the amount of acinetobactin present in the culture supernatant of this mutant is due to a decrease in siderophore secretion and not a decrease in production.

Table 3. Siderophore utilization assay

Compounds tested	***A. baumannii* s1 indicator strain (growth halo in mm)***
$FeCl_3$	16.38±0.75
H_2O	0
19606 culture supernatant†	13±0.84
3213 culture supernatant†	11.58±0.68

*Bacterial growth around 7-mm filter disk on LB agar plates containing 225 µM DIP was determined after 34 h incubation at 37^{o}C.

† Culture supernatants of *A. baumannii* strains incubated in M9 minimal medium.

The role of BarA/B in virulence

The role of BarA/BarB in the virulence of *A. baumannii* ATCC 19606^T was determined using A549 human alveolar epithelial cells and *G. mellonella* caterpillars as *ex vivo* and *in vivo* experimental models, respectively. The tissue culture assay showed a significant reduction in the number of bacteria recovered from A549 human alveolar epithelial cells with the 3213 *barA/B* mutant (P= 0.0039) when compared with the number of bacteria recovered from A549 cells infected with the parental strain (Fig. 8A). However, the decrease in persistence of the 3213 isogenic derivative was not as great as that of the ATCC 19606 s1 mutant (P=0.0001), which showed a 2-log decrease in the number of bacteria recovered from the infected A549 monolayer. The results of the *ex vivo* model indicate that the 3213 mutant is able to persist better than the s1 mutant but not as well as the parental strain.

The *G. mellonella* infection model showed that 60% of caterpillars died after 6 d following infection with the parental strain, a value that is significantly different from those injected with sterile PBS (P = 0.001) (Fig. 8B). Both the 3213 and the s1 isogenic derivatives, which killed 33% (P= 0.1638) and 27% (P= 0.4052) of the caterpillars, respectively, were statistically indistinguishable from the PBS control group. Fig 8B shows that both mutants were less virulent than the parental strain, with s1 killing significantly fewer worms (P = 0.0097) than the parental strain, but killing by 3213 *barA/B* mutant was at an intermediate and almost significant difference (P = 0.057) when compared to ATCC 19606^T. In both models, the 3213 *barA/B* mutant is able to persist better in the *ex vivo* model and kill more caterpillars in the *in vivo* models than the s1 isogenic derivative. This could be because the 3213 isogenic derivative still secretes some acinetobactin, which allows this mutant to acquire iron and exhibit an elevated virulence phenotype when compared to the s1 acinetobactin-deficient mutant. However, the reduction in the amount of siderophore secreted by the 3213 *barA/B* mutant does not allow for this derivative to persist in an A549 monolayer or kill caterpillars as well as the wild-type does. Taken together, the results of both the *ex vivo* and *in vivo* assays indicate that BarA/B plays a role in the virulence of *A. baumannii* ATCC 19606^T and that efficient secretion of acinetobactin is needed for persistence in the presence of human epithelial cells and killing of *G. mellonella* caterpillars.

Figure 8. The role of BarA/B in virulence. (A) Persistence of *A. baumannii* in the presence of A549 monolayers. Bacteria (10^3) were added to 95% confluent monolayer maintained in mHBSS. The bacterial counts are represented as the ratio between the CFU/ml of recovered bacteria and the CFU/ml of infecting bacteria after 24 h of incubation at 37°C in 5% CO_2. (B) *G. mellonella* killing assays. Caterpillars were infected with 1 x 10^4 bacteria of the ATCC 19606^T parental strain (blue), 3213 *barA/B* mutant (red) or the s1 mutant (yellow) iron-deficient isogenic derivatives. Moth death was determined daily over 6 d. Caterpillars injected with comparable volumes of PBS (black) were used as negative controls.

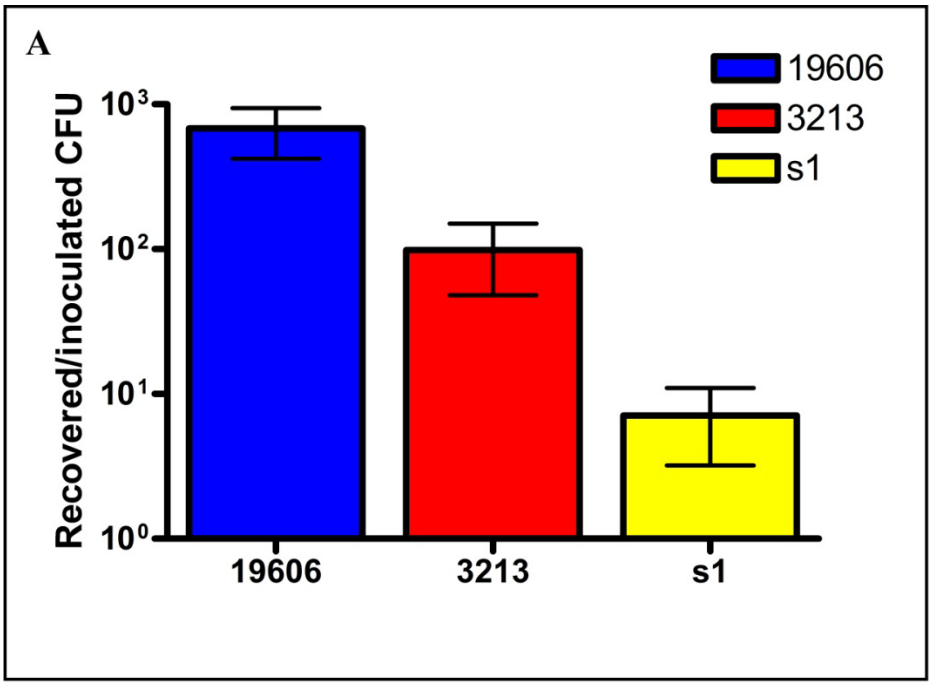
A
19606
3213
s1
Recovered/inoculated CFU
10^3
10^2
10^1
10^0
19606
3213
s1

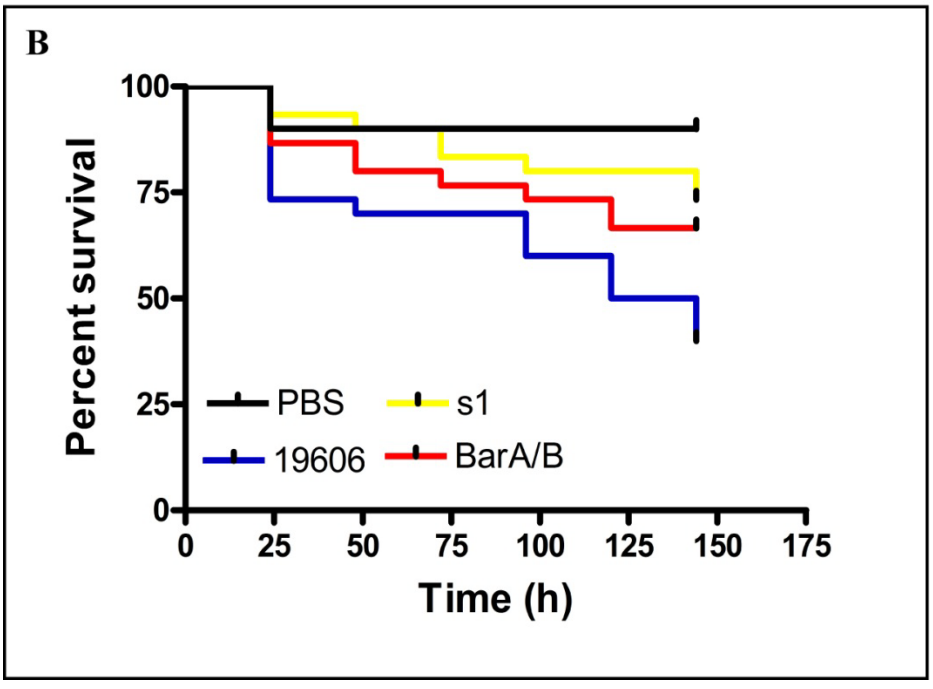
B
Percent survival
100
75
50
25
0
PBS
s1
19606
BarA/B
0
25
50
75
100
125
150
175
Time (h)

Discussion

Under iron-limiting conditions, *A. baumannii* produces the siderophore acinetobactin, which is not only important for acquiring this essential nutrient but is also needed for successful infection (51, 165). Proteins that are important in the production and uptake of acinetobactin have been examined; however, little is known about its export from the cell. Identification of two genes within the acinetobactin cluster coding for proteins with homology to ABC exporters, *barA* and *barB*, suggests that their products function in acinetobactin secretion. The *barA*/B isogenic derivative 3213 exhibited 60% less growth than the parental strain in M9 minimal medium supplemented with 100 µM DIP. The diminished growth seen in the *barA/B* mutant is not as pronounced as in the s1 mutant, whose growth was reduced by 97%. The severe growth defect of the s1 mutant in iron-chelated conditions could be attributed to the lack of acinetobactin production by this mutant, whereas the growth reduction of the 3213 isogenic derivative could be linked to reduced acinetobactin secretion (51). HPLC analysis of the culture supernatant from the 3213 *barA/B* mutant resulted in a 40% reduction of acinetobactin secreted below that of wild-type after 24 h of growth in M9 minimal medium.

The reduction in siderophore secretion by the BarA/B deficient strain could lead to an intracellular accumulation of newly synthesized acinetobactin, which has the ability to sequester iron from its own cofactors, causing deleterious effects for the cell. To prevent detrimental levels of intracellular siderophore, acinetobactin could be degraded by the cells to either an intermediate product or to precursors, such as DHBA. Interestingly, HPLC analyses did not detect increased level of acinetobactin breakdown products or precursors in the culture supernatant of the 3213 isogenic derivative. This contrasts with other mutants deficient in siderophore secretion. For example, a mutation in the MFS pump EntS from *E. coli* leads to the increased secretion of enterobactin breakdown products when grown under iron-limiting conditions (93). Perhaps an accumulation of breakdown products is not seen because non-specific export systems may pump out excess acinetobactin, thus limiting harmful effects associated with an increased intracellular concentration of siderophore. However, we cannot rule out the possibility that feedback inhibition prevents the accumulation of intracellular acinetobactin to detrimental levels, which has also been speculated with other siderophore secretion mutants.

The discovery of a reduction in as opposed to a complete lack of acinetobactin secretion was unanticipated, as previous reports have indicated that mutations in other ABC exporters involving siderophore secretion resulted in either a severe reduction in or a complete loss of siderophore secretion. Previous reports demonstrated that a mutation in the pyoverdine export protein PvdE in *P. aeruginosa* resulted in a severe decrease in efflux of pyoverdine from the cytoplasm to the periplasmic space (105). A complete absence of salmochelin was observed in IroC-deficient *S. enterica* serovar Typhimurium isogenic derivative (106). Tolmasky *et al*. (170) also demonstrated that a disruption in ORF14, a BarA homolog, in *V. anguillarum* 775 strain resulted in a severe iron acquisition deficiency due to the lack of anguibactin production.

Conceivably, the difference in phenotypes between the *A. baumannii* BarA/B mutant and the *V. anguillarum* ORF14 mutant could be attributed to secretion of some acinetobactin by non-specific export systems, such as those associated with antibiotic resistance. These systems are more prevalent in *A. baumannii*, possibly helping this nosocomial pathogen persist in a hospital setting, which is in contrast to the susceptible fish pathogen, *V. anguillarum* (7, 193, 194). Genomes from several different isolates indicate that *A. baumannii* has a large number of efflux genes. Strains differ in their content of efflux proteins from different classes of exporters, which include 30 MFS family, 8 ABC family, 7 resistance-nodulation-division (RND) family, and 26 multidrug and toxic compound extrusion (MATE) protein families (195, 196). The high abundance of efflux pumps might contribute to the resistance to a broad range of antibiotics, a virulence factor which has allowed *A. baumannii* to become a highly prevalent pathogen. The RND exporters, AdeABC, AdeFGH and AdeJKL, have been experimentally proven to secrete a broad range of antibiotics, dyes, and detergents (197-200). All three systems are present in ATCC 19606^{T}, and further investigation is needed to determine if any of the above mentioned export systems are involved in acinetobactin secretion (197). Another possible explanation for a reduction in but not a loss of acinetobactin secretion is that acinetobactin might be secreted by another exporter. One candidate is the MFS efflux protein AedD, which belongs to the drug: H^{+} antiporter 2 (DHA2) family of exporters (201). In *A. baylyi* ADP1 and *A. baumannii*, AedD is found within a genetic cluster that encodes proteins involved in the biosynthesis and utilization of an uncharacterized hydroxamate siderophore, and AedD is annotated as a MFS protein involved in secretion of this siderophore (see chapter 3) (150, 151, 201), and has similarity to the YhcA export protein from *Erwinia chrysanthemi*, which is an MFS pump experimentally

demonstrated to be involved in the secretion of achromobactin (201, 202). Genes coding for this uncharacterized hydroxamate siderophore are present in the ATCC 19606^T strain but the growth defect of the s1 derivative confirms that acinetobactin is the only siderophore produced (51).

The inability of the *A. baumannii* 3213 *barA/B* mutant to achieve a virulence phenotype that is statistically distinguishable from that of the wild-type in the complex hemolymph of *G. mellonella* contrasts with the statistical difference seen with the A549 persistence assay. This difference could be explained in part by the presence of a greater pool of extracellular host iron-binding proteins in the hemolymph of the caterpillar, which could lead to more efficient loading of apo-acinetobactin prior to dilution in the extracellular milieu. This would allow for a higher concentration of ferric-acinetobactin complexes in proximity to the bacterium and a greater likelihood of binding to the BauA acinetobactin receptor. Despite the potential of iron reserves like transferrin found in the hemolymph (203), the 3213 *barA/B* isogenic derivative still killed 50% less caterpillars than the wild-type and *G. mellonella* death after injection with the *barA/B* mutant is also statistically indistinguishable from *G. mellonella* killing after injection with PBS. These results suggest that the BarA/B complex is needed for efficient export of acinetobactin within the caterpillar. It is important to note that in this *in vivo* model, the s1 derivative was significantly different in the killing of injected caterpillars compared to the parental strain, which contradicts previous reports that show this derivative is approaching significance (165). Nevertheless, both reports confirm the fact that ATCC 19606^T needs a fully functioning acinetobactin-mediated system to cause a successful infection, as has been demonstrated with both *G. mellonella* and mouse sepsis models (165).

Taken together, these results demonstrate that the BarA/B proteins are needed for efficient secretion of acinetobactin. BarA/B also may require additional components to secrete acinetobactin from the cytoplasm to the extracellular milieu. ABC transporters interact with a periplasmic linker protein, known as membrane fusion protein (MFP), which connects the cytoplasmic membrane proteins to an outer membrane channel (204). These genes are not proximal to the acinetobactin cluster and are located in a different chromosomal region. It is also possible that acinetobactin is secreted from the cell in a two-step process, in which BarA/B is needed for secretion into the periplasmic space and another export system is responsible for efflux from the periplasmic space to the extracellular milieu. A similar two-step siderophore secretion process has been demonstrated for the *P. aeruginosa* efflux pump PvdE (105), which is

needed for secretion of pyoverdine to the periplasmic space. The PvdRT-OpmQ export system, which has similarities to an ABC transporter system, is needed for secretion from the periplasmic space to the extracellular milieu (105, 110). It is possible that one of the many efflux pumps encoded in the *A. baumannii* genome could have a similar function and work in combination with BarA/B to secrete acinetobactin from the cell.

In conclusion, our findings provide evidence that BarA and BarB are involved in the secretion of acinetobactin from *A. baumannii* ATCC 19606^{T}. These results not only provide additional information about the acinetobactin-mediated siderophore system, but also indicate that alternative secretion pathways may exist for acinetobactin secretion in *A. baumannii*. Further research is needed to identify these other acinetobactin efflux pumps, which would broaden our current understanding on the mechanisms involved in siderophore secretion. Understanding all mechanisms involved in acinetobactin secretion may lead to new therapeutic targets to help treat infections caused by multidrug-resistant *A. baumannii*.

Chapter 3

The *Acinetobacter baumannii entA* gene located outside the acinetobactin cluster is critical for siderophore production, iron acquisition and virulence

William F. Penwell, Brock A. Arivett and Luis A. Actis

© PlosOne 2012. Vol. **7** (5): e36493

Abstract

Acinetobacter baumannii causes severe infections in compromised patients, who present an iron-limited environment that controls bacterial growth. This pathogen has responded to this restriction by expressing high-affinity iron acquisition systems including that mediated by the siderophore acinetobactin. Gene cloning, functional assays and biochemical tests showed that the *A. baumannii* genome contains a single functional copy of an *entA* ortholog. This gene, which is essential for the biosynthesis of the acinetobactin precursor 2,3-dihydroxybenzoic acid (DHBA), locates outside of the acinetobactin gene cluster, which otherwise harbors all genes needed for acinetobactin biosynthesis, export and transport. *In silico* analyses and genetic complementation tests showed that *entA* locates next to an *entB* ortholog, which codes for a putative protein that contains the isochorismatase lyase domain, which is needed for DHBA biosynthesis from isochorismic acid, but lacks the aryl carrier protein domain, which is needed for tethering activated DHBA and completion of siderophore biosynthesis. Thus, *basF*, which locates within the acinetobactin gene cluster, is the only fully functional *entB* ortholog present in ATCC 19606^{T}. The differences in amino acid length and sequences between these two EntB orthologs and the differences in the genetic context within which the *entA* and *entB* genes are found in different *A. baumannii* isolates indicate that they were acquired from different sources by horizontal transfer. Interestingly, the AYE strain proved to be a natural *entA* mutant capable of acquiring iron through an uncharacterized siderophore-mediated system, an observation that underlines the ability of different *A. baumannii* isolates to acquire iron using different systems. Finally, experimental infections using *in vivo* and *ex vivo* models demonstrate the role of DHBA and acinetobactin intermediates in the virulence of the ATCC 19606^{T} cells, although to a lesser extent when compared to the responses obtained with bacteria producing and using fully matured acinetobactin to acquire iron.

Introduction

Acinetobacter baumannii is being increasingly recognized as an important pathogen that causes severe infections in hospitalized patients as well as deadly cases of community-acquired pneumonia (7, 8, 205, 206). More recently, it has been described as the etiological agent of severe wound infections in military personnel injured in the Middle East (22, 207) and cases of necrotizing fasciitis (20). A serious concern with this pathogen is its remarkable ability to acquire genes and express resistance to a wide range of antibiotics as well as to evade the human defense responses (7). Among the latter is the capacity of *A. baumannii* to prosper under the iron-limited conditions imposed by the human host's high-affinity chelators lactoferrin and transferrin (208, 209). Although some progress has been made in recent years, not much is known about the pathobiology of this bacterium and the nature of its virulence factors involved in the serious diseases it causes in humans.

Bacterial pathogens respond to iron limitation imposed by the human host by expressing different high-affinity uptake systems including siderophore-dependent and siderophore-independent systems, as well as systems that remove iron from host compounds, such as hemin, by either direct contact or by producing scavengers known as hemophores (58, 210). In the case of *A. baumannii*, experimental data (51, 148, 149, 211) and *in silico* analyses of fully sequenced and annotated genomes (150, 212) show that different *A. baumannii* clinical isolates could express different iron uptake systems. Currently, the best-characterized system is that expressed by the ATCC 19606^T type strain, which is based on the production and utilization of acinetobactin (51, 52, 171). This catechol-hydroxamate siderophore is a non-cyclic derivative of 2,3-dihydroxybenzoic acid (DHBA) linked to threonine and *N*-hydroxyhistamine (171). Genetic and functional analyses indicate that the acinetobactin-mediated system is the only high-affinity iron acquisition system expressed by the ATCC 19606^T type strain (51). The *bas*, *bau* and *bar* genes needed for the production, transport and secretion of acinetobactin, respectively, are located in a 26.5-kb chromosomal region harboring seven operons (51, 52). However, this locus does not include an *entA* ortholog coding for a 2,3-dihydro-2,3-dihydroxy-benzoate dehydrogenase. This enzyme is involved in the last step of the conversion of chorismate into DHBA, which is essential for the biosynthesis of the catechol moiety of siderophores such as enterobactin (213, 214). This observation indicates that at least two chromosomal regions are involved in the biosynthesis of acinetobactin in the ATCC 19606^T strain; one containing the *bas*,

bau and *bar* genes and another harboring at least the *entA* gene. In this report, we present experimental and genomic evidence supporting this hypothesis as well as showing that there are variations not only in nucleotide sequence but also in genetic arrangements among the *A. baumannii* loci harboring the *entA* genetic determinant. In addition, we demonstrate that the expression of an active *entA* gene is needed for the full virulence of the ATCC 19606^T strain when tested using A549 human alveolar epithelial cells and *Galleria mellonella* caterpillars as experimental infection models. We also report the observation that the *A. baumannii* AYE strain is a natural *entA* mutant that acquires iron through a siderophore-mediated system that remains to be characterized.

Materials and Methods

Bacterial strains, plasmids, and culture conditions

Bacterial strains and plasmids used in this work are shown in Table 4. Strains were routinely cultured in Luria Bertani (LB) broth or agar (172) at 37ºC in the presence of appropriate antibiotics. Iron-rich and iron-limiting conditions were achieved by the addition of $FeCl_3$ dissolved in 0.01M HCl and 2,2' dipyridyl (DIP), respectively, to liquid or solid media.

Recombinant DNA techniques

Chromosomal and plasmid DNA were isolated by ultracentrifugation in CsCl density gradients (172, 176) or using commercial kits (Qiagen). DNA restriction and Southern blot analyses were conducted using standard protocols and [^{32}P]a-dCTP-labelled probes prepared as described before (172, 215).

Construction of a gene library and cloning of the *entA* gene

An *A. baumannii* ATCC 19606^T genomic library was prepared using *Escherichia coli* LE392 and the cosmid vector pVK100 as described before (149). Cosmid DNA was isolated *en masse* from *E. coli* LE392 clones and used to transform *E. coli* AN193 by electroporation as described before (149). Transformants harboring the ATCC 19606^T *entA* genes were selected on LB agar containing 20 µg/ml tetracycline (Tet) and 250 µM DIP. Cosmid DNA was isolated from one of the *E. coli* AN193 complemented clones, which was named 2631, digested with

Table 4. Bacterial strains and plasmids used in this work.

Strain/plasmid	Relevant characteristics[a]	Source/reference
Strains		
A. baumannii		
ATCC 19606^T	Nosocomial isolate	ATCC
ATCC 19606^T s1	ATCC 19606^T *basD* mutant, Km^R	(51)
ATCC 19606^T 3069	ATCC 19606^T *entA* mutant, Km^R	This work
ATCC 19606^T 3069.C	ATCC 19606^T 3069 harboring pMU951	This work
ATCC 19606^T 3069.E	ATCC 19606^T 3069 harboring pWH1266	This work
ATCC 17978	Nosocomial isolate	ATCC
AYE	Nosocomial isolate	(216)
E. coli		
LE392	Used for *in vitro* DNA packaging	(217)
DH5α	Used for recombinant DNA methods	Gibco-BRL
AB1515	*purE42*, *proC14*, *leu-6*, *trpE38*, *thi-1*, *fhuA23*, *lacYl*, *mtl-l*, *xyl-5*, *rpsL109*, *azi-6*, *tsx-67*	CGSC[b]
AN192	*entB* mutant of AB1515	(218)
AN192-3170	AN192 harboring pMU964	This work
AN192-3171	AN192 harboring pMU925	This work
AN193	*entA* mutant	C. Earhart
AN193-2631	AN193 harboring pMU711	This work
AN193-2942	AN193 harboring pMU748	This work
AN193-2943	AN193 harboring pMU804	This work
AN193-2944	AN193 harboring pMU807	This work
AN193-3101	AN193 harboring pMU858	This work
AN193-3172	AN193 harboring pMU925	This work
AN193-3179	AN193 harboring pMU968	This work
S. typhimurium		
enb-7	Uses DHBA to produce enterobactin and grow under iron-chelated conditions	(219)
Plasmids		
pVK100	Cosmid cloning vector, Tet^R, Km^R	(220)
pUC118	Cloning vector, *Hin*dIII/BAP, Amp^R	Takara
pUC4K	Source of Km^R DNA cassette, Amp^R, Km^R	Pharmacia
PCR-Blunt	PCR cloning vector, Km^R, Zeo^R	Invitrogen
PCR8/GW/TOPO	PCR cloning vector, Sp^R	Invitrogen
pEX100T	Mobilizable suicide plasmid in ATCC 19606^T, Amp^R	ATCC
pWH1266	*E. coli-A. baumannii* shuttle cloning vector, Amp^R, Tet^R	(221)
pMU711	pVK100 harboring the 19606^T *entA* gene, Tet^R, Km^R	This work

pMU748	pUC118 with a 2.7-kb *Hin*dIII fragment from pMU711 harboring *entA*, *modB*, *modC* and the 3'end of *modA*, Amp^R	This work
pMU804	PCR8/GW/TOPO harboring the ATCC 17978 *entA* and *entB* genes, Sp^R	This work
pMU807	*entA*::EZ-Tn*5*<KAN-2> derivative of pMU804, Sp^R, Km^R	This work
pMU858	pMU748 derivative with ATCC 19606^T *entA*::*aph* insertion, Amp^R, Km^R	This work
pMU902	pEX100T with a 1.2 kb amplicon harboring *entA*::*aph,* Amp^R, Km^R	This work
pMU925	PCR-Blunt derivative harboring the ATCC 19606^T *entA* and *entB* genes, Km^R	This work
pMU951	pWH1266 harboring the ATCC 19606^T *entA* allele, Amp^R	This work
pMU964	PCR-Blunt derivative harboring the ATCC 19606^T *basF* gene, Km^R	This work
pMU968	PCR-Blunt derivative harboring the AYE chromosomal region encompassing the predicted *entA*-*entB* orthologs, Km^R	This work

[a]Amp, ampicillin; Km, kanamycin; Sp, spectinomycin; Tet, tetracycline; Zeo, zeocin; R, resistance/resistant. [b]CGSC, Coli Genetic Stock Center, Yale University, New Haven, Conn

Figure 9. Genetic organization of *A. baumannii* chromosomal regions harboring genes coding for siderophore production and utilization. (A) Genetic map of the ATCC 19606^T gene cluster containing the *entA* and *entB* orthologs. H, *Hin*dIII; E, *Eco*RI. (B) Genetic map of the ATCC 17978 gene cluster that includes the predicted *entA* and *entB* orthologs. The horizontal arrows and their direction indicate the location and direction of transcription of predicted genes, respectively. The horizontal lines indicate the chromosomal regions either cloned or used to confirm recombinant derivatives by PCR or Southern blotting. The numbers next to each bar indicate the location of primers used in PCR amplification. The vertical arrows indicate the insertion of the DNA cassette harboring the *aph* gene, which code for kanamycin resistance, or the EZ-Tn*5*<KAN-2> transposon (Tn). Numbers under ORFs shown in panel B correspond to those listed in Table 6. Numbers on top of short vertical bars indicate DNA size in kb.

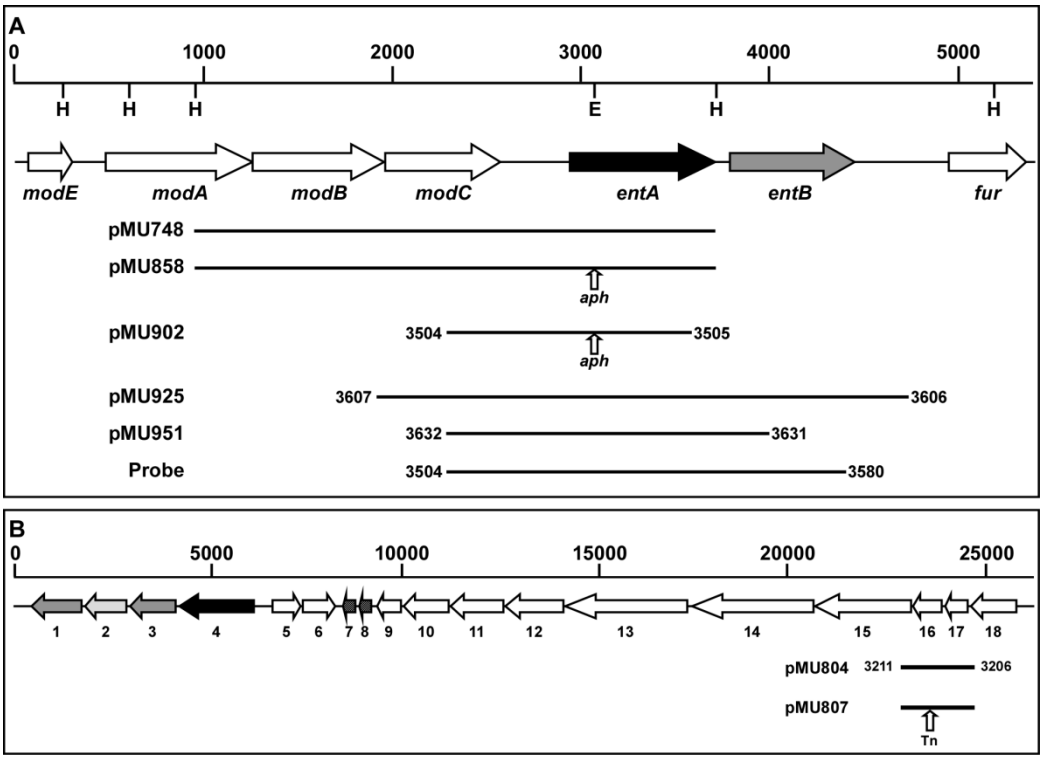
A
0
1000
2000
3000
4000
5000
H
H
H
E
H
H
modE
modA
modB
modC
entA
entB
fur
pMU748
pMU858
aph
pMU902
3504
3505
aph
pMU925
3607
3606
pMU951
3632
3631
Probe
3504
3580
B
0
5000
10000
15000
20000
25000
1
2
3
4
5
6
7
8
9
10
11
12
13
14
15
16
17
18
pMU804
3211
3206
pMU807
Tn

*Hin*dIII and subcloned into pUC118 to generate pMU748 (Fig. 9A). Plasmid DNA was isolated from *E. coli* DH5α recombinant subclones and sequenced with standard automated DNA sequencing methods using M13 forward and reverse (222) and custom-designed primers. Sequences were assembled using Sequencher 4.2 (Gene Codes Corp.). Nucleotide and amino acid sequences were analyzed with DNASTAR, BLAST (223), and the software available through the ExPASy Molecular Biology Server (http://www.expasy.ch).

Construction of an ATCC 19606^T *entA*::*aph* isogenic derivative

To generate the ATCC 19606^T *entA*::*aph* insertion mutant 3069, a 2.5-kb pMU858 fragment, which encompasses the pUC4K DNA cassette inserted into an *Eco*RV site located within *entA*, was PCR amplified with primers 3504 (5'-CCAACAAGAACGTCACTT-3') and 3505 (5'-ATTCCTGTTCGGTACTGG-3') (Fig. 9A) and Phusion DNA polymerase (NEB). The amplicon was cloned into the SmaI site of the pEX100T and *E. coli* DH5α transformants were selected on LB agar containing 40 mg/ml kanamycin (Km) and 150 mg/ml ampicillin (Amp). Plasmid DNA (pMU902) was isolated from one of these derivatives and the appropriate cloning was confirmed by automated sequencing using primers 3187 (5'-AGGCTGCGCAACTGTTGG-3') and 3188 (5'-TTAGCTCACTCATTAGGC-3'), which anneal close to the pEX100T SmaI site. ATCC 19606^T cells were electroporated with pMU902 as described before (224) recovering the cells in SOC medium (172) for 6 h in a shaking incubator at 37°C. Transformants were selected on LB agar containing 40 mg/ml Km. The generation of the appropriate ATCC 19606^T *entA*::*aph* derivative was confirmed by PCR using primers 3504 and 3580 (5'-CCATGCTTGGATTACTTG-3') (Fig. 9A) as well as Southern blotting (172) using as a probe the amplicon obtained with primers 3504 and 3580 (Fig. 9A) and parental DNA as a template. The ATCC 19606^T 3069 derivative was genetically complemented with pMU951 (Fig. 9A), a derivative of the shuttle vector pWH1266 harboring an amplicon encompassing the parental *entA* allele that was obtained with Phusion DNA polymerase using primers 3631 (5'-GGATCCGGGAATATTAGACTGGCG-3') and 3632 (5'-GGATCCCCAACAAGAACGTCACTT-3'), both of which included *BamHI* restriction sites.

Production and utilization of catechol and siderophore compounds and expression of EntA and EntB activity by cloned genes

A. baumannii cells were cultured in a chemically defined medium containing sodium succinate as a carbon source (171). Production of extracellular compounds with siderophore activity was investigated with the Chrome Azurol S (CAS) reagent (225). The presence of catechol compounds in cell-free succinate culture supernatants (171) was detected with the Arnow test (185). Briefly, 1 volume of reagent A (0.5 N HCl), reagent B (10% $NaNO_3$, $NaMoO_4$), and reagent C (1 N NaOH) were successively added to 1 volume of culture supernatant cleared by centrifugation at 16,000 x *g*. The reaction was measure by determining OD_{510} after 10 min incubation at room temperature. DHBA (Sigma-Aldrich) was used as a standard in chemical and biological assays. Production of DHBA was biologically examined with cross-feeding assays using the *Salmonella typhimurium enb*-7 enterobactin mutant as previously described (211). Minimal inhibitory concentrations (MICs) of DIP, which were repeated at least three times in duplicate each time, were determined using M9 minimal medium (175) containing increasing concentrations of DIP. OD_{600} was used to monitor cell growth after overnight incubation at 37ºC. Expression of EntA and EntB activity of cloned DNA was tested by transforming the *E. coli* AN193 and *E. coli* AN192 mutants with pMU925, which was obtained by PCR amplification and cloning of the ATCC 19606^T genomic region encompassing the predicted *entA* and *entB* genes with primers 3606 (5'-GAACTGAACCATATGGCG-3') and 3607 (5'-CGCAGTGGTTTCATCGTT-3') (Fig 9A). The same set of primers were used to PCR clone the cognate chromosomal region from the AYE clinical isolate to generate the derivative pMU968. Primers 3206 (5'-CGCAGGCATCGTAAAGGG-3') and 3211 (5'-TCTGCACAGCATCAACCG-3') were used to PCR amplify and clone the ATCC 17978 *entA* and *entB* orthologs (pMU804) (Fig. 9B).

The genetic nature of the *entB* deficient phenotype of *E. coli* AN192 was examined by automated DNA sequencing of amplicons obtained using the primers 3783 (5'-CGTGAACAGGGTATTGCC- 3') and 3785 (5'-CAGCTAACAGTCGCTGAC-3') and chromosomal DNA obtained from this mutant and the parental strain AB1515 (218) as templates. PCR sequencing reactions were done using primers 3783, 3785, 3784 (5'-CCTTTGAACCGCAACGTG-3'), 3786 (5'-CGATATCACCATGCACTT), 3792 (5'-CACATTGGCTGTATGACC-3'), and 3793 (5'-CTCCAGCGGAGAACGATG-3').

Production of DHBA and acinetobactin was examined by HPLC analysis with an Agilent 1100 LC instrument using succinate culture supernatants filtered with 0.45 µm cellulose acetate filter units (Spin-x centrifuge filter units, Costar, Cambridge, MA). Supernatants were fractionated with a Vydac C-8, 5 mm, 250 mm x 4.6 mm reversed-phase column (Grace Davison Discovery Sciences, Deerfield, IL). Water and acetonitrile containing 0.13% and 0.1% trifluoroacetic acid, respectively, were used as mobile phases. The gradient was as follows: 17% acetonitrile for 5 min and then from 17% to 30% within 30 min, and thereafter held for 15 min. Detection was at 317 nm with a flow rate of 0.5 ml/min.

A549 infection assays

A549 human alveolar epithelial cells (187), which were provided by Dr. E. Lafontaine (College of Veterinary Medicine, University of Georgia, USA) were cultured and maintained in DMEM supplemented with 10% heat-inactivated fetal bovine serum at 37°C in the presence of 5% CO_2 as previously described (44). A549 monolayers maintained in modified Hank's balanced salt solution (mHBSS, same as HBSS but without glucose) for 24 h at 37°C in 5% CO_2 without infection remained viable as determined by trypan blue exclusion assays. 24-well tissue culture plates were seeded with approximately 10^4 epithelial cells per well and then incubated for 16 h. Bacterial cells were grown 24 hr in LB broth at 37ºC with shaking at 200 rpm, collected by centrifugation at 15,000 rpm for 10 min, washed, resuspended, and diluted in mHBSS. The A549 monolayers were singly infected with 10^3 cells of the ATCC 19606^T parental strain, the S1 (*basD*) or 3069 (*entA*) isogenic derivatives. Inocula were estimated spectrophotometrically at OD_{600} and confirmed by plate count. Infected monolayers were incubated 24 h in mHBSS at 37°C in 5% CO_2. The tissue culture supernatants were collected, the A549 monolayers were lysed with sterile distilled H_2O and lysates were added to the cognate tissue culture supernatants. Bacteria were collected from the resulting suspensions by centrifugation, resuspended in 1 ml sterile distilled H_2O, serially diluted and then plated on nutrient agar. After overnight incubation at 37ºC, the colony forming units (CFUs) were counted and CFU/ml values for each sample were calculated and recorded. Counts were compared using the Student's t-test; P values < 0.05 were considered significant. Experiments were done four times in triplicate using fresh biological samples each time. To determine bacterial relative fitness, the recovered CFUs were divided by the CFUs of the inoculum used to infect monolayers.

***G. mellonella* killing assays**

Bacteria grown in LB broth were collected by centrifugation and suspended in phosphate-buffered saline solution (PBS). The number of bacteria was estimated spectrophotometrically at OD_{600} and diluted in PBS to appropriate concentrations. All bacterial inocula were confirmed by plating serial dilutions on LB agar and determining colony counts after overnight incubation at 37°C. Ten freshly-received final-instar *G. mellonella* larvae (Grubco, Fairfield, OH) weighing 250-350 mg were randomly selected and used in killing assays as described previously (189). Briefly, the hemocoel at the last left proleg was injected with 5-µl inocula containing 1×10^5 bacteria ± 0.25 log of each tested strain using a syringe pump (New Era Pump Systems, Inc., Wantagh, NY) with a 26 G½ needle. Each test series included control groups of non-injected larvae or larvae injected with sterile PBS or PBS containing 100 µM $FeCl_3$. The test groups included larvae infected with the parental strain ATCC 19606^T, the s1 *basD* mutant or the 3069 *entA* insertion derivative, which were injected in the absence or presence of 100 µM $FeCl_3$. Injected larvae were incubated at 37°C in darkness, assessing death at 24-h intervals over six days. Larvae were considered dead and removed if they did not respond to probing. Results were not considered if more than two deaths occurred in the control groups. Experiments were repeated three times using 10 larvae per experimental group and the survival curves were plotted using the Kaplan-Meier method (190). *P* values < 0.05 were considered statistically significant for the log-rank test of survival curves (SAS Institute Inc., Cary, NC).

Results and Discussion

The acinetobactin locus in different *A. baumannii* strains

Previous reports described a 26.5-kb *A. baumannii* ATCC 19606^T chromosomal gene cluster involved in acinetobactin production and utilization (51, 52). Table 5 shows that the same *bas-bau-bar* 18-gene cluster, recently referred to as the acinetobactin gene cluster (150), is also found in *A. baumannii* AYE (216). In contrast, the cognate clusters in strains AB0057 and ACICU include the additional putative genes AB57_2807 and AB57_2818 (226), and ACICU_02575 and ACICU_02586 (227), respectively. Furthermore, the *A. baumannii* AB307-294 *bas-bau-bar* gene cluster has three additional predicted genes; ABBFA_001054, ABBFA_001053, and ABBFA_001065 (226). It is not clear whether these additional coding units are the result of sequencing and/or annotation artifacts and their potential role in siderophore production and utilization remains to be tested considering that most of them (AB57_2807, AB57_2818, ACICU_02575, ACICU_02586, ABBFA_001054 and ABBFA_001065) code for polypeptides containing 43 to 51 amino acid residues. Similarly, the annotation of the ATCC 17978 *bas-bau-bar* gene cluster (153) encompasses 21 rather than 18 predicted genes because of potential nucleotide sequencing errors (Table 5). The products of coding regions A1S_2382 and A1S_2383 are highly related to the BasD predicted protein, while the products of the A1S_2376-A1S_2378 coding regions highly match that of the *barA* gene originally described in the ATCC 19606^T type strain (52). Unfortunately, these errors were also included in a recent report analyzing potential iron acquisition functions expressed by *A. baumannii* using bioinformatics (150).

In spite of all these differences, a common feature of the *bas-bau-bar* gene cluster present in all these strains is the absence of an *entA* gene coding for a 2,3-dihydro-2,3-dihydroxybenzoate dehydrogenase needed for the biosynthesis of DHBA, which is a precursor needed for the production of catechol siderophores, such as enterobactin (214). This observation indicates that a second locus must contain the *entA* ortholog, a possibility that is supported by our initial finding that the genome of the *A. baumannii* ATCC 17978 strain has an additional gene cluster (Table 6) potentially involved in siderophore biosynthesis and utilization (53). The coding region A1S_2579 of this cluster, which was identified as cluster 2 (150), was annotated as a putative *entA* ortholog (153). However, initial BLAST searches using A1S_2579 as a query did.

Table 5. Components of the *bas-bau-bar* gene cluster in different *A. baumannii* genomes.

Strain	Annotated coding regions	Additional coding regions[a]	Accession #
19606[T]	BAC87896-BAC87913	NA[b]	AB101202
AYE	ABAYE1087-ABAYE1104	None	NC_010410
AB0057	AB57_2802-AB57_2822	2807/2818	NC_011586.1
ACICU	ACICU_02570-ACICU_02589	02575/02586	NC_010611.1
AB307-294	ABBFA_001050-ABBFA_001070	001054-001053/001065	NC_011595.1
17978	A1S_2372-A1S_2392	2382-2383[c]/2376-2378[d]	NC_009085.1

[a]Additional coding regions compared to the ATCC 19606 *bas-bau-bar* gene cluster. Numbers should be preceded by the cognate letters and underscore symbols. [b]Not applicable. [c]*basD*-related coding sequences. [d]*barA*-related coding sequences.

Table 6. Revised annotation of the *A. baumannii* ATCC 17978 A1S_2562-A1S_2581 gene cluster.

Coding region #[a]	Annotated coding region[b]	Predicted function[c]
1	A1S_2562	MDR efflux pump protein
2	A1S_2563/ A1S_2564	Siderophore interacting protein
3	A1S_2565	MFS family transport protein
4	A1S_2566	Ferric siderophore receptor protein
5	A1S_2567	Thioesterase
6	A1S_2568	Phosphopantetheinyl transferase
7	Omitted	Transposase fragment
8	A1S_2569	Transposase fragment
9	A1S_2570	Acetyltransferase
10	A1S_2571	Ornithine decarboxylase
11	A1S_2572	Lysine/ornithine monooxygenese
12	A1S_2573/A1S_2574	2,3 DHB-AMP ligase
13	A1S_2575	Nonribosomal peptide synthetase
14	A1S_2576/A1S_2577	Nonribosomal peptide synthetase
15	A1S_2578	Nonribosomal peptide synthetase
16	A1S_2579	2,3 DHB-2,3-dehydrogenase
17	A1S_2580	Isochorismatase
18	A1S_2581	Isochorismate synthetase

[a]Numbers correspond to coding regions shown in Fig 9B. [b]Coding regions reported by Smith et al. (153) and deposited in GenBank under accession number NC_009085.1. [c]MDR, Multidrug Resistance; MFS, Major Facilitator Superfamily; DHB, dihydroxybenzoate.

not identified *entA* orthologs as top matches in any of the fully sequenced and annotated *A baumannii* genomes and the ATCC 19606^T partial genomic data (GenBank accession number NZ_ACQB00000000.1) deposited in GenBank by the Broad Institute as part of the Human Microbiome Project (http://www.broadinstitute.org/). Furthermore, attempts to identify the ATCC 19606^T *entA* gene by PCR amplification or Southern blotting, using ATCC 17978 genomic information to design appropriate primers and probes, failed to produce positive results (data not shown). Taken together, all these observations indicate that there are variations in the nucleotide sequence and chromosomal arrangements among the *entA* genes present in different *A. baumannii* strains.

Cloning and testing of the ATCC 19606^T *entA* gene

Since the *in silico* approach failed to locate the ATCC 19606^T *entA* gene, a functional complementation approach was applied using *E. coli* AN193, an *entA* mutant that does not produce enterobactin because of its inability to make the DHBA precursor. Transformation of this mutant with plasmid DNA isolated *en masse* from an ATCC 19606^T genomic library made in *E. coli* LE392, using the cloning cosmid vector pVK100, resulted in the isolation of the AN193-2631 derivative capable of growing in the presence of significantly higher DIP concentrations when compared with AN193 transformed with empty cloning vector. Transformation of *E. coli* AN193 with plasmid pMU711 isolated from the AN193-2631 derivative confirmed the ability of this cosmid clone to restore the iron uptake capacity of *E. coli* AN193 (data not shown). Restriction analysis of pMU711 digested with *Hin*dIII showed that it has an insert larger than 20 kb (data not shown). Subcloning into *Hin*dIII-digested pUC118 and nucleotide sequencing resulted in the identification of pMU748, which has a 2.7-kb *Hin*dIII insert (Fig. 9A). This restriction fragment harbors a 771-nucleotide gene, the nucleotide sequence of which is identical to the ATCC 19606^T HMPREF0010_00620.1 locus found in the scaffold supercont 1.1 of the whole genome sequence uploaded to GenBank by the Broad Institute under accession number NZ_GG704572. This gene codes for a 28-kDa predicted protein highly related (E values lower than 1xe^{-5}) to the EntA protein found in a wide range of bacteria, showing the top BLASTx scores with products of the cognate *A. baumannii* AB0057 (AB57_1983), AB307-294 (ABBFA_001741), and ACICU (ACICU_01790) genes (Table 7). Transformation of the *E. coli* AN193 *entA* mutant with either pMU748 (data not shown) or the PCR derivative pMU925, which includes a downstream *entB* ortholog (Fig. 9A), restored iron uptake proficiency to this derivative (Fig. 10A). The function of the ATCC 19606^T *entA* ortholog was confirmed by the observation that the AN193-3101 transformant harboring pMU858, a pUC118 *Hin*dIII subclone in which *entA* was inactivated by inserting a DNA cassette coding for Km resistance into a unique *Eco*RV site (Fig. 9A), showed a growth similar to that of untransformed *E. coli* AN193 cells when cultured in the presence of 250 μM DIP (Fig. 10A).

The role of the ATCC 19606^T *entA* ortholog in the acinetobactin-mediated iron acquisition process was confirmed further with the isogenic derivative 3069, which was generated by allelic exchange using pMU902 (Fig. 9A). This is a derivative of pEX100T, which does not replicate in ATCC 19606^T, harboring the *entA*::*aph* construct. Compared with the ATCC 19606^T parental

Figure 10. Iron acquisition phenotype of *E. coli* enterobactin deficient mutants. (A) Growth of the *E. coli* AN193 *entA* mutant harboring no plasmid or transformed with pMU925, pMU858, pMU968, pMU804 or pMU807 in LB broth in the absence or the presence of 250 µM DIP. (B) Growth of the *E. coli* AN192 *entB* mutant harboring no plasmid or transformed with pMU925 or pMU964 in LB broth in the absence or the presence of 250 µM DIP. The plasmids pMU925, pMU968 and pMU804 harbor the *entA*/*entB* orthologs cloned from ATCC 19606^T, AYE, and ATCC 17978, respectively. Plasmid pMU858 harbors an insertionally inactivated ATCC 19606^T *entA* derivative. Plasmid pMU964 harbors the ATCC 19606^T *basF* gene.

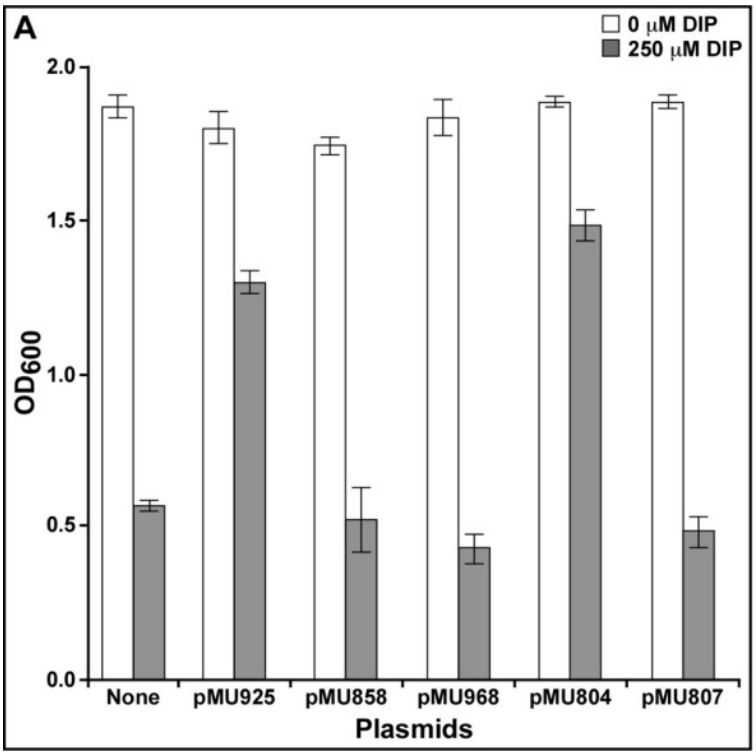
A
0 μM DIP
250 μM DIP
2.0
1.5
1.0
0.5
0.0
OD600
None
pMU925
pMU858
pMU968
pMU804
pMU807
Plasmids

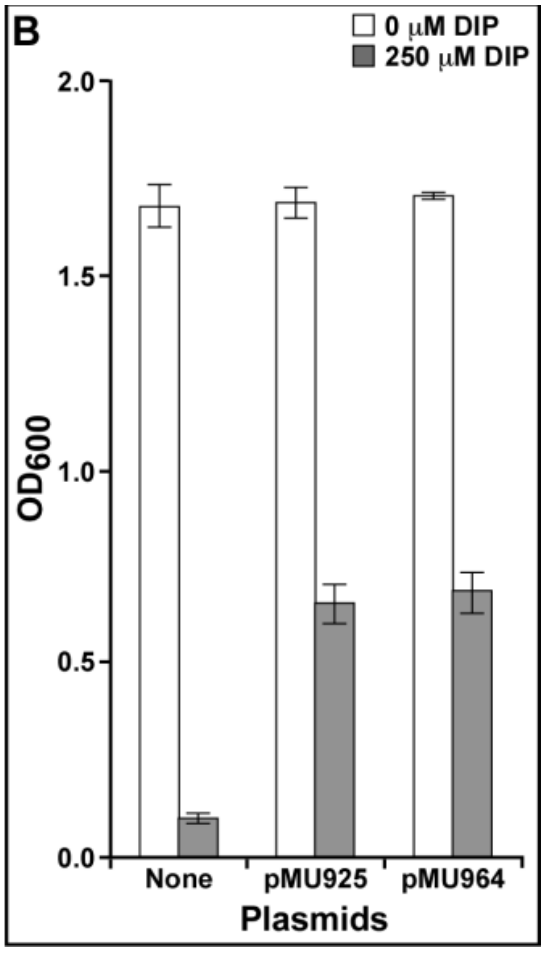
B
0 μM DIP
250 μM DIP
2.0
1.5
1.0
0.5
0.0
OD600
None
pMU925
pMU964
Plasmids

strain, the 3069 derivative, which showed the predicted genetic arrangement by PCR and Southern blotting (data not shown), displayed a drastic growth defect ($P = 0.0001$) when cultured in M9 minimal medium containing increasing DIP concentrations (Fig. 11A). This response is similar to that displayed by the ATCC 19606^T s1 mutant impaired in BasD-mediated acinetobactin biosynthesis activity (51), which was used as a control. The CAS colorimetric assay showed that while the ATCC 19606^T succinate culture supernatants tested positive, no reaction could be detected with culture supernatants of the ATCC 19606^T 3069 and s1 mutants (data not shown). Furthermore, Arnow colorimetric assays showed that 3069 cells produced drastically reduced amounts of DHBA ($P = 0.002$), which were within the detection limit of the Arnow test (Fig. 11B). This finding was supported by the lack of crossfeeding of the *S. typhimurium enb*-7 reporter mutant (Fig. 11C), which uses DHBA as a precursor to produce enterobactin and grow under iron-chelated conditions. Finally, HPLC analysis of culture supernatants of cells grown in succinate medium showed the presence of two peaks with elution times of 8.925 and 10.272 min (Fig. 11D). Although these two peaks were absent in the sterile medium as well as in the supernatant of the ATCC 19606^T 3069 mutant, they could be detected in the ATCC 19606^T 3069 sample only when it was spiked with either pure DHBA or purified acinetobactin before HPLC analysis (Fig. 11D). These observations showed that the two peaks detected in ATCC 19606^T culture supernatants indeed correspond to DHBA and mature acinetobactin. Interestingly, the chromatograms shown in Fig. 11D and Fig. 12 indicate that ATCC 19606^T cells produce and secrete a significant amount of DHBA in addition to fully matured acinetobactin. A similar analysis of s1 succinate culture supernatants showed the presence of DHBA but not fully matured acinetobactin (data not shown), a result that is in accordance with the colorimetric data shown in Fig. 11B.

Finally, the role of the ATCC 19606^T *entA* ortholog was confirmed with genetic complementation assays, which proved that electroporation of pMU951, a derivative of the shuttle vector pWH1266 harboring the *entA* wild-type allele expressed under the promoter controlling the expression of tetracycline resistance, was enough to restore the parental iron utilization phenotype in the ATCC 19606^T 3069.C derivative (Fig. 11A) as well as its capacity to produce DHBA (Fig. 11, panels B and C). This complementation was not observed with the ATCC 19606^T 3069.E derivative harboring the empty cloning vector pWH1266. Although not shown, there were no significant growth differences among the parental strain, the mutants and

Figure 11. Iron acquisition phenotype of *A. baumannii* derivatives and their capacity to produce catechol, DHBA and acinetobactin. (A) The ATCC 19606^T parental strain (19606), the s1 BasD acinetobactin synthesis mutant (s1) and the 3069 *entA* isogenic derivative harboring no plasmid (3069) or transformed with empty pWH1266 vector (3069.E) or pMU951 harboring (3069.C) were cultured in M9 minimal medium in the absence or the presence of increasing concentrations of DIP. pMU951 is a pWH1266 derivative harboring the ATCC 19606^T *entA* allele. (B) Arnow's reaction of succinate culture supernatants obtained from the strains shown in panel A. (C) Crossfeeding of the *S. typhimurium enb*-7 enterobactin deficient derivative by $FeCl_3$, distilled water or succinate culture supernatants from the ATCC 19606^T parental strain (19606) or the 3069 *entA* isogenic derivative harboring either no plasmid (3069) or pMU951 (3069.C) under iron-chelated conditions. (D) HPLC profiles of sterile succinate medium (medium) or culture supernatants from the ATCC 19606^T parental strain (19606) or the 3069 *entA* mutant (3069). Succinate culture supernatants cleared by high-speed centrifugation and filtration trough 0.45 µm cartridges were spiked with either DHBA (3069+DHBA) or purified acinetobactin (3069+Ab) immediately before HPLC analysis. The elution time for DHBA and acinetobactin are indicated on top of the cognate peaks.

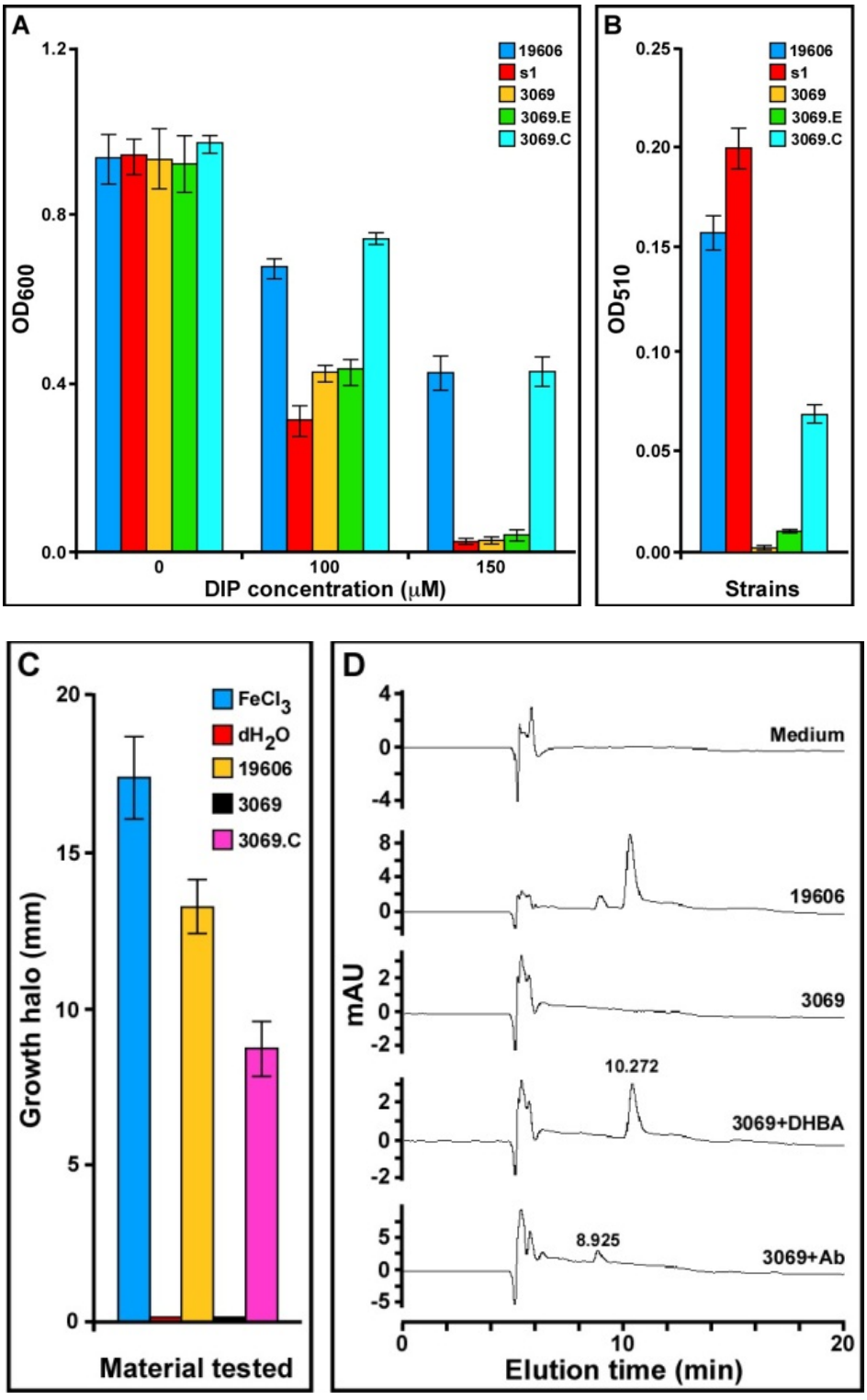
A
1.2
0.8
0.4
0.0
OD600
19606
s1
3069
3069.E
3069.C
0
100
150
DIP concentration (μM)
B
0.25
0.20
0.15
0.10
0.05
0.00
OD510
19606
s1
3069
3069.E
3069.C
Strains
C
20
15
10
5
0
Growth halo (mm)
FeCl3
dH2O
19606
3069
3069.C
Material tested
D
Medium
19606
3069
10.272
3069+DHBA
8.925
3069+Ab
mAU
0
10
20
Elution time (min)

the complemented strains used in these experiments when they were cultured in LB broth without any selection pressure. Furthermore, the plasmid pMU951 was stably maintained in the ATCC 19606^T 3069.C strain as an independent replicon without detectable rearrangements.

Taken together, all these results strongly indicate that the *entA* ortholog shown in Fig. 9A is essential for the production of DHBA, which is used by *A. baumannii* ATCC 19606^T cells as a key precursor for acinetobactin biosynthesis. The location of the *entA* gene outside the main locus involved in the biosynthesis, transport and secretion of acinetobactin resembles the arrangement of genes needed for the biosynthesis of anguibactin in the fish pathogen *V. anguillarum* 775 (228). The pJM1 plasmid present in this strain contains most of the genes coding for anguibactin biosynthesis and transport functions, including an *angA* ortholog that is inactive because of a frameshift mutation (107). Further analysis showed that the 2,3-dihydro-2,3-dihydroxy-benzoate dehydrogenase activity needed for anguibactin biosynthesis is indeed encoded by the chromosomal ortholog *vabA*, which is located within a 11-gene cluster that contains all the genetic determinants needed for the production and utilization of vanchrobactin (229). Although this system is fully active in *V. anguillarum* RV22, an O2 serotype isolate that lacks pJM1, vanchrobactin is not produced in the serotype O1 *V. anguillarum* 775 (pJM1) strain because of an RS1 transposon insertion within *vabF*. Furthermore, *in silico* analysis of the predicted product of *vabA* and *angA* loci, after virtual correction of the frameshift present in the later gene, showed that they are only 32% identical (228). These observations and the fact that the *angA* pJM1 plasmid copy is near transposable elements led to the hypothesis that transposition events resulted in the acquisition by horizontal transfer of two genes potentially coding for the same function that may have evolved independently (228). A mechanism similar to this one could also explain the location of the ATCC 19606^T *entA* gene outside the acinetobactin cluster (150), a possibility that is supported by the recent observation that *A. baumannii* has an underappreciated capacity to rearrange its genome by swapping, acquiring or deleting genes coding for a wide range of functions, including those involved in iron acquisition (230).

Our results also provide strong support to our previous report that acinetobactin is the only high-affinity siderophore produced by this strain (51), when cultured under iron-chelated laboratory conditions, although it contains genetic determinants that could code for additional iron acquisition functions as deduced from recent comparative genomic analyses (150, 212).

Considering these reports and the experimental data presented here, it is possible to speculate that the additional iron acquisition related genes present in *A. baumannii* ATCC 19606^{T} are either not expressed or do not code for complete functional iron acquisition systems and represent remnants of DNA fragments acquired from other sources by horizontal gene transfer. Such outcomes, which are currently being explored, could be due to a situation similar to that reported for the fish pathogen *V. anguillarum***,** where a vanchrobactin-producing ancestor acquired the pJM1 plasmid coding for the production and utilization of anguibactin (229). Since anguibactin is potentially a better iron chelator than vanchrobactin, evolution and adaptation processes favored the emergence of *V. anguillarum* O1 serotype strains harboring the pJM1 plasmid and producing only anguibactin because of mutations in the vanchrobactin coding genes, but capable of using both anguibactin and vanchrobactin as it is the case with the 775 (pMJ1) strain (231).

Analysis of the ATCC 19606^T chromosomal region harboring *entA* and *entB* orthologs

Sequence analysis of flanking DNA regions showed that a *modE-modA-modB-modC* gene cluster, which could code for an uncharacterized molybdenum transport system, locates upstream of ATCC 19606^T *entA* gene (Fig. 9A). Downstream, *entA* is separated by a 72-nt intergenic region from a predicted gene coding for an isochorismatase (EntB) ortholog, which is followed by a 524-nt intergenic region preceding a *fur* iron-dependent regulatory gene. The nucleotide sequence and genetic arrangement is the same as that reported for this strain by the Broad Institute Human Microbiome Project. Table 7 shows that the same gene cluster is also found in the genome of *A. baumannii* AB0057, AB307-294 and ACICU.

The predicted product of the ATCC 19606^T *entB* gene depicted in Fig. 9A showed significant amino acid sequence similarity and the same length when compared with the products of the cognate AB0057 (AB57_1984), AB307-294 (ABBFA_001740), ACICU (ACICU_01791), and AYE (ABAYE1888) genes. The product of the ATCC 19606^T *entB* ortholog is also related to that of *basF*, which is located within the acinetobactin gene cluster originally described in this strain (52). The product of *basF* is a 289-amino acid protein that contains the N-terminal isochorismatase lyase (ICL) domain, which is needed for DHBA biosynthesis from isochorismic acid, and the C-terminal aryl carrier (ArCP) protein domain, which is needed for tethering activated DHBA and chain elongation in the biosynthesis of siderophores such as enterobactin (232) and anguibactin (233). In contrast, *in silico* analysis showed that the *entB* ortholog shown in Fig 9A codes for a 213-amino acid residue protein that includes the N-terminal ICL domain but lacks the C-terminal ArCP protein domain. Based on this predicted protein structure, it is possible to speculate that this shorter EntB ortholog should code for the isochorismatase lyase activity. This possibility was examined by testing the iron-uptake proficiency of the *E. coli* AN192 *entB* mutant harboring either no plasmid or the derivatives AN192-3171 and AN192-3170 transformed with pMU925, which harbors the *entA* and *entB* genes shown in Fig. 9A, or pMU964, which harbors a copy of the *basF* gene present in the acinetobactin cluster, respectively. Fig. 10B shows that AN192-3171 (pMU925) and AN192-3170 (pMU964) grew significantly better ($P < 0.0001$ and $P = 0.0013$, respectively) than the non-transformed AN192 strain when cultured in LB broth containing 250 µM DIP. This response indicates that both ATCC 19606^T *entB* orthologs complement the *E. coli* AN1932 *entB* mutant, allowing it to produce enterobactin and grow under iron-chelated conditions. The complementation by the

Table 7. Components of the gene cluster containing the *entA-entB* genes in different *A. baumannii* genomes.

Strain	Annotated coding regions	Additional coding regions[a]	Accession #
19606^T	00624.1-00618.1[b]	NA[c]	NZ_GG704572
AB0057	AB57_1980-AB57_1985	None	NC_011586.1
AB307-294	ABBFA_001744-ABBFA_001739	None	NC_011595.1
ACICU	ACICU_01787-ACICU_01792	None	NC_010611.1
AYE	AABAYE1887-ABAYE1894	ABAYE1890	NC_010410

[a]Additional coding regions compared to the ATCC 19606^T gene cluster shown in Fig. 9A. [b]Numbers should be preceded by the annotation HMPREF0010_ according to the information presented in the *A. baumannii* Broad Institute genome site. [c]Not applicable.

BasF ortholog is straightforward since this protein contains the ICL and ArCP protein domains needed for enterobactin biosynthesis. On the other hand, the complementation by the shorter ATCC 19606^T EntB ortholog can be explained by the previous observation that the mutation in *E. coli* AN192 affects only the functionality of the ICL domain of the protein produced by this derivative that was obtained by chemical mutagenesis (218). This functional observation is further supported by our DNA sequencing data showing that the AN192 *entB* ortholog has two point mutations when compared with the parental AB1515 allele. One is a silent mutation that resulted in a G-to-A base transition at position 801 of the gene, which maps within the ArCP protein domain and produced no change in amino acid sequence. In contrast, the other mutation, which locates at position 593 and is also a G-to-A base transition, produced a Gly-to-Asp amino acid change at position 198 that maps within the ICL domain. This amino acid change, which is one residue away from Arg196 that is predicted to play a role in the interaction of the ICL domains in the functional EntB dimer protein (234), could be responsible for the lack of isochorismatase lyase in the AN192 mutant. Taken together, these results indicate that *basF*, which locates within the acinetobactin gene cluster, is the only fully functional *entB* ortholog present in the genome of the *A. baumannii* strains fully sequenced and annotated.

Considering the different genetic context in which *basF* and the *entB* ortholog shown in Fig. 9A are found in different *A. baumannii* genomes and the differences in length (289 vs. 213 amino acid residues) and amino acid composition (52.4% similarity and 40.1% identity to one another) of their predicted products, it is possible to speculate that these two genes were transferred from unrelated sources by at least two independent horizontal mechanisms, one of which may have been driven by the need of acquiring the *entA* trait required for acinetobactin biosynthesis. These observations are in agreement with the recently described capacity of *A. baumannii* to rearrange its genome content (230), as proposed above for the presence of the *entA* ortholog in a genomic region outside the acinetobactin cluster.

Analysis of the *A. baumannii* AYE *entA* ortholog

The comparative genomic analysis of the ATCC 19606^T *entA* ortholog with other *A. baumannii* sequenced genomes showed that the clinical isolate AYE also harbors the gene cluster shown in Fig. 9A, which was annotated as ABAYE1887-ABAYE1894 (216). However, this cluster contains an additional 210-nucleotide gene (ABAYE1890) (Table 7), which was not included in any of the other fully sequenced *A. baumannii* genomes. ABAYE1890 codes for a hypothetical 69-amino acid protein and overlaps by 35 nucleotides with ABAYE1889, which codes for a predicted 229-amino acid protein. Both genes were recently recognized by comparative genomic analysis as components of the siderophore biosynthesis gene cluster 5 (150). However, it is important to note that the predicted product of ABAYE1889 is 26 amino acids shorter than the putative ACICU, AB0057 and AB307-0294 EntA orthologs. This observation suggests that the *A. baumannii* AYE ABAYE1889 *entA* gene may not code for a functional product needed for the biosynthesis of DHBA and acinetobactin. This possibility was supported by the HPLC analysis of AYE succinate culture supernatants, which showed an elution profile that does not include peaks corresponding to DHBA and acinetobactin that were detected in the ATCC 19606^T culture supernatant (Fig. 12). Interestingly, AYE succinate culture supernatants promoted the growth of *S. typhimurium enb*-7 in the presence of DIP in spite of the fact that it does not produce DHBA (data not shown). This observation indicates that *A. baumannii* AYE produces an uncharacterized non-catechol-based siderophore(s) capable of promoting growth under iron-chelated conditions.

The failure of the ABAYE1889-ABAYE1890 genetic region to code for EntA activity was further confirmed by the fact that AN193-3179, a derivative transformed with pMU968 harboring the 2.8-kb AYE chromosomal region encompassing these predicted genes, grew as poorly as the non-complemented AN193 mutant when cultured in the presence of 250 µM DIP (Fig. 10A). All these results indicate that the AYE isolate is a natural *A. baumannii entA* mutant that does not make acinetobactin because of the lack of DHBA production. HPLC analysis of AYE culture supernatants of cells grown in succinate medium supplemented with 100 µM DHBA confirmed this possibility since a peak with a retention time corresponding to acinetobactin could be detected only under this experimental condition (Fig. 12).

Cloning, DNA sequencing and bioinformatic analysis of the 2.8-kb AYE chromosomal region encompassing the ABAYE1889 and ABAYE1890 genes confirmed the original genome

Figure12. HPLC profiles of sterile succinate medium (medium) or culture supernatants from the ATCC 19606^{T} parental strain (19606) or the AYE clinical isolate cultured in the absence (AYE) or the presence of 100 µM DHBA (AYE+DHBA).

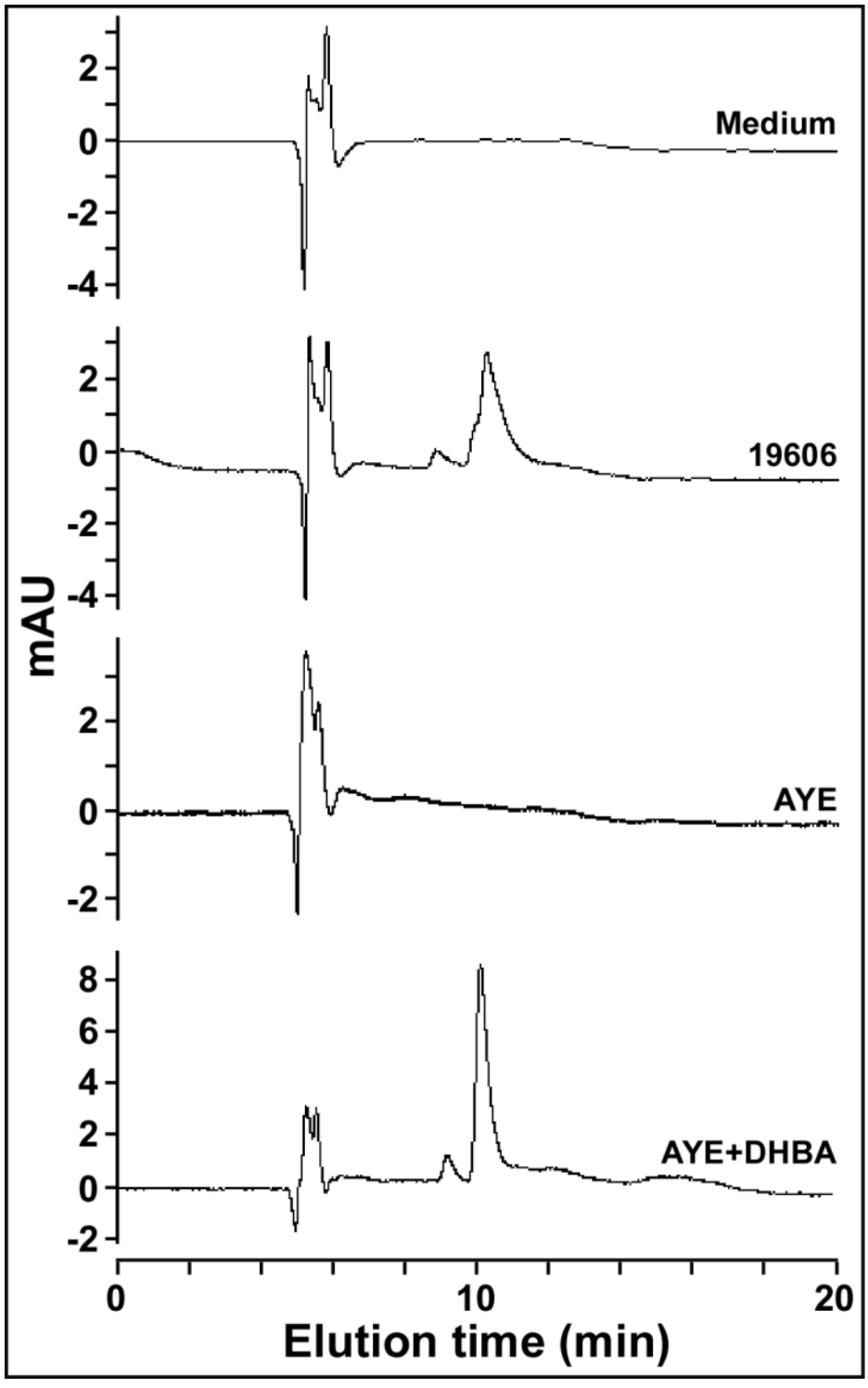
Medium
19606
AYE
AYE+DHBA
mAU
Elution time (min)
2
0
-2
-4
8
6
4
10
20

sequence report (216) and showed that the only difference between this region and the cognate regions of other *A. baumannii* chromosomes is the presence of an extra T at position 1,946,969 in the AYE genome. This single-base insertion, which could be due to DNA slippage, results in the two predicted annotated genes, neither of which code for a full-length EntA ortholog. Accordingly, *in silico* deletion of the extra T from the AYE genomic region results in a single predicted coding region, the product of which is an ortholog displaying the same number of amino acid residues predicted for the product of the ATCC 19606^T *entA* gene shown in Fig. 9A. All these results indicate that the AYE clinical isolate is a natural *entA* mutant incapable of producing acinetobactin, although this isolate tests positive with the CAS reagent. This situation could be similar to that of *V. anguillarum* 775 (pJM1) that only produces anguibactin but uses this siderophore as well as externally provided vanchrobactin to acquire iron under chelated conditions (229). This is due to the inactivation of the *vabF* vanchrobactin chromosomal gene and the possibility that anguibactin is an iron chelator stronger than vanchrobactin, a condition that does not justify the production of two siderophores. Accordingly, the production and utilization of the AYE uncharacterized siderophore, which may have a higher affinity for iron than acinetobactin, could be mediated by genes located in cluster 1 identified by *in silico* genomic analysis (150) that remain to be characterized genetically and functionally. Furthermore, preliminary siderophore utilization bioassays showed that AYE cell-free succinate culture supernatants crossfeed the ATCC 19606^T s1 (*basD*) and 3069 (*entA*) acinetobactin production deficient mutants as well as the t6 (*bauA*) acinetobactin uptake mutant. These findings indicate that *A. baumannii* AYE acquires iron through an uncharacterized siderophore, which is different from acinetobactin but can be used by ATCC 19606^T cells through acinetobactin-independent mechanisms. All these results provide evidence supporting the ability of the ATCC 19606^T strain to use xenosiderophores produced by related and unrelated bacterial pathogens.

Analysis of the ATCC 17978 chromosomal region harboring the *entA* ortholog

The ATCC 17978 A1S_2562-A1S_2581 cluster (Table 6), cluster 2 according to Eijkelkamp *et al*. (150), includes the A1S_2579 gene coding for a putative EntA ortholog (153). The role of this gene in DHBA production was confirmed by the observation that the AN193-2943 transformant harboring pMU804 (Fig. 9B) displays an iron-restricted response similar to that detected with AN193-3172 harboring pMU925, a response that was not detected with AN193-2944 harboring pMU807 (Fig. 10A). The latter plasmid is a derivative of pMU804 with a transposon insertion within the annotated *entA* (A1S_2579) coding region (Fig. 9B).

Detailed analysis of the nucleotide sequence and annotation of the A1S_2562-A1S_2581 cluster (GenBank accession number NC_009085.1) showed that because of potential DNA sequencing errors, this cluster is most likely composed of 18 predicted coding regions rather than the 20 genes originally reported (153). Fig. 9B and Table 6 show that A1S_2563 and A1S_2564 could be a single genetic unit coding for a predicted siderophore interacting protein that belongs to the ferrodoxin reductase protein family. Our DNA sequencing data, which confirmed the DNA sequence originally reported (153), and *in silico* analysis showed that there are two potential coding regions between A1S_2568 and A1S_2570 (Fig. 9B and Table 6), with one of them annotated as the A1S_2569 coding region and the other omitted in the original report. Our analysis showed that the predicted products of these two genes are truncated transposases found in a wide range of bacterial genomes including members of the *Acinetobacter* genus. We also observed that A1S_2573 and A1S_2574 most likely correspond to a single genetic unit coding for a predicted 2,3 dihydroxybenzoate-AMP ligase (EntE) (Fig. 9B and Table 6), which is needed for the activation of DHBA and further biosynthesis of DHBA-containing siderophores such as enterobactin and anguibactin (58). Nucleotide and amino acid comparative analyses also showed that the products of A1S_2573/A1S_2574, A1S_2580 and A1S_2581 are significantly related to that of the *basE*, *basF* and *basJ* genes, respectively. The products of these three genes, which work together with EntA, are needed for the biosynthesis and activation of DHBA using chorismate as a precursor. Taken together, all these observations indicate that there is a potential redundancy in the *A. baumannii* ATCC 17978 functions needed for the biosynthesis and utilization of DHBA as a siderophore precursor. In contrast, and as it was observed with the other *A. baumannii* genomes, the ATCC 17978 *entA* ortholog, which is represented by the

coding region A1S_2579 (Fig. 9B and Table 6), is a unique coding region that locates outside the *bas-bau-bar* gene cluster. Furthermore, the genetic arrangement and content of this ATCC 17978 gene cluster containing the *entA* ortholog is different from that shown in Fig. 9A and described in the genome of other *A. baumannii* strains. This observation resulted in the classification of this cluster as cluster 2 (150), which at the time that report was published was found only in the ATCC 17978 genome. However, genomic data recently uploaded into the BaumannoScope web site (https://www.genoscope.cns.fr/agc/microscope/about/collabprojects.php?P_id=8) indicate that the same gene cluster is also present in the genome of the *A. baumannii* strains 6013113 (GenBank accession number ACYR02000000.2) and 6013150 (GenBank accession number ACYQ00000000.2).

Interestingly, the ATCC 17978 A1S_2562-A1S_2581 gene cluster has the same genetic content and organization as that of the *A. baylyi* ADP1 ACIAD2761-ACIAD2776 gene cluster (GenBank accession number NC_005966.1) with the exception of the presence of the transposase coding regions. A gene potentially coding for a transposase fragment is located outside the *A. baylyi* ADP1 ACIAD2761-ACIAD2776 gene cluster, downstream of ACIAD2761 (235). In contrast, the ATCC 17978 cluster 2 includes two putative genes coding for transposase-related proteins located between the A1S_2568 and A1S_2570 annotated coding regions (Fig. 9B and Table 6), one of which was not included in the original report (153). Furthermore, our previous analysis showed that cluster 2 includes perfect inverted repeats located at the ends of the cluster (53). Taken together, these observations suggest that this particular cluster was mobilized by horizontal gene transfer among environmental and clinical *Acinetobacter* strains, which must acquire iron in different free-iron restricted ecological niches.

Role of the ATCC 19606^T *entA* gene in virulence

The role of the *entA* gene in the virulence of *A. baumannii* ATCC 19606^T was tested using A549 human alveolar epithelial cells and *G. mellonella* caterpillars as *ex vivo* and *in vivo* experimental models. The tissue culture assays showed that the number of ATCC 19606^T bacteria recovered after 24 h incubation was significantly greater than the s1 (P = 0.0048) and 3069 (P = 0.000045) derivatives (Fig. 13A), affected in acinetobactin biosynthesis at intermediate (*basD*) and early (*entA*) biosynthetic stages, respectively. It was also noted that the persistence of 3069 was significantly lower than that of the s1 mutant (P = 0.0024) (Fig. 13A). It is important to mention that incubation of *A. baumannii* ATCC 19606^T in mHBSS at 37°C for 24 h did not result in significant bacterial growth.

Infection of *G. mellonella* larvae showed that more than 40% of them died six days after injected with the parental ATCC 19606^T strain, a value that is significantly different (P = 0.0014) from that obtained with animals injected with sterile PBS (Fig. 13B). Infection of caterpillars with the 3069 *entA* mutant showed that the killing rate of this derivative is not statistically different from that of the PBS negative control (P = 0.6705) but significantly different from the killing rate of the parental strain (P = 0.0005). On the other hand, the s1 derivative is significantly more virulent than the 3069 mutant (P = 0.043) and almost significantly different from the parental strain (P = 0.0820). The killing rates of the s1 and 3069 mutants were corrected to values statistically indistinguishable from the parental strain when the inocula used to infect the larvae were supplemented with 100 µM $FeCl_3$ (Fig. 13C). This response shows that the virulence defect of the s1 and 3069 isogenic mutants is due to their inability to acquire iron when injected into *G. mellonella*.

Taken together, these results demonstrate that inactivation of *entA* produces a more drastic reduction in the capacity of *A. baumannii* ATCC 19606^T cells to persist in the presence of A549 cells, which represent a target affected during the respiratory infections this pathogen causes in humans, or infect and kill *G. mellonella* larvae, an invertebrate host capable of mounting a complex innate immune response similar to that of vertebrate animals (236), when compared to the response obtained with the *basD* mutant. This response could be due to the fact that the 3069 derivative does not produce DHBA and acinetobactin intermediates, which are secreted by the s1 mutant and could have some functions in iron acquisition and virulence as it was shown with *Brucella abortus* (237, 238). Thus, these acinetobactin precursors together with

DHBA could bind iron, although less efficiently than acinetobactin, and provide s1 cells with enough iron to persist and cause host injury, although to a much reduced extent when compared with the response obtained with ATCC 19606^{T} cells.

Figure 13. Virulence of *A. baumannii* ATCC 19606^T parental and isogenic derivatives. (A) Persistence of bacteria in the presence of A549 monolayers. Bacteria (10^3) we added to 95% confluent monolayer maintained in mHBSS. The resulting CFUs were quantified after 24 h incubation at 37°C in 5% CO_2. (B and C) *G. mellonella* killing assays. Caterpillars were infected with 1 x 10^5 bacteria of the ATCC 19606^T parental strain (19606), or the s1 or 3069 iron-deficient isogenic derivatives in the absence (panel B) or the presence (panel C) of 100 µM Fe_3Cl and incubated at 37°C in darkness. Moth death was determined daily for six days. Caterpillars injected with comparable volumes of PBS or PBS plus 100 µM Fe_3Cl were used as negative controls.

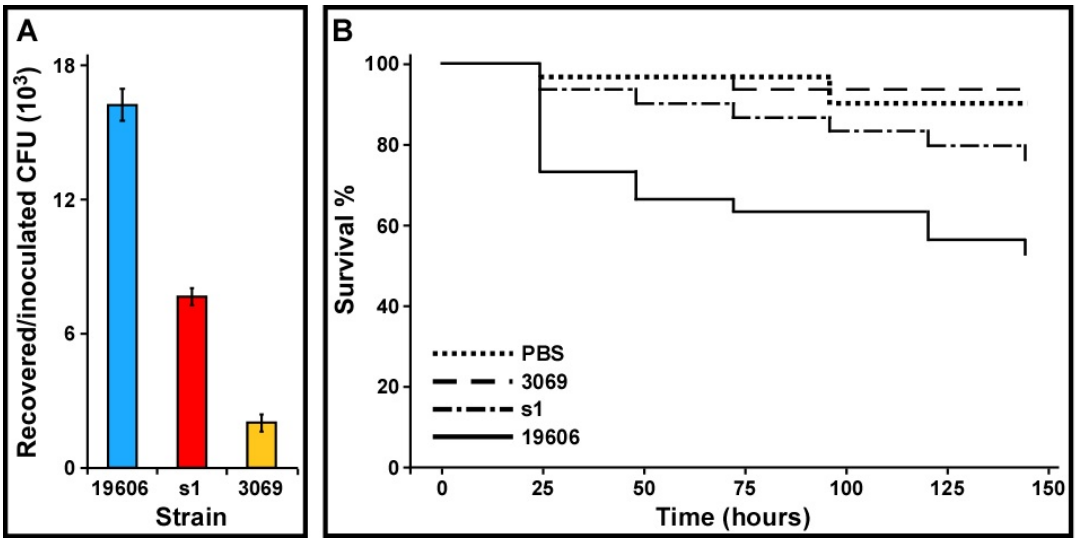
A
Recovered/inoculated CFU (10^3)
18
12
6
0
19606
s1
3069
Strain
B
Survival %
100
80
60
40
20
0
PBS
3069
s1
19606
0
25
50
75
100
125
150
Time (hours)

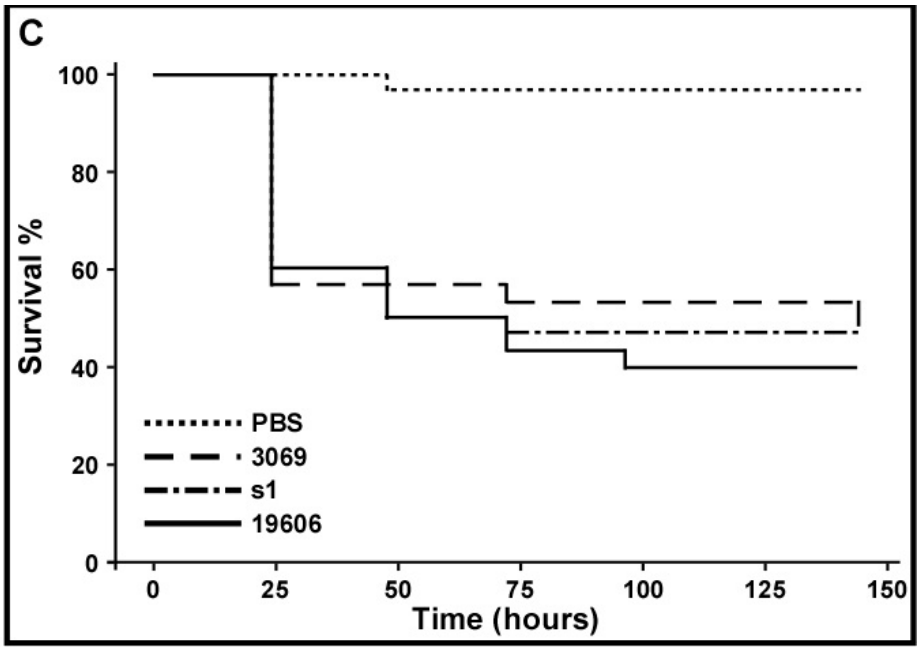
C
Survival %
100
80
60
40
20
0
PBS
3069
s1
19606
0
25
50
75
100
125
150
Time (hours)

Conclusions

The work described in this report shows that a single *A. baumannii entA* functional ortholog, which is essential for the biosynthesis of the acinetobactin precursor DHBA, is located outside the acinetobactin gene cluster, which otherwise codes for all biosynthesis, secretion and transport functions related to iron acquisition mediated by this high-affinity siderophore. Although the same genetic arrangement is found in all fully sequenced and annotated *A. baumannii* genomes, the genetic context within which the *entA* ortholog is found varies among different clinical isolates. In one group of strains this gene is next to genes coding for putative molybdenum transport, as in ATCC 19606^T. In another group, *entA* is located within a large gene cluster, which could code for an alternative uncharacterized siderophore-mediated system, as in ATCC 17978. Interestingly, this cluster also includes genes coding for potential DNA mobility functions and is flanked by perfect inverted repeats, a feature that may explain its transfer by lateral processes. Nevertheless, in all cases examined the *entA* ortholog is always next to an *entB* ortholog, which codes for a protein that is able to catalyze the production of DHBA from isochorismic acid but cannot promote the completion of the acinetobactin biosynthesis process because of the lack of the C-terminal aryl carrier (ArCP) protein domain. This is in contrast to the presence of *basF* within the acinetobactin cluster that codes for a fully functional EntB ortholog. All these findings indicate that all genetic components needed for iron acquisition by the acinetobactin-mediated system involved horizontal transfer as well as complex chromosomal rearrangement processes. All these observations are in agreement with the recent observation that *A. baumannii* has the capacity to acquire, lose and/or shuffle genes, a number of which could code for virulence factors involved in the pathogenesis of the infections this bacterium causes in humans (230). Our study also shows that the presence of all genetic determinants needed for the biosynthesis and utilization of acinetobactin does not warrant its active expression and may not reflect a virulence advantage when compared to other strains; the AYE clinical isolate is a natural *entA* mutant incapable of producing DHBA and acinetobactin. However, AYE is an iron-uptake proficient strain that seems to acquire this essential metal due to the expression of a siderophore-mediated system that remains to be functionally characterized. This finding reinforces our initial observation that different *A. baumannii* clinical isolates can express different iron acquisition systems (148). Finally, we show that acinetobactin intermediates and DHBA, which are produced in addition to acinetobactin in the ATCC 19606^T strain, play a role

in the virulence of *A. baumannii* when tested using *ex vivo* and *in vivo* infection experimental models, although to a lesser extent when compared to the role of the fully matured acinetobactin-mediated system.

Acknowledgments

US Public Health AI070174 and NSF 0420479 grants and Miami University funds supported this work. We are grateful to the Miami University Center of Bioinformatics and Functional Genomics for its support and assistance with automated DNA sequencing and nucleotide sequence analysis. We are also grateful to Dr. E. Lafontaine (College of Veterinary Medicine, University of Georgia, USA) for providing the A549 human epithelial cell line.

Chapter 4

Characterization of the hydroxamate siderophore produced by *A. baumannii* AYE

William F. Penwell and Luis A. Actis

Abstract

Acinetobacter baumannii produces the siderophore acinetobactin under iron-limiting conditions; however, we recently determined that the clinical isolate AYE does not make acinetobactin due to a point mutation in the *entA* ortholog yet still displays siderophore activity, indicating the production of an uncharacterized siderophore. Here we determined the chemical nature of this siderophore that was purified from culture supernatants of AYE. *In silico* analysis of the gene cluster identified by comparative genomics to be involved in the production of this siderophore revealed that protein products coded for by genes from this cluster have similarity to proteins involved in production of acinetoferrin and achromobactin. Based on *in silico* analysis of the predicted protein involved in siderophore production, we proposed a structure and pathway for the synthesis of the siderophore we called baumannoferrin. Furthermore, the type strain ATCC 19606^{T} contains the baumannoferrin gene cluster and can use this siderophore to grow under iron-chelated conditions but does not produce baumannoferrin, possibly due to a change in critical amino acids needed for activity of enzymes involved in synthesis. This is the first report examining the chemical nature of the previously uncharacterized siderophore.

Introduction

Iron is an essential element for the growth of nearly all microorganisms. However, despite being the fourth most abundant element in the Earth's crust, in the presence of oxygen and at physiological pH, iron is only found in insoluble ferric oxyhydroxide complexes (55, 59). Iron is also limited in the host largely due to sequestration by host iron-binding proteins like transferrin and lactoferrin (57, 63). These restrictions on the availability of iron leave the concentration well below the 10^{-6} M needed for proper metabolism and cellular functions in microorganisms (55, 59). Bacteria have developed several mechanisms to acquire this essential metal, including the use of low molecular weight iron-chelating compounds called siderophores (58, 68). Siderophores are secreted from the cell, sequester ferric iron by forming ferric-siderophore complexes, and are then transported back into the cell through specific outer membrane receptors (58, 88). Siderophores are important virulence factors for many pathogenic bacteria, and siderophore-deficient strains are attenuated in their virulence phenotype as compared with siderophore producing strains (106, 165, 186, 239, 240). This fact has made components of the siderophore-mediated iron acquisition systems, like those involved in transport or biosynthesis, attractive targets for drug design to treat pathogenic bacteria, especially against those that are multi-drug resistant, such as *Acinetobacter baumannii*.

A. baumannii is the cause of a significant number of nosocomial infections in immunocompromised patients over the last few decades (1, 2). Pneumonia and bacteremia are two diseases that are most often linked with this pathogen but other diseases, such as necrotizing fasciitis and urinary tract infections, are also associated with *A. baumannii* (1, 7). Many clinical isolates of *A. baumannii* exhibit a multiple- or pan-drug resistant phenotype, which has not only limited the number of treatment options but has also led to the global emergence of this pathogen (7, 241, 242). *A. baumannii* uses multiple, extensively studied mechanisms to resist a broad spectrum of antibiotics, which are considered to play major roles in its virulence (7, 35, 242-244).

Another virulence factor that has been studied in *A. baumannii* is the acinetobactin-mediated iron uptake system expressed under iron-limiting conditions. The acinetobactin-mediated system is the only high-affinity siderophore system to be comprehensively studied in *A. baumannii* (51, 186). All genes needed for the biosynthesis, export, and uptake of this siderophore are present within the 26.5-kb acinetobactin cluster, with the exception of the *entA*

ortholog (52, 171, 186). Furthermore, this siderophore is essential for the type strain ATCC 19606^T to grow under iron-limiting conditions and cause a successful infection in an *in vivo* virulence model (165, 171, 186).

Recent comparative genomic analysis of sequenced genomes from fifty different clinical isolates has indicated that the acinetobactin cluster is highly conserved in *A. baumannii* (151). However, this bioinformatic study also identified an uncharacterized siderophore-mediated system, found ubiquitously among the clinical *A. baumannii* isolates examined (151, 245). In a study that investigated *A. baumannii* ATCC 17978 under iron-limiting conditions, Eijkelkamp *et al.* (150) determined that components of this uncharacterized siderophore system were up-regulated, suggesting that this siderophore system could play a role in iron acquisition. This uncharacterized siderophore gene cluster was also found in the genome of ATCC 19606^T, but acinetobactin-deficient mutants generated in this strain were found to be negative for siderophore activity when tested with the Chrome Azurol S reagent (CAS), indicating that the type strain is solely dependent upon acinetobactin for iron acquisition (51, 186). Despite these *in silico* studies, no experimental data have been reported demonstrating production of this uncharacterized siderophore by any *A. baumannii* strain.

The *A. baumannii* clinical isolate AYE possesses a natural mutation in the *entA* ortholog and cannot synthesize the DHBA precursor needed for the production of acinetobactin (186). Interestingly, AYE can grow under iron-limiting conditions and culture supernatants from this strain are still positive for siderophore activity when tested with the CAS reagent, indicating that this clinical isolate still produces a siderophore (186). The comparative genomic studies by Antunes *et al*. (151) demonstrated that AYE possesses genes coding for the aforementioned uncharacterized siderophore-mediated system, which this strain might use to acquire iron.

The objectives of this study were to characterize the unidentified siderophore produced by the *A. baumannii* AYE clinical isolate and to examine the putative proteins encoded by the genes present in this uncharacterized siderophore cluster. To accomplish this goal, we used biochemical analyses on M9 culture supernatant or purified siderophore isolated from AYE iron-restricted culture supernatant to determine the chemical nature of this siderophore. Homology searches of the predicted protein products from this uncharacterized siderophore gene cluster indicated that some components of this system are similar to proteins located in the acinetoferrin cluster found in *A. haemolyticus* ATCC 17906^T, whereas other components are related to

proteins involved in the biosynthesis and export of the siderophore achromobactin, which is produced by different *Pseudomonas* species. The results from this study indicate that the AYE clinical isolate produces a hydroxamate siderophore, which can be utilized by ATCC 19606^T to grow under iron limitation. Even though we could not determine the actual structure, we predicted the structure of this siderophore using *in silico* examination of the proteins potentially involved in its biosynthesis. The results of this study emphasize the ability of different *A. baumannii* isolates to acquire iron using different siderophore-mediated systems.

Materials and Methods

Bacterial strains, plasmids, and culture conditions

Bacterial strains used in this work are described in Table 8. Strains were routinely cultured in Luria Bertani (LB) broth or agar (172) at 37ºC in the presence of appropriate antibiotics. M9 minimal medium was used for growth under chemically defined conditions (175). Iron-limiting conditions were achieved by the addition of 2,2' dipyridyl (DIP) to LB broth.

XAD-7 purification of hydroxamate siderophore from AYE

The uncharacterized siderophore was isolated from *A. baumannii* AYE iron-restricted culture supernatants by adsorption onto XAD-7 resin. Briefly, AYE was grown in 9 L of succinate medium (246), and the supernatant was recovered by centrifugation at 10,000 x *g* for 10 min. Clear supernatant was added to the XAD-7 resin (20 g) and the suspension was shaken slowly in an incubator for 3.5 h at 37^{o}C to adsorb the siderophore. The suspension was filtered over a glass filter funnel and the resin was washed with 500 ml of distilled water three times. The resin was then washed with 300 ml of methanol to elute the siderophore from the resin and the samples were dried by rotary evaporation and then resuspended in 3 ml of methanol.

Chrome azurol sulfonate assay

The CAS assay (225, 247) was used to detect the presence of siderophore in the supernatants. Cell-free culture supernatant (0.5 ml) was mixed with an equal volume of CAS solution and 10 µl of shuttling solution. After 20 min of incubation at room temperature the absorbance of the resultant solution was measured at 630 nm. M9 minimal medium was used as a blank and when combined with the CAS and shuttle solution was used as a reference solution.

Siderophore concentrations were determined as $[(A_{ref} - A_{std})/A_{ref}]*100$ = % siderophore concentration.

Table 8. Bacterial strains and plasmids used in this work.

A. baumannii strains	Relevant characteristics[a]	Source/reference
A. baumannii		
ATCC 19606^T	Nosocomial isolate	ATCC
ATCC 19606^T s1	ATCC 19606^T *basD* mutant, Km^R	(51)
ATCC 19606^T t6	ATCC 19606^T *bauA*::Ez::TN<R6Kγori/KAN-2> derivative, Km^R	(51)
ATCC 19606^T 3069	ATCC 19606^T *entA* mutant, Km^R	(186)
AYE	Nosocomial isolate	(216)

Arnow's colorimetric assay

The Arnow's colorimetric assay (14) was used to detect catechol compounds. One volume of culture supernatant was successively mixed with 1 volume of reagent A (0.5 N HCl), reagent B (10% $NaNO_3$, $NaMoO_4$) and reagent C (1 N NaOH). The reaction was measured by determining the OD_{510} after 10 min incubation at room temperature.

Ferric perchlorate hydroxamate assay

Ferric perchlorate (248) was used to detect hydroxamate compounds. Methanolic solutions of the purified siderophore from AYE were evaporated to dryness under a stream of nitrogen gas and resuspended in 0.5 ml of deionized water and then 0.5 ml of 5 mM $Fe(ClO_4)_3$ in 0.1 M $HClO_4$ was added. The OD_{450} of the sample was measured against a blank reference of water and $Fe(ClO_4)_3$-$HClO_4$ reagent (1:1).

Siderophore utilization assay

The ability of *A. baumannii* ATCC 19606^T to utilize the siderophore produced by AYE was determined by the size of growth halos around 7-mm filter disks that were spotted with cell-free culture supernatant from AYE. The *A. baumannii* acinetobactin production deficient 3069 (*entA*) and s1 (*basD*) and the acinetobactin receptor deficient t6 (*bauA*) isogenic derivatives were used as indicator strains (51, 186). The 3069 and s1 mutants were grown in LB agar supplemented with 225 µM DIP and the t6 mutant was grown in 200 µM DIP. Growth halos were measured after incubation for 30 h at 37^oC.

HPLC analysis of catechol and siderophore compounds

Production of DHBA and acinetobactin was examined by HPLC analysis with an Agilent 1100 LC instrument using M9 culture supernatants filtered through 0.45-mm cellulose acetate filter units (Spin-x centrifuge filter units, Costar, Cambridge, MA). For analysis of acinetobactin and DHBA, M9 culture supernatants were fractionated with an Acclaim C-8, 5 µm, 250 mm x 4.6 mm reversed-phase column (Thermo Fisher Scientific, Sunnydale, CA). Water and acetonitrile containing 0.13% and 0.1% trifluoroacetic acid (TFA), respectively, were used as mobile phases. The gradient was as follows: 17% acetonitrile for 5 min and then from 17% to

30% within 30 min, and thereafter held for 15 min. Detection was at 317 nm with a flow rate of 0.5 ml/min.

XAD-7 purified siderophore from AYE was fractionated using a Vydax C-18, 5 µM, 250 mm x 4.6 mm reversed-phase column (Grace Davison Discovery Sciences, Deerfield, IL). Water and acetonitrile both containing 0.1% TFA were used as mobile phases. The gradient was as follows: 0% acetonitrile for 2 min and then from 0% to 100% within 25 min, and thereafter held for 2 min. Detection was at 254 nm with a flow rate of 1 ml/min. Siderophore activity from collected fractions was assessed with the CAS reagent and also tested for biological activity using siderophore utilization bioassays as described above.

Spectroscopy

UV and visible (UV/Vis) spectra of the XAD-7 purified siderophore from AYE dissolved in distilled water were recorded on a Nanodrop 2000 spectrometer (Thermo Fisher Scientific, Sunnydale, CA).

***In silico* analyses**

NCBI BLASTP was used for comparative genome analyses (184). ScanProsite was used for motif and domain scans of predicted proteins (249).

RNA isolation and transcriptional analysis of gene expression

A. baumannii ATCC 19606^T was grown in 1 ml LB broth supplemented with 100 µM DIP. Cells were grown in triplicate at 37^{o}C and then pooled together after 24 h of incubation. The pooled samples were mixed with 2 ml lysis buffer (0.3 M $C_2H_3NaO_2$, 30 mM EDTA, and 3% SDS) in a boiling water bath. Two acid phenol extractions were performed at 65^{o}C and was followed by one extraction with chloroform at room temperature. RNA was precipitated in 100% ethanol at -20^{o}C overnight and then washed with 70% ethanol. RNA pellets were vacuum-dried and resuspended in diethyl pyrocarbonate (DEPC)-treated with distilled water. An RNeasy column (Qiagen) was used to remove contaminating DNA and further purified the RNA samples. To determine if the genes from the uncharacterized siderophore gene cluster were transcribed in ATCC 19606^T, total RNA samples were used as a template for reverse transcriptase-PCR (RT-PCR) with primers that are listed in Table 9 and shown in Fig. 17A. A

commercial RT-PCR kit (Qiagen) was used as suggested by the manufacturer. Samples were amplified under the following cycle conditions: 50°C for 30 min, 95°C for 15 min, and 25 cycles of 1 min denaturation at 94°C, 1 min annealing at 55°C, and 1 min extension at 72°C. The amplicons were analyzed following ethidium bromide agarose gel electrophoresis (172).

Table 9. Primers used in this study

Number	Nucleotide sequence
3726	5’- GGAGCAACTGGCTATATC -3’
3727	5’- CGATGACACTCTTTTGCC -3’
3728	5’- GTTGTGCAACTGAGCAGC -3’
3729	5’- GGCAATTGCATACCAGCA -3’
3730	5’- GGTACGCCTGATTTAGGC -3’
3731	5’- GTCAGAAGTACGTAGCGT -3’
3732	5’-GTCAGGTTCAGTATCCTC -3’
3733	5’- GGCATAACCCACGTCTTG -3’
3734	5’- GAGCTTTGGTGCCCAGTA -3’
3735	5’- CTGCATAAGCCTGCTGTG -3’
3731	5’- CTGGAGATCTGATTGTAG -3’
3722	5’- CTGATTGAGACTGGTTACAGAAG -3’
2531	5’- ATTGAAGCTGATTTCCACC -3’
2532	5’- TCCGCAATCACAGAAAGG -3’

Results and Discussion

Characterization of *A. baumannii* AYE under iron-limiting conditions

In Chapter 2, we determined that the *entA* ortholog of *A. baumannii* ATCC 19606^T was located outside the acinetobactin cluster and is essential for the production of the acinetobactin precursor 2,3-dihydroxybenzoic acid (DHBA) (186). The *entA* gene was also confirmed to be necessary for ATCC 19606^T to cause a successful infection in A549 persistent assays and *G. mellonella* killing assays. Analysis of the nucleotide sequence of this ortholog with other *A. baumannii* sequenced genomes revealed that the clinical isolate AYE encodes an EntA protein that is 29 amino acids shorter than other predicted EntA proteins (186). Genetic complementation experiments showed that *entA* from AYE was not able to complement the growth phenotype of the *E. coli entA*-deficient strain, AN193, demonstrating that AYE was a natural *entA* mutant (186). This was confirmed by HPLC analysis of AYE culture supernatant (Fig. 14A). This analysis showed that the supernatant of both AYE and ATCC 19606^T *entA*-deficient strain 3069 were missing the peaks that correspond to acinetobactin (~19 min) and DHBA (~25 min), which were detected in the ATCC 19606^T culture supernatant (Fig. 14A).

To test whether the natural mutation in the *entA* gene of AYE caused a growth defect phenotype consistent with a disruption in acinetobactin production, both AYE and ATCC 19606^T cells were grown in LB broth supplemented with increasing concentrations of DIP. Interestingly, AYE was able to grow at a much higher concentration of DIP than the type strain ATCC 19606^T (Fig. 14B), suggesting that this clinical isolate is able to grow under iron-limiting conditions independently of acinetobactin and might use an uncharacterized siderophore to acquire iron. Furthermore, the siderophore produced by AYE might have a higher affinity for iron compared to acinetobactin, which could explain why AYE is able to grow at a higher concentration of DIP than ATCC 19606^T.

To test the possibility that AYE produces an uncharacterized siderophore, a CAS assay was performed using M9 culture supernatant obtained from AYE and was compared to the supernatant obtained from ATCC 19606^T and the ATCC 19606^T 3069 *entA* mutant. The results of this assay demonstrated that culture supernatant from AYE produces a molecule that can chelate iron from the ferric-CAS complex (Fig. 14C). As expected, ATCC 19606^T was also positive for siderophore activity, but no significant iron chelation of the CAS reagent was

Figure 14. Detection of DHBA and acinetobactin in the culture supernatant of *A. baumannii* AYE. (A) HPLC analysis of culture supernatant of sterile M9 minimal medium (M9) or culture supernatant from ATCC 19606^T (19606), the 3069 acinetobactin-deficient strain (3069) or the AYE clinical isolate. (B) ATCC 19606^T (blue) and AYE (purple) were cultured in LB broth in the presence of increasing concentrations of DIP. (C) Iron-chelating activity of ATCC 19606^T (blue), 3069 (orange) and AYE (purple) detected by CAS assay. (D) Arnow's colorimetric assay of M9 culture supernatant obtained from strains shown in panel C.

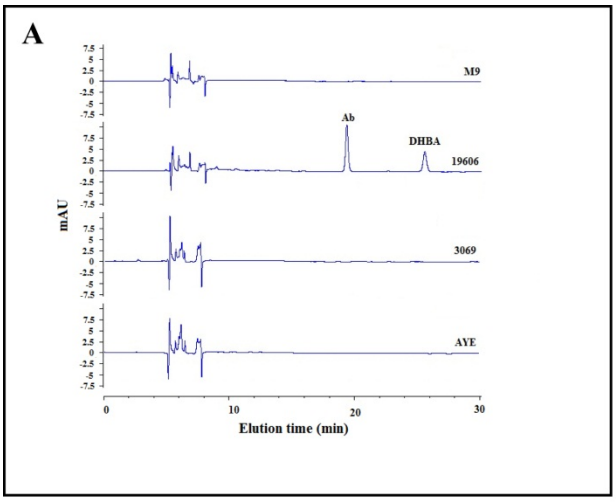
A
M9
Ab
DHBA
19606
3069
AYE
mAU
Elution time (min)

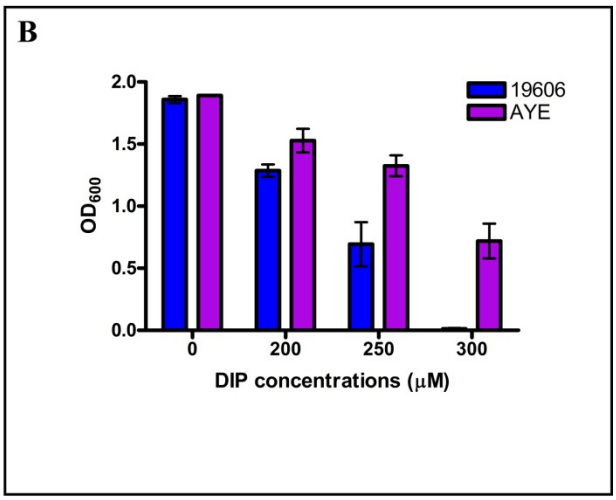
B
19606
AYE
OD600
DIP concentrations (μM)

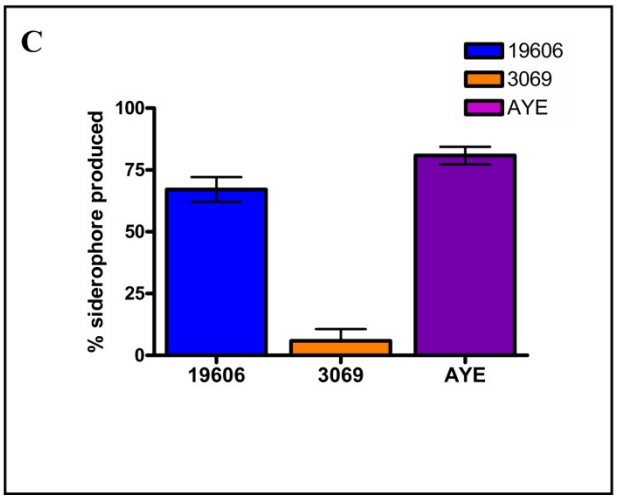
C
19606
3069
AYE
% siderophore produced

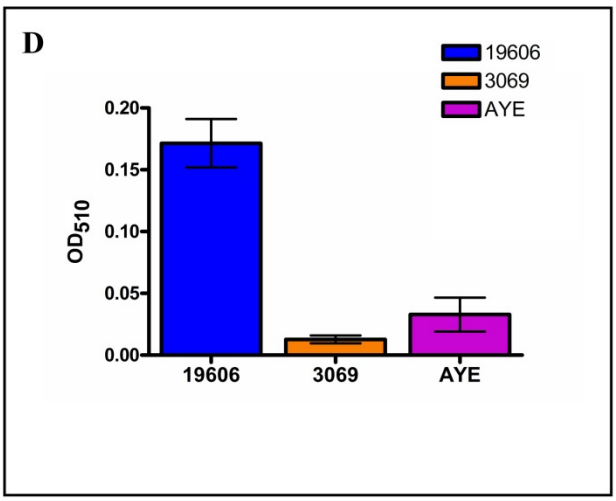
D
19606
3069
AYE
OD510

observed with the ATCC 19606^T *entA* mutant, which is consistent with previous data showing that acinetobactin is the only high-affinity siderophore produced by ATCC 19606^T (51, 186). Because AYE has a natural *entA* mutation and does not produce DHBA, this uncharacterized siderophore might be a non-catechol based siderophore. This was confirmed by the failure to detect a catechol by the Arnow's colorimetric assay (Fig. 14D).

To determine whether the uncharacterized siderophore produced by AYE could be utilized by ATCC 19606^T, a siderophore utilization bioassay was performed using ATCC 19606^T 3069 (*entA*) and s1 (*basD*) acinetobactin production-deficient mutants and the t6 (*bauA*) acinetobactin uptake mutant as indicator strains. Both 3069 and s1 were able to grow under iron-limiting conditions around filter disks containing cell-free supernatants from AYE and ATCC 19606^T (Fig. 15). However, the t6 isogenic derivative grew only around a filter disk containing cell-free culture supernatant from AYE and not around a filter disk containing the supernatant from ATCC 19606^T (Fig. 15C). These results indicate that ATCC 19606^T can utilize this uncharacterized siderophore for growth in iron-limiting conditions and that the uptake of this siderophore is mediated by an acinetobactin-independent transport mechanism.

Data presented here correlate with recent research, which demonstrated that the culture supernatant from *A. baumannii* AYE was positive for siderophore activity as determined by the CAS assay (151, 155). The detection of the chemical moiety present in the supernatant revealed low levels of catechol but high levels of hydroxamate as determined by Arnow's colorimetric assay and the Csàky reaction, respectively (151, 155). Despite these correlations, the authors suggest that different *A. baumannii* strains may produce more than one type of siderophore but failed to recognize that AYE does not produce acinetobactin. It is worth noting that if provided with exogenous DHBA, AYE can produce acinetobactin, which was demonstrated in Chapter 2. Antunes *et al.* (151) also demonstrated that AYE successfully kills *G. mellonella* caterpillars at a similar rate as other *A. baumannii* clinical strains. Therefore, AYE is not dependent upon acinetobactin for virulence, unlike ATCC 19606^T, which needs a fully functioning acinetobactin system to cause killing of infected caterpillars (155, 165, 186).

Taken together, the results show that *A. baumannii* AYE is able to acquire iron using an uncharacterized siderophore that is not structurally related to acinetobactin. AYE displayed an increased growth phenotype compared to ATCC 19606^T when both were grown in iron-chelated conditions, which might be attributable to the physicochemical properties of this uncharacterized

siderophore. The results of the bioassay show that ATCC 19606^{T} can use this uncharacterized siderophore by a mechanism that is independent of acinetobactin uptake.

Figure 15. Siderophore utilization assay with culture supernatant from *A. baumannii* AYE. Growth of *A. baumannii* ATCC 19606^T 3069 (A), s1 (B) and t6 (C) mutants under iron-chelated conditions around filter disks spotted with $FeCl_3$ (green), H_2O (grey), or cell-free culture supernatant from ATCC 19606^T (blue) or AYE (purple).

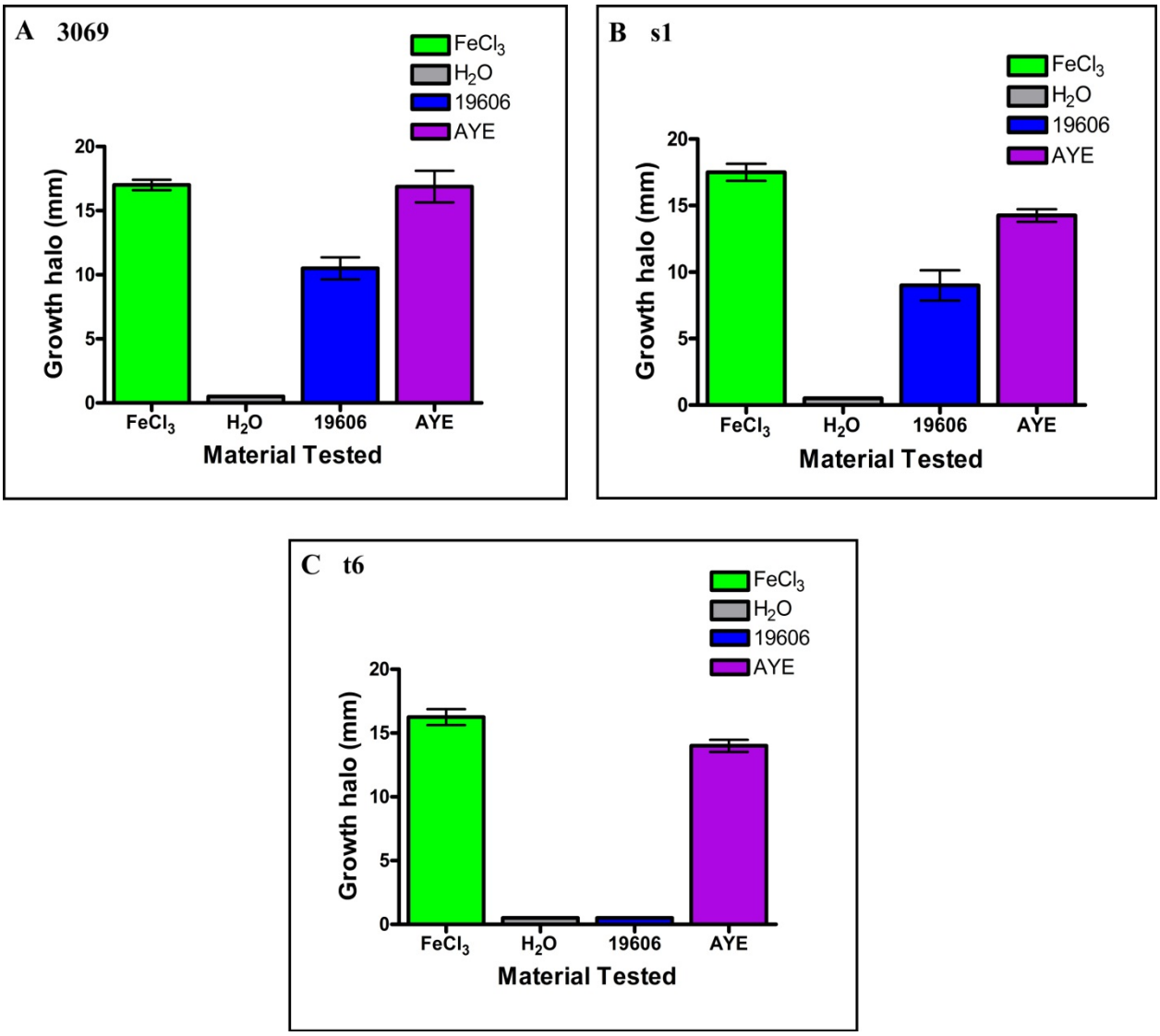
A 3069
FeCl3
H2O
19606
AYE
Growth halo (mm)
20
15
10
5
0
FeCl3
H2O
19606
AYE
Material Tested
B s1
FeCl3
H2O
19606
AYE
Growth halo (mm)
20
15
10
5
0
FeCl3
H2O
19606
AYE
Material Tested
C t6
FeCl3
H2O
19606
AYE
Growth halo (mm)
20
15
10
5
0
FeCl3
H2O
19606
AYE
Material Tested

Purification of the hydroxamate siderophore from *A. baumannii* AYE

To further characterize the chemical nature of this siderophore and possibly elucidate its structure, we purified it from cell-free supernatants of *A. baumannii* AYE using XAD-7 resin. The retained siderophore was washed with deionized water and then eluted from the resin with methanol. To assess for siderophore activity, the XAD-7-purified material was tested with the CAS reagents and also for the ability to cross-feed the ATCC 19606^T t6 (*bauA*) acinetobactin receptor-deficient mutant. The XAD-7-purified material was positive for both the CAS reaction (Fig. 16A) and for the ability to cross-feed the ATCC 19606^T t6 mutant (Fig. 16B), indicating that a siderophore was present in the collected material.

We then examined the chemical characteristics of this siderophore by using Arnow's colorimetric assay and the ferric perchlorate assay to detect the presence of catechol and hydroxamate moieties, respectively. No catechol group was detected in the purified siderophore but hydroxamate was detected (Fig. 16C). This indicates that this siderophore is a hydroxamate siderophore and does not contain a catechol moiety, presumably due to the natural mutation in *entA* in the AYE strain. The UV/Vis spectrum of the purified siderophore displayed a maximum absorption at 250 nm. Upon addition of $FeCl_3$, a shoulder appeared at 250 nm and a broad absorption band at 450 nm, which corresponds to the characteristic charge-transfer band of ligand from the siderophore binding to metal (Fig. 16D). The addition of $FeCl_3$ caused the purified siderophore solution to turn from colorless to reddish brown, which suggests that the siderophore was isolated predominantly in the iron-free form and formed a ferric-siderophore complex upon the addition of $FeCl_3$.

Since the hydroxamate siderophore from AYE was present in the purified material, the XAD-7-associated siderophore preparation was further purified by using a reverse-phase HPLC C-18 column to fractionate and collect the samples. HPLC analysis of the purified siderophore revealed six peaks with an absorbance over 200 mAU, with the major peak eluting off the column at 14.4 min (Fig. 16E). We tested these six peaks for siderophore activity using both the CAS reagent and a siderophore utilization bioassay. The CAS assay identified one eluted fraction, which corresponds to the absorption peak at 14.4 min that was positive for siderophore activity (Fig. 16A). This fraction and another, which corresponds to the peak at 12.4 min, were able to cross-feed the ATCC 19606^T BauA-deficient strain (data not shown). Thus, two different fractions had siderophore activity.

Figure 16. Chemical characterization of XAD-7 purified siderophore from AYE. (A) CAS assay to detect siderophore activity of sterile succinate medium (1), XAD-7 purified siderophore (2) and the HPLC collected fraction at 14.4 min (3) using the CAS reagent. (B) Cross-feeding of the *A. baumannii* ATCC 19606^{T} t6 BauA mutant by $FeCl_3$ (green), H_2O (grey) and purified siderophore from AYE (purple). (C) Arnow's colorimetric assay (purple) and ferric perchlorate (pink) performed on a 1:4 dilution of purified siderophore. (D) Absorption spectrum of XAD-7 purified siderophore (blue) and the ferric-siderophore (red). (E) HPLC profile of the purified siderophore.

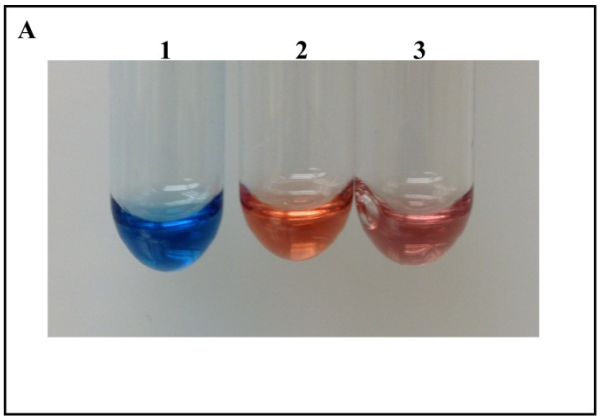
A
1
2
3

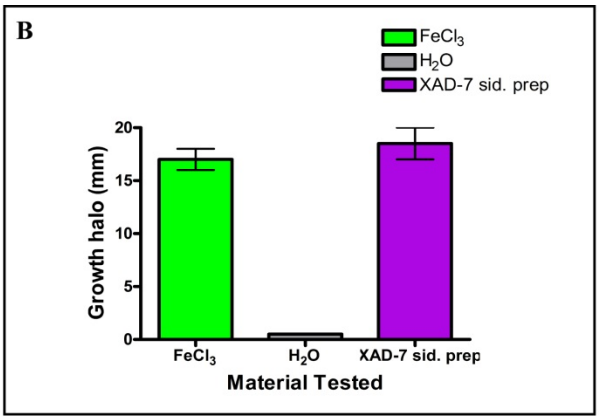
B
FeCl3
H2O
XAD-7 sid. prep
Growth halo (mm)
20
15
10
5
0
FeCl3
H2O
XAD-7 sid. prep
Material Tested

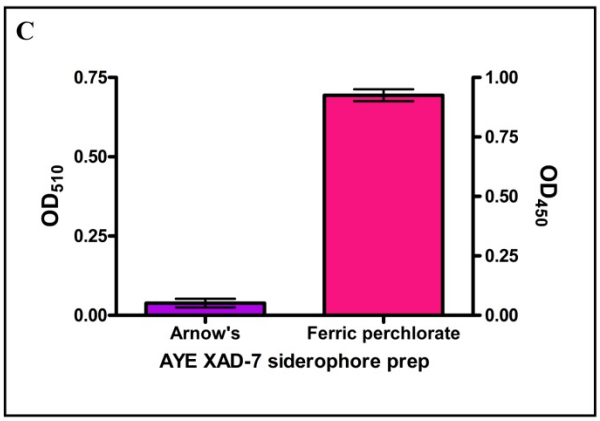
C
0.75
0.50
0.25
0.00
OD510
1.00
0.75
0.50
0.25
0.00
OD450
Arnow's
Ferric perchlorate
AYE XAD-7 siderophore prep

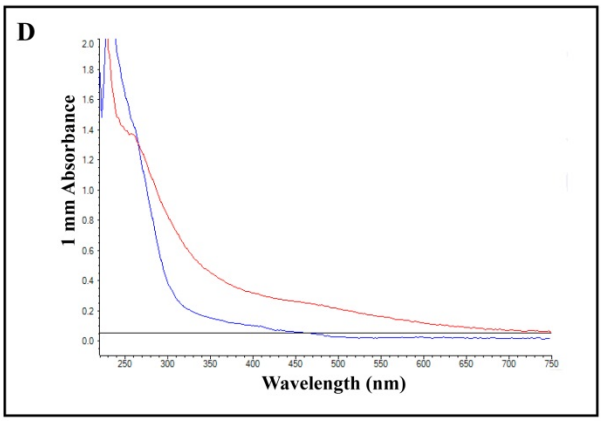
D
1 mm Absorbance
Wavelength (nm)

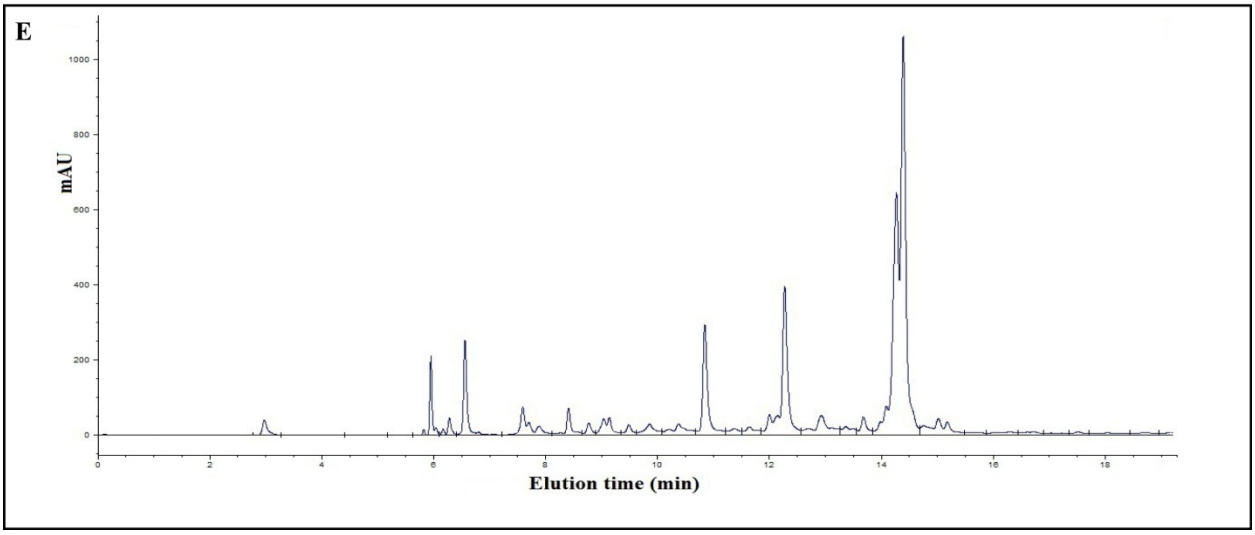
E
mAU
Elution time (min)

It is possible that the smaller absorption peak at 12.4 min is either an intermediate in siderophore biosynthesis or a breakdown product of the 14.4 min peak that retains siderophore activity. This is similar to *E. coli,* in which enterobactin intermediate and breakdown products have siderophore activity and are able to cross-feed enterobactin-deficient strains (93). It is also important to note that there are two peaks present in the fraction at 14.4 min and further HPLC analysis is needed to determine if this could be a shift in the siderophore molecule due to the binding of iron or an artifact of the HPLC procedure. It is also possible that these two peaks are two closely related products that elute off the column at similar times.

Taken together, these results strongly support the identification and isolation of a novel siderophore in *A. baumannii.* Efforts to elucidate the structure of this uncharacterized siderophore are ongoing. Pending identification of this siderophore with one that was previously identified from another organism, we name this siderophore baumannoferrin.

***In silico* analysis of baumannoferrin gene cluster from *A. baumannii* AYE**

In silico genomic analysis performed by Antunes *et al.* (150) and Eijkelkamp *et al.* (151) identified the baumannoferrin gene cluster, which was found to be present in almost all sequenced *A. baumannii* genomes. This gene cluster (Fig. 17A) is comprised of twelve ORFs, which encode six proteins related to siderophore biosynthesis, two involved in siderophore utilization, one involved in siderophore export and three proteins of unknown function (Table 10) (151). Sequence similarity searches determined that components of the AYE baumannoferrin cluster have homology to proteins from the acinetoferrin system from *A. haemolyticus* ATCC 17906^T (Fig. 17B). This finding is in agreement with a recent comparative genomic study between species of the *Acinetobacter* genus performed by Sahl *et al.* (245). Acinetoferrin is a citrate-based dihydroxamate siderophore that was first described by Okujo *et al.* (246). The gene cluster responsible for the production of this siderophore in *A. haemolyticus* ATCC 17906^T was recently described by Funahashi *et al.* (250), who determined that this cluster contains four genes, AcbABCD, that are involved in the production of acinetoferrin and four genes, ActBCAD, that code for putative proteins involved in the secretion and uptake of this siderophore (Fig. 17B). However, not all genes present in the AYE baumannoferrin gene cluster code for putative proteins related to products from the acinetoferrin cluster of *A. haemolyticus* ATCC 17906^T. Some putative proteins are similar to products of the achromobactin gene clusters found in *Pseudomonas* species and other siderophore clusters found in unrelated bacteria (Table 10).

Homology searches of the proteins encoded by the AYE baumannoferrin gene cluster revealed that ORF1, ORF2, and ORF12 have 77%, 50%, and 75% identity (87%, 70%, and 87% similarity) to the proteins AcbA, AcbB, and AcbD, which are involved in the production of acinetoferrin (Fig. 17B and Table 10). ORF4, ORF5, and ORF7 have 49%, 38%, and 40% identity (67%, 56%, and 61% similarity) to proteins involved in the synthesis of achromobactin from *Pseudomonas chlororaphis* and *Pseudomonas savastanoi*, respectively (Fig. 17A, Table 10). The products of ORF4 and ORF5 are related to AcsC and AcsA, which belong to the nonribosomal peptide synthetase-independent (NIS) class of siderophore synthetases, and ORF7 encodes a protein similar to a dimethylmenaquinone methyltransferase, whose function in achromobactin production is still unknown (251).

Figure 17. Genetic organization of chromosomal regions harboring genes coding for the production and utilization of siderophores from *Acinetobacter* species. (A) Genetic map of the baumannoferrin gene cluster found in *A. baumannii*. (B) Genetic map of the acinetoferrin gene cluster found in *A. haemolyticus* ATCC 17906^{T}. The horizontal arrows and their direction indicate the location and direction of transcription of predicted genes, respectively. The horizontal lines indicate the region of the baumannoferrin cluster used for RT-PCR. The numbers next to each bar indicates the location of the primers used for RT-PCR. Numbers of ORFs shown in panel A correspond to those listed in Table 10. Those genes predicted to be involved in the biosynthesis, export and uptake of siderophores are colored blue, orange and red respectively. Genes that code for hypothetical proteins are shown in black. Numbers on top of short vertical bars indicate DNA size in kb. Fig. 17A was adapted from Antunes *et al.* (151), and Fig. 17B Funahashi *et al.* (250).

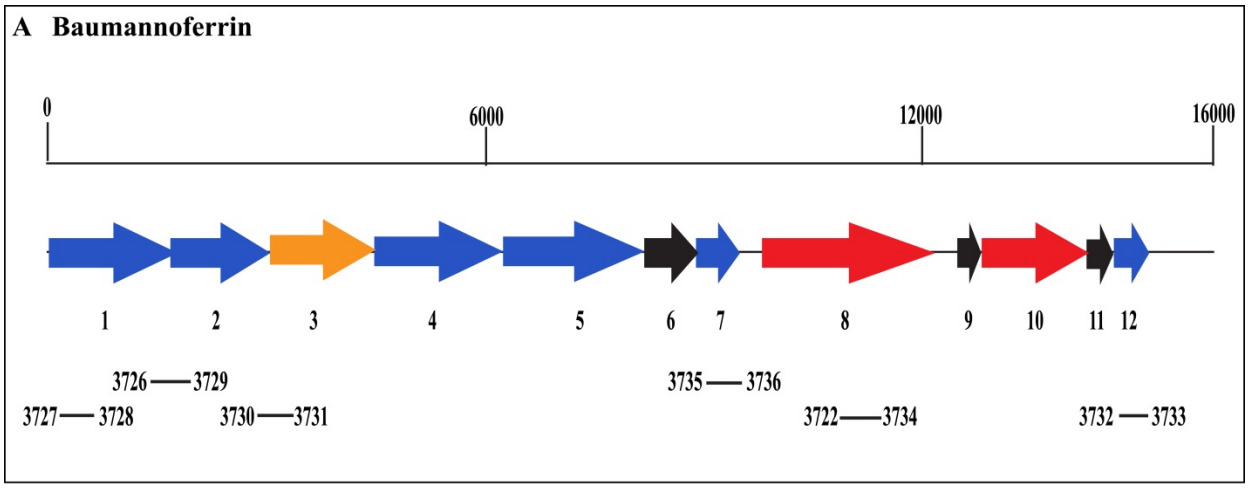
A Baumannoferrin
0
6000
12000
16000
1
2
3
4
5
6
7
8
9
10
11
12
3726—3729
3727—3728
3730—3731
3735—3736
3722—3734
3732—3733

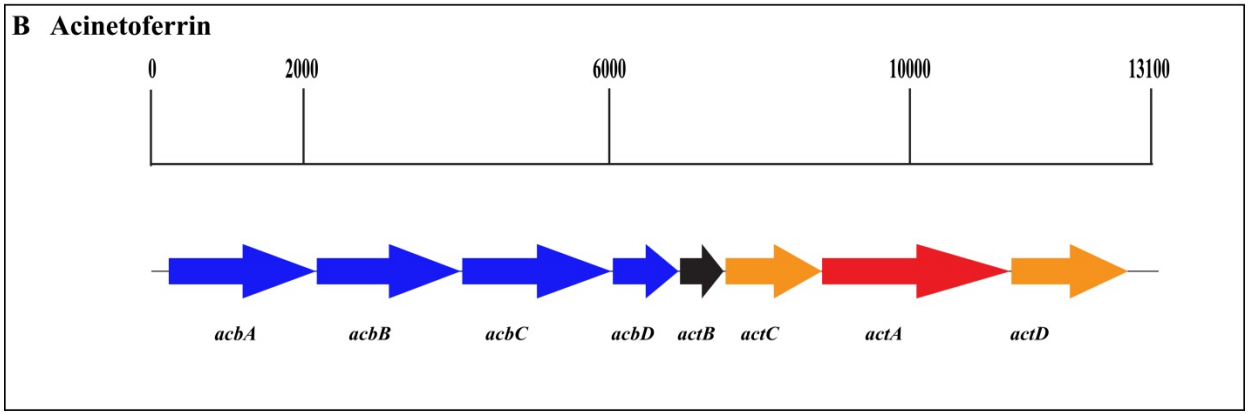
B Acinetoferrin
0
2000
6000
10000
13100
acbA
acbB
acbC
acbD
actB
actC
actA
actD

Table 10. Proposed genes and encoded proteins of the baumannoferrin gen locus of *A. baumannii* AYE and comparisons with similar proteins from NCBI database.

ORF	Length (aa)	Homologous protein	Organism	Identity, similarity (%)	Accession No.
1	595	AcbA acinetoferrin biosynthesis protein	*A. haemolyticus ATCC 17906*^{T}	77, 87	BAM09326
2	477	AcbB acinetoferrin biosynthesis protein	*A. haemolyticus ATCC 17906*^{T}	56, 70	BAM09327
3	481	YhcA achromobactin exporter	*Pseudomonas syringae*	43, 64	ZP_06460555
4	613	AcsC achromobactin biosynthesis protein	*Pseudomonas chlororaphis*	49, 67	ZP_10175683
5	636	AcsA achromobactin biosynthesis protein	*P. chlororaphis*	38, 56	ZP_10175790
6	256	Ferric reductase protein	*Bacillus pseudofirmus*	24, 43	YP_003427160
7	204	Achromobactin biosynthesis-associated methyltransferase	*P. syringae*	40, 61	ZP_21127699
8	772	ActA acinetoferrin receptor	*A. haemolyticus ATCC 17906*^{T}	57, 71	BAM09332
9	97	Hypothetical protein	*Pseudomonas fluorescens*	25, 52	YP_002870703
10	507	PepSY-associated TM helix domain	*Shewanella baltica*	32, 52	YP_001048513
11	112	ABC transporter permease protein	*Oribacterium sp.*	31, 54	ZP_06599419
12	206	AcbD acinetoferrin biosynthesis protein	*A. haemolyticus ATCC 17906*^{T}	77, 87	BAM09329

The baumannoferrin cluster contains several genes whose products are involved in the secretion, uptake, and utilization of this siderophore. ORF3 codes for a protein product that has 43% identity (64 % similarity) to YhcA from *Pseudomonas syringae*, which is a major facilitator superfamily (MFS) efflux protein experimentally demonstrated to export achromobactin in *Dickeya dadantii* (formly *Erwinia chrysanthemi*) (202). ORF8 could be the receptor needed for the uptake of baumannoferrin in AYE since it has 57% identity (71% similarity) to ActA, which is the putative acinetoferrin receptor (Fig. 17 B and Table 10). ORF6 codes for a ferric reductase protein that has 24% identity (43% similarity) to a protein from *Bacillus pseudofirmus* (Table 10). The C-terminal end of ORF6 contains the FhuF domain, which has been demonstrated in *E. coli* to be needed for the reduction of iron from ferrioxamine B (252). This suggests that ORF6 could be involved in the reduction and release of iron from ferric-hydroxamate complexes, pending experimental verification.

The protein products of ORF10 and ORF11 have 32% identity and 31% identity (52% and 54% similarity) to the pepsy-associated transmembrane helix from *Shewanella baltica* and an ABC transporter permease from *Orinbacterium* spp., respectively. These two proteins might be involved in either the secretion or uptake of baumannoferrin, but further work is needed to determine their function. ORF9 codes for a protein product that has 25% identity (52% similarity) to a hypothetical protein from *P. fluorescens* with unknown function.

While these results demonstrated similarities between the baumannoferrin gene cluster of AYE and the acinetoferrin locus of *A. haemolyticus* ATCC 17906^{T}, there are major differences between these two siderophore clusters. One difference is that the baumannoferrin gene cluster contains eight genes that code for proteins that are not homologous to proteins located within the acinetoferrin cluster but are similar to proteins encoded within other siderophore clusters, particularly those involved in the production and secretion of achromobactin (Fig. 17 and Table 10). Another difference between these two siderophore clusters is that the baumannoferrin locus contains three genes, ORF1, ORF4, and ORF5, which encode putative siderophore synthetases, whereas the acinetoferrin cluster contains only two genes, *acbA* and *acbC*, which code for synthetases (Fig. 17). The difference in the number of synthetases between the two clusters could allow for variation in the structure of the siderophores. Since the hydroxamate cluster contains proteins involved in siderophore synthesis that are similar to both acinetoferrin and

achromobactin, we speculate that the structure of this siderophore could contain structural components of both of these siderophores.

Proposed model and structure of baumannoferrin

Sequence similarity searches of putative baumannoferrin biosynthesis proteins revealed that these proteins are homologous to enzymes that comprise the NIS pathway. Enzymes from the NIS pathway assemble hydroxamate or carboxylate siderophores using alternating dicarboxylic acid and amino acid derivatives, like diamines or amino alcohols, as precursors, which are linked together by amide or ester bonds (87). Examples of siderophores that are assembled by this pathway include aerobactin (253, 254), acinetoferrin (250), rhizobactin 1021(255), vibrioferrin (256) and achromobactin (257, 258).

Based on the homologies with other proteins involved in siderophore biosynthesis and the protein products of the five genes located in the baumannoferrin cluster (ORF1, ORF2, ORF4, ORF5, and ORF12) that are involved in siderophore production (17A), we propose a hypothetical pathway for the synthesis of this siderophore and also speculate on the structure of baumannoferrin. Since *in silico* examination of ORF2 showed that it has similarities to AcbB, which is related to 1,3-diaminopropane monooxygenase, this protein might be involved in the hydroxylation of 1,3-diaminopropane (1,3-DAP) to N^3-hydroxy-1,3-diaminopropane (Fig. 18, reaction **[1]**). This molecule could then be acetylated by ORF12, which has similarity to AcbD, and subsequently transfer a molecule of 2-(E)-octenoic acid to N^3-hydroxy-1,3-diaminopropane forming N^3-2-octenoyl-N^3-hydroxy-1,3-diaminopropane (reaction [**2]**). The genes encoding the proteins involved in forming 1,3-DAP are not found within the acinetoferrin cluster of *A. haemolyticus* ATCC 17906^T but are found in a different genome region, which is also the case for the *A. baumannii* baumannoferrin locus. Two separate reports identified two genes that encode proteins needed for the production of this compound in *A. baumannii* ATCC 19606^T (259, 260), in which it is important for surface-associated motility and virulence in (261).

The rest of the proteins involved in production of baumannoferrin belong to the superfamily of NIS synthetases. These proteins are needed to catalyze the formation of amide bonds to link citrate and the hydroxamate moiety to form a functional siderophore (87, 262). The synthetase superfamily can be divided into 3 subfamilies, type A, type B, and type C, based on sequence analysis between the proteins involved in the assembly of siderophores by the NIS pathway. Type A is responsible for the formation of amide or ester bonds between polyamines or amino alcohols and the prochiral carboxyl group of citrate (87, 263). Type B is needed for the

Figure 18. The proposed structure and pathway for the biosynthesis of the siderophore baumannoferrin.

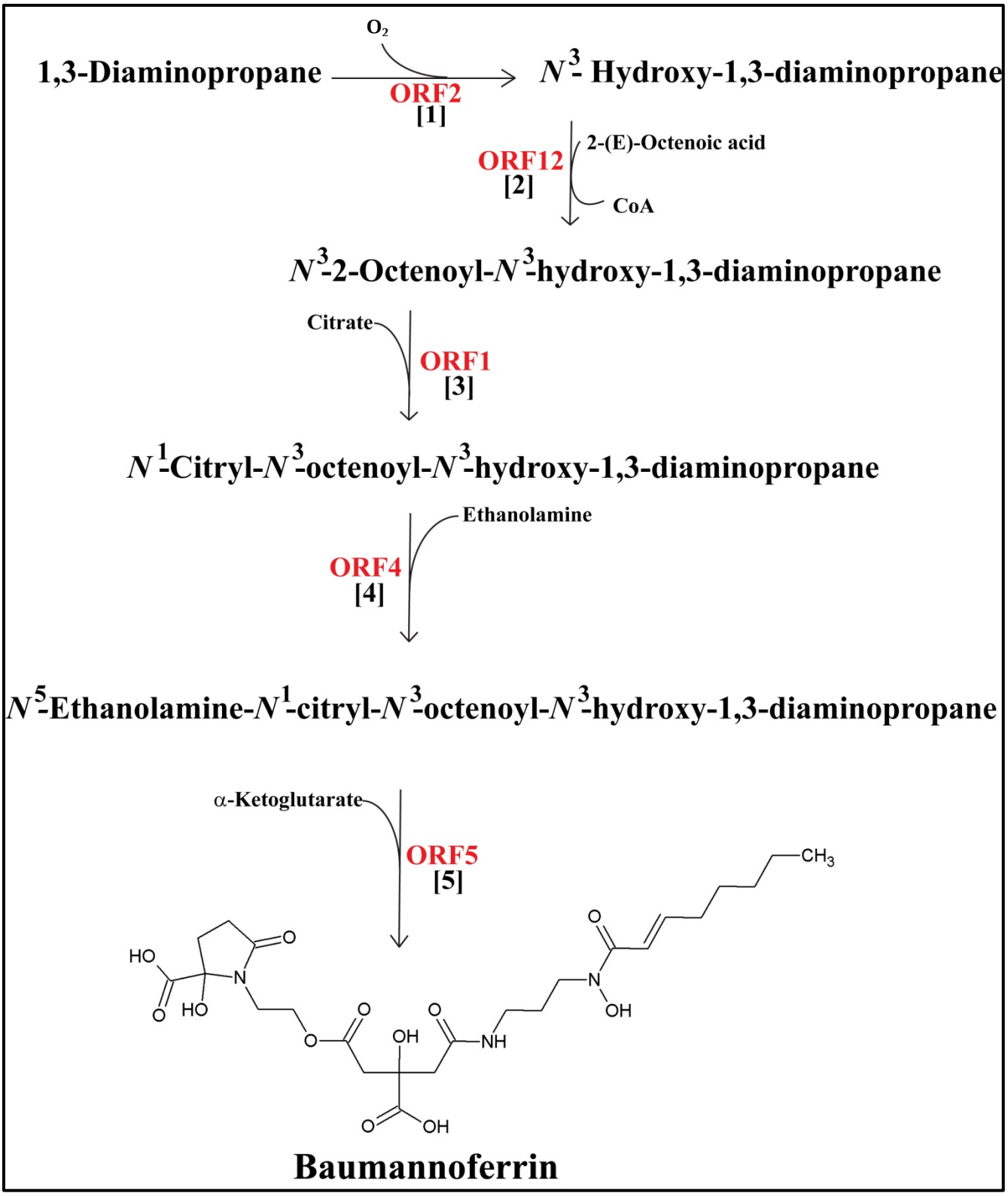
1,3-Diaminopropane
O2
ORF2
[1]
N3- Hydroxy-1,3-diaminopropane
ORF12
[2]
2-(E)-Octenoic acid
CoA
N3-2-Octenoyl-N3-hydroxy-1,3-diaminopropane
Citrate
ORF1
[3]
N1-Citryl-N3-octenoyl-N3-hydroxy-1,3-diaminopropane
Ethanolamine
ORF4
[4]
N5-Ethanolamine-N1-citryl-N3-octenoyl-N3-hydroxy-1,3-diaminopropane
α-Ketoglutarate
ORF5
[5]
Baumannoferrin

formation of amide or ester bonds between the amino or hydroxyl group of a variety of substrates with the C5 carboxyl group of α–ketoglutarate (87, 263). Type C catalyzes the formation of amine or ester bonds between a variety of substrates and the other prochiral carboxyl group of citrate (87, 263). The baumannoferrin gene cluster from AYE encodes three such NIS synthetases, ORF1, ORF4, and ORF5 (Fig. 17A), which are classified as type A, type C, and type B siderophore synthetases, respectively.

ORF1, which has similarity to a type A synthetase that is related to AcbA of the acinetoferrin cluster, could transfer N^3-2-octenoyl-N^3-hydroxy-1,3-diaminopropane to the carboxyl end of citrate forming N^1-citryl-N^3-octenoyl-N^3-1,3-diaminopropane (reaction **[3]**). ORF4 has similarity to the type C synthetase AcsC which transfers ethanolamine to the carboxyl end of citrate in the assembly of achromobactin. Therefore, we speculate that ORF4 has a similar function in the assembly of baumannoferrin, catalyzing the formation of the intermediate N^5-ethanolamine-N^1-citryl-N^3-octenoyl-N^3-hydroxy-1,3-diaminopropane (reaction **[4]**). ORF5, which has homology to the type B achromobactin synthetase, AcsA, could be responsible for condensing the C5 carboxyl portion of α-ketoglutarate with either an amino or hydroxyl group of the substrate, that has been linked to citrate by the type A and type C synthetases. Therefore, in baumannoferrin assembly, ORF5 could transfer α-ketoglutarate to the amino end of ethanolamine (reaction **[5]**). However, ORF5 could not link a molecule of α-ketoglutarate to 1,3-DAP because the carboxyl group on 1,3-DAP would act as a steric obstacle. Steric hindrance by the carboxyl group has been proposed for other siderophores, like staphyloferrin B, which has a derivative of diaminopropane as a precursor (264).

This mechanism for the production of the baumannoferrin siderophore proposes that this siderophore could be assembled from one molecule of citrate, 1,3-diaminopropane, ethanolamine and α-ketoglutarate (Fig. 18). The predicted general structure of baumannoferrin shares similarities with acinetoferrin (Fig. 19) and could use some of the same precursors for the synthesis of this hydroxamate siderophore. However, this model differs from the synthesis of acinetoferrin in that the baumannoferrin cluster contains three siderophore synthetases instead of two. The third siderophore synthetase is predicted to be responsible for the addition of α-ketoglutarate to the ethanolamine group on baumannoferrin. One explanation for why a type B synthetase is not needed for the production of acinetoferrin is because this siderophore contains

two 1,3-DAP molecules linked to citrate, and the carboxyl groups on this precursor would hinder the addition of α-ketoglutarate by the synthetase.

Once baumannoferrin is synthesized it could be secreted to the extracellular milieu by the protein coded for by ORF3 (Fig. 17A), which has similarity to the MFS pump YhcA (Table 10), which is responsible for the export of achromobactin in *D. dadantii* (258). Once secreted into the extracellular milieu, baumannoferrin binds iron and then could be transported back into the cell through the outer membrane receptor coded for by ORF8 (Fig. 17A). A ScanProsite (249) search on putative receptor proteins coded by ORF8 revealed that a plug domain is formed by residues of the N-terminal region, while residues of the C-terminal regions form channel and TonB-interacting domains, similar to other membrane receptors involved in siderophore import (88). Furthermore, this receptor coded by ORF8 is similar to the acinetoferrin receptor, ActA, from *A. haemolyticus* ATCC 17906^T (Table 10) and was demonstrated by Funahashi *et al.* (250) to be needed for the growth under iron-chelated conditions. Once inside the cell, iron might be removed from the ferric-baumannoferrin complex by the product of ORF6 (Fig. 17A), which contains an FhuF domain, which is needed to bind the iron-sulfur clusters that are needed for removal of iron from siderophores by a redox reaction (252).

Figure 19. The structure of baumannoferrin and acinetoferrin. The structure of acinetoferrin was modified from (246)

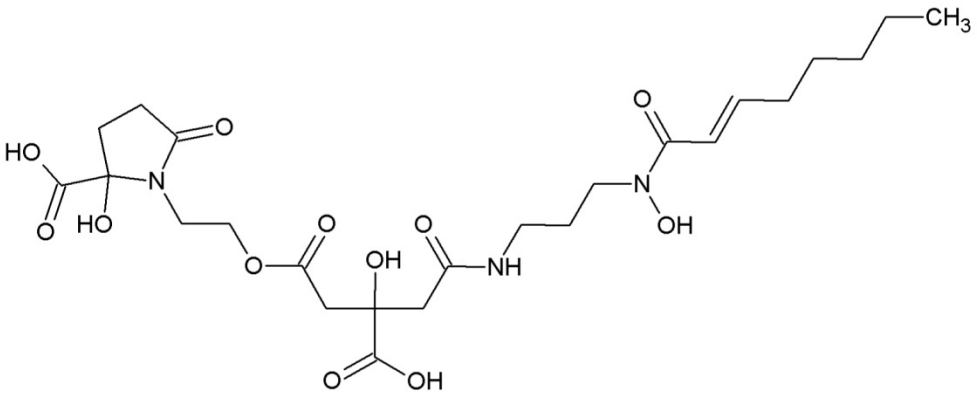

Baumannoferrin

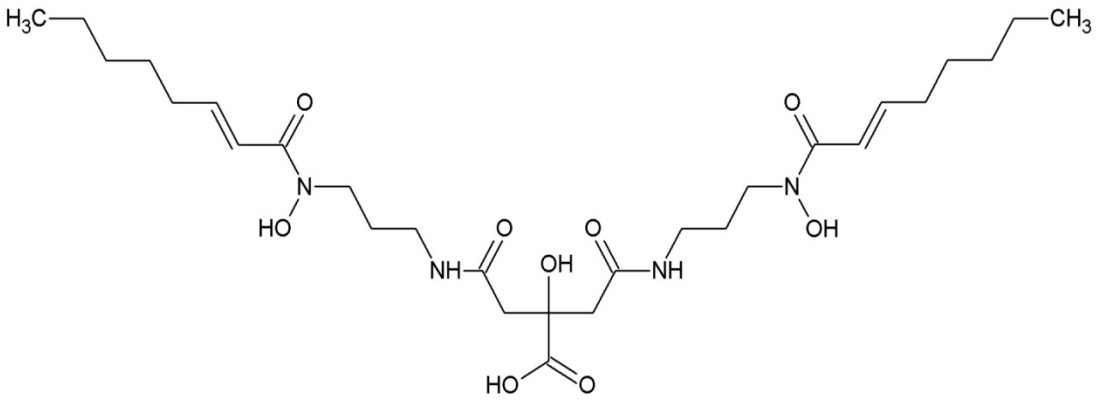

Acinetoferrin

Transcriptional analysis of the baumannoferrin gene cluster in *A. baumannii* ATCC 19606^T

Comparative genome analysis identified the baumannoferrin gene cluster in the sequenced genome of fifty *A. baumannii* clinical isolates, including ATCC 19606^T (151). However, previous research demonstrated that this hydroxamate siderophore is not produced by the type strain (51, 186). One potential reason that baumannoferrin could not be produced is that the genes from this cluster are not expressed. To investigate the expression of this hydroxamate cluster in the ATCC 19606^T type strain, RT-PCR analysis (Fig. 20) was performed on total RNA isolated from cells grown under iron-limiting conditions, using primers described in Fig. 17A. PCR products for 3727-3728 (334 bp), 3726-3729 (385 bp), 3730-3731 (352 bp), 3735-3736 (376 bp), and 3722-3734 (301 bp) were detected in ATCC 19606^T cDNA and corresponded to amplicon sizes that were obtained with control PCR reactions using ATCC 19606^T genomic DNA as a template (data not shown). Furthermore, without the addition of reverse transcriptase, no products were amplified from the RNA template (Fig. 20, lane 9), indicating that the RT-PCR products detected were attributable to the mRNA present in the template sample. These results indicate that genes from the baumannoferrin cluster in ATCC 19606^T are transcribed under iron-limiting conditions. The putative receptor protein (ORF8) that is located within the siderophore gene cluster (Fig. 17A) was also expressed under iron-limiting conditions (Fig. 20, lane 5) and could be responsible for the uptake of this siderophore, explaining the ability of ATCC 19606^T to utilize baumannoferrin. However, further research is needed to characterize this receptor and to determine its role in uptake. Transcriptional analysis of the baumannoferrin gene cluster revealed that the failure of ATCC 19606^T to produce this siderophore might not be due to lack of transcription, although not all genes involved in the biosynthesis, secretion, and uptake of this siderophore were examined. Bioinformatics prediction suggests that ORF4 and ORF5, whose gene expression was not investigated, are part of a polycistronic operon (from ORF1 to ORF7) and that a lack of or disruption to their transcription would be evidenced by the absence of a cDNA amplicon with the primers 3735 and 3736.

It is possible that the cause of the lack of production of this hydroxamate siderophore lies in the activity of proteins involved in synthesis of baumannoferrin. A comparison of the predicted amino acid sequences of enzymes involved in baumannoferrin production from AYE and ATCC 19606^T revealed a small number of differences in the amino acid residues between the proteins needed for siderophore synthesis. However, the identity of the critical amino acids

Figure 20. Transcriptional analysis of the baumannoferrin cluster in *A. baumannii* ATCC 19606^{T}. RT-PCR was performed on RNA samples isolated from ATCC 19606^{T} grown under iron-limiting conditions. Agarose gel electrophoresis was used to analyze the RT-PCR products of 3727-3728 (lane 1), 3726-3729 (lane 2), 3730-3731 (lane 3), 3733-3736 (lane 4), 3722-3734 (lane 5) and 3732-3733 (lane 6). Transcription of *recA* (2531-2532) was employed as a control (lane 7). RT-PCR reactions with *recA* were also spiked with DNA (lane 8) or contained no RT-enzymes (lane 9). Lambda *Hin*dIII (λ) was used as a size marker.

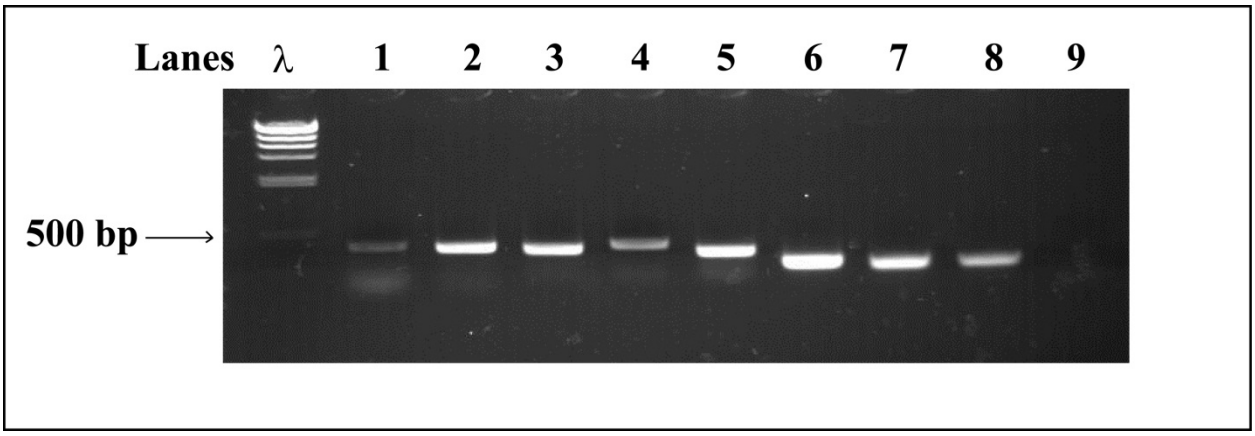
Lanes λ 1 2 3 4 5 6 7 8 9
500 bp ⟶

needed for activity of these proteins is unknown. Similarly, in *Yersinia pseudotuberculosis*, the inability to produce aerobactin is most likely due to a mutation in an amino acid of a conserved domain of an enzyme involved in its synthesis (265). *In silico* examination of the amino acid sequence of ORF7 revealed that the protein product from ATCC 19606^T was one amino acid (205 aa) longer than the putative protein product of AYE (204 aa). However, we cannot rule out the possibility that this amino acid addition is due to a sequencing error in one of the two genomes; further research is needed to determine not only if this difference is genuine but also what role this protein plays in siderophore biosynthesis.

Another possibility is that ATCC 19606^T does not produce baumannoferrin because it lacks the necessary precursor for the production of the hydroxamate siderophore. The gene(s) needed for the synthesis of this precursor could be located in another region of the genome. This situation resembles what is seen with the *entA* gene in *A. baumannii* and the ornithine decarboxylase gene that is needed for the production of alcaligin in *Bordetella* spp. (186, 266). Alternatively, this precursor may not be produced because either ATCC 19606^T does not possess the gene(s) or, these gene(s) are not functional due to a mutation. This latter scenario is similar to AYE and its inability to produce DHBA due to a point mutation in *entA* (186).

Conclusions

In this chapter, we presented biochemical and functional evidence that demonstrates the acinetobactin-deficient *A. baumannii* AYE strain grows under iron-limiting conditions by producing an uncharacterized hydroxamate siderophore to acquire iron. This work is the first to show directly the production of a siderophore, which we have named baumannoferrin. Comparative genomic analysis identified the putative siderophore cluster that is responsible for the production of baumannoferrin and is present in the genome of fifty *A. baumannii* clinical isolates, including the type strain ATCC 19606^T (150, 151). This baumannoferrin gene cluster has a total of twelve ORFs, which include genes that encode proteins involved in synthesis, secretion and uptake of this siderophore. Sequence similarity searches revealed that proteins from this cluster have homology to proteins from the recently identified acinetoferrin cluster in *A. haemolyticus* ATCC 17906^T and the achromobactin gene cluster that is found in different *Pseudomonas* species. Because the baumannoferrin cluster contains proteins that are part of the NIS siderophore assembly pathway, we were able to use the similarities of the synthetases involved in production of this uncharacterized hydroxamate siderophore to propose a structure for baumannoferrin, which could be synthesized from citrate, 1,3-diaminopropane, ethanolamine and α-ketoglutarate (Fig. 18). The structure of this hydroxamate siderophore remains to be experimentally confirmed to validate our proposed model and the proteins that comprise the components of the baumannoferrin-mediate systems need to be functionally characterized.

Results from the *in silico* studies indicated that the *A. baumannii* type strain ATCC 19606^T also contains the baumannoferrin gene cluster, but previous reports have demonstrated that this strain is solely dependent upon acinetobactin for acquisition of iron (51, 186). We were unsuccessful in determining the reason why ATCC 19606^T does not produce baumannoferrin but we speculate that it could be due to a change in amino acids that comprise critical residues needed for the activity of enzymes involved in the synthesis of the siderophore. A more comprehensive study of the *A. baumannii* strains that actually produce baumannoferrin could allow for *in silico* identification of important residues needed for activity. We also cannot rule out the possibility that the additional amino acid found in ORF7 in ATCC 19606^T could result in an inactive protein that would not allow for the production of baumannoferrin. However, even though the type strain does not produce this siderophore, the putative receptor proteins encoded by ORF8 could still be functional, as data from the siderophore utilization assay indicate that

ATCC 19606^T can utilize baumannoferrin under iron-limiting conditions by a BauA-independent mechanism.

A comparison of the siderophore-mediated iron acquisition capability of AYE and ATCC 19606^T reinforce initial observations that were proposed by Dorsey *et al.* (148) who demonstrated that different *A. baumannii* clinical isolates express different iron acquisition systems. Additional research is needed to determine whether other *A. baumannii* isolates have the ability to produce the siderophore from both the acinetobactin and baumannoferrin systems or if strains select the siderophore that is best adaptive to their environment. Examination of a strain that produces both siderophores would allow for the determination of the role these siderophores play in virulence and whether one siderophore is preferentially employed at different stages of infection. It is also possible that one siderophore is more important for growth *in vitro* under iron limitation than *in vivo,* as observed for enterobactin and yersiniabactin in *Klebsiella pneumoniae* (267).

Chapter 5

Summary

A. baumannii has emerged as a global pathogen that is responsible for a wide range of nosocomial infections. Diseases associated with this opportunistic pathogen normally occur in immunocompromised patients in the form of pneumonia, bacteremia, urinary tract infections, and necrotizing fasciitis (1, 8, 20). Infections are not limited to hospital settings, as evident by the significant number of infections in military personnel who sustained traumatic injuries during war conflicts (23). The ability of this pathogen to adapt to the hospital environment and express resistance to a broad range of antimicrobials has led to *A. baumannii* outbreaks and therapeutic challenges in treating infected individuals. With the advent of pan-drug resistant clinical isolates, the number of available antibiotics to use for treatment has decreased and because of this, research into the discovery of new therapeutic targets is needed. A comprehensive understanding of the virulence factors used by this pathogen to cause infection could help in the discovery of these potential targets. One such factor that has been experimentally proven to be necessary for the pathogenesis of *A. baumannii* in multiple virulence models is the production and utilization of the iron-chelating siderophore acinetobactin.

Acinetobactin enables *A. baumannii* to circumvent iron limitation in the host caused by innate immune proteins, like transferrin and lactoferrin, resulting in "nutritional immunity" (68). Acinetobactin was first reported in 1994 by Yamamoto *et al.* (171), who elucidated the structure of this siderophore, which is synthesized from *N*-hydroxyhistamine, L-threonine, and 2,3-dihydroxybenzoic acid (DHBA). Its structure is closely related to the structure of anguibactin, which is produced by the fish pathogen *V. anguillarum* (51). The acinetobactin gene cluster was identified and described in the type strain ATCC 19606^T by Dorsey *et al.* (51) and Mihara *et al.* (52). Nucleotide sequence analysis of this gene cluster determined that it is comprised of 18 genes that are involved in the production, secretion and utilization of this siderophore. However, the acinetobactin gene cluster lacks the gene coding for an EntA-like protein, which is needed for the production of the acinetobactin precursor DHBA.

The characterization of the *entA* ortholog in ATCC 19606^T

A main objective of this work was to locate the *entA* ortholog of *A. baumannii* ATCC 19606^T and determine its role in siderophore production and virulence. We located this gene in a

non-contiguous genomic region, and further *in silico* analysis of this region indicated that *entA* is flanked by genes coding for a possible uncharacterized molybdenum transporter system and a putative *entB* gene coding for an isochorismatase. To characterize the involvement of the *entA* ortholog in acinetobactin production, we generated the isogenic derivative 3069. The 3069 *entA* deficient mutant was unable to grow under iron-restricted conditions imposed by the presence of the synthetic iron chelator, DIP. Biochemical and HPLC analyses also indicated that this isogenic derivative did not produce the DHBA moiety that is needed for synthesis of acinetobactin.

This non-contiguous cluster also contains an *entB* ortholog that is related to the *basF* gene found within the acinetobactin gene cluster. *In silico* analysis of the protein products coded for by these two genes showed that both proteins have the isochorismatase lyase (ICL) domain needed to convert isochorismate to 2,3-dihydroxy-2,3-dihydrobenzoic acid but only BasF contains the aryl carrier protein (ArCP) domain that is needed for the tethering of an activated DHBA molecule that allows for chain elongation in siderophore biosynthesis (268). To confirm that EntB possessed a functional ICL domain, we performed genetic complementation experiments on an *E. coli entB*-deficient AN192 strain and determined that the ATCC 19606^T EntB could restore the production of enterobactin. Interestingly, in this study, we determined the location of a point mutation that affected the activity of the ICL domain of EntB in the *E. coli* AN192 isogenic derivative, which was generated over 40 years ago by chemical mutagenesis (269). Even though the EntB of ATCC 19606^T is missing the domain needed for tethering DHBA, it was able to complement the AN192 strain because this point mutation disturbed the activity of ICL domain but not the ArCP domain of EntB in the AN192 strain.

The fact that both the *entA* and the *entB* orthologs are found outside the acinetobactin cluster in *A. baumannii* ATCC 19606^T and other *A. baumannii* strains that were investigated in this study could indicate that this non-contiguous locus may have arisen through horizontal gene transfer or chromosomal rearrangement. This claim is supported by the observation that *A. baumannii* has the ability to rearrange its genome by swapping, acquiring, or deleting genes that code for a wide range of functions and that this ability has led to genomic diversity among clinical isolates (270, 271). For example, *A. baumannii* ATCC 17978 contains a gene cluster that codes for the fimsbactin siderophore, which was most likely acquired by horizontal gene transfer, as evidenced by fact that this cluster is flanked by inverted repeats and has an open

reading frame coding for putative transposition function (53, 154, 156). Interestingly, *entA* is found within the fimsbactin gene cluster and is not located in the non-contiguous locus that was described in ATCC 19606^T, and it shares low sequence similarity with *entA* from ATCC 17978. ATCC 17978 does not contain the non-contiguous locus that is present in ATCC 19606^T and other strains, which strengths the argument of genome diversity among *A. baumannii* strains.

Another reason that *entA* is located outside the acinetobactin cluster might be that it is a remnant of an ancestral DHBA-based siderophore system that was used for iron acquisition prior to the procurement of the acinetobactin gene cluster. This ancestral siderophore system might have consisted of DHBA as in *Brucella abortus* (272). However, Chipperfield and Ratledge (273)proposed that DHBA can act as a low-affinity siderophore when ferric iron is readily soluble but cannot act as a siderophore when iron is complexed with iron-binding proteins such as transferrin or lactoferrin. This suggests a selective advantage for *A. baumannii* acquiring and retaining the acinetobactin-mediated system, which can act as a high-affinity siderophore system to sequester iron from host proteins to obtain this essential micronutrient and mount a successful infection in the human host.

In this study, we also demonstrated that the *entA* ortholog was essential for ATCC 19606^T to cause a successful infection in both A549 human alveolar epithelial cells and *G. mellonella* virulence assays. In both models, the 3069 *entA* mutant displayed a decreased virulence phenotype when compared to the parental strain and also to the s1 *basD* mutant. This could be explained by the fact that the s1 mutant retains the ability to produce acinetobactin intermediates and the DHBA moiety, which could act as low-affinity siderophores.

Taken together, the results show that DHBA is essential for the pathogenesis of ATCC 19606^T, making EntA a potential target for new antimicrobial drugs. Drugs that inhibit the function of EntA will block the production of DHBA and consequently prevent the synthesis of siderophores that use the catechol moiety as a precursor. However, EntA may not be a good potential target if bacteria produce a catechol-based siderophore and a hydroxamate or carboxylate siderophore, which do not use DHBA as a precursor. To effectively inhibit the productions of two different siderophores from two different structural classes one would have to either find a common target needed for the synthesis of both siderophore-mediated systems or use different inhibitors in combination.

Iron acquisition by the baumannoferrin-mediated system in *A. baumannii* AYE

We also examined the components of the ATCC 19606^T gene cluster containing the *entA* ortholog with four other *A. baumannii* genomes (AB0057, AB307-294, ACICU, and AYE) and observed that the predicted EntA protein from the AYE clinical isolate is 29 amino acids shorter than the predicted protein of ATCC 19606^T (186). Biochemical and HPLC analyses of AYE revealed that this clinical isolate does not produce DHBA or acinetobactin. Our initial expectation was that AYE would have a growth phenotype that mirrors the ATCC 19606^T 3069 *entA* isogenic derivative when grown in iron-chelated conditions. Surprisingly, this clinical isolate actually grew better than ATCC 19606^T in LB broth supplemented with increasing concentrations of DIP. The fact that this natural *entA* mutant is able to grow under iron-limiting conditions suggests that AYE might produce an uncharacterized siderophore to acquire iron. The production of this siderophore could be mediated by the gene cluster that was identified by Antunes *et al.* (151) and Eijkelkamp *et al.* (150) using *in silico* approaches. Interestingly, Antunes *et al.* (155) also demonstrated that the acinetobactin-deficient AYE strain can successfully kill *G. mellonella* caterpillars at a similar rate as other *A. baumannii* clinical strains, indicating that this clinical isolate can utilize this uncharacterized siderophore to acquire the iron needed for pathogenesis. Taken together, these results indicate that this strain is not dependent upon acinetobactin to cause an infection, thus demonstrating that *entA* is not essential for all *A. baumannii* strains.

Since we found that AYE does not make acinetobactin due to a mutation in *entA* but produces a siderophore, we wanted to determine the chemical nature of this uncharacterized siderophore produced by AYE and possibly elucidate the structure. Chemical analysis performed on XAD-7 purified siderophore revealed that it contained a hydroxamate moiety but did not possess a catechol group, which is consistent with the fact that this strain is a natural *entA* mutant. To further purify the XAD-7 preparation, we ran the purified material over a C-18 HPLC column and collected the resulting fractions. Analysis of the collected fractions using the CAS reagent and siderophore utilization assays revealed that we obtained two fractions that were positive for siderophore activity. The results from the CAS assay and other biochemical assays performed throughout this study strongly support the fact that we have isolated a hydroxamate siderophore, which the structure still needed to be determined. Until the structure has been elucidated, we gave this uncharacterized siderophore the tentative name of baumannoferrin.

To establish a possible structure for baumannoferrin, we examined the gene cluster that was identified by Antunes *et al.* (151), which contains genes coding for protein products involved in the production, synthesis, and utilization of this siderophore. The results from similarity searches revealed that proteins coded for by ORFs involved in siderophore production from the baumannoferrin locus belong to the NRPS-independent siderophore (NIS) biosynthesis pathway class of synthetases. The NIS pathway, which is responsible for the production of hydroxamate and carboxylate siderophores, has only recently began to be studied, and how siderophores are assembled by enzymes from this pathway is not understood as well as how catechol siderophores are produced by non-ribosomal peptide synthetases (NRPS) (87, 274). This NIS pathway uses nucleotide triphosphate-dependent synthetase to condense substrates to either citrate or succinate and these enzymes only contain one active site, which is in contrast to the NRPS, which are multimodular enzymes responsible for the production of siderophores, like acinetobactin (87, 263, 274). The first NIS biosynthetic pathway described was for the production of aerobactin, which is produced in enteric bacteria, like *E. coli* (88, 254). The aerobactin pathway possesses two synthetases, IucA and IucC, that are needed to condense lysine moieties to a molecule of citrate (262). Every NIS pathway that has been identified to date contains at least one synthetase that has sequence similarity to a synthetase in the aerobactin pathway, and this has become the hallmark of the NIS pathway (87). Analysis of the proteins encoded by the genes involved in baumannoferrin synthesis revealed three enzymes, ORF1, ORF4, and ORF5, which are NIS synthetases and could be used to assemble this siderophore from one molecule each of citrate, 1,3-diaminopropane, ethanolamine, and α-ketoglutarate. The elucidation of the structure of baumannoferrin is needed to validate our proposed model (Fig. 18) for the synthesis of this siderophore. The structure is also required for further investigations into the physicochemical properties of baumannoferrin.

RT-PCR data from this study showed that genes from the ATCC 19606^T baumannoferrin locus are transcribed, and that failure to produce this siderophore in this particular strain could be due to the lack of activity of proteins produced by these ORFs. *In silico* analysis revealed differences in the amino acid sequence of the proteins potentially involved in synthesis of baumannoferrin between ATCC 19606^T and AYE. We speculate that ATCC 19606^T does not produce this hydroxamate siderophore because of changes in the amino acid sequence in one protein involved in production of baumannoferrin. The fact that ATCC 19606^T contains the gene

clusters needed for the synthesis of acinetobactin and baumannoferrin but only produces acinetobactin resembles a situation reported in *V. anguillarum*. This fish pathogen has the ability to produce the chromosome-encoded vanchrobactin. Additionally, strains of the O1 serotype contain the pJM1 plasmid for the production of anguibactin (275-277); however, they only produce anguibactin. It was determined that vanchrobactin is not produced by these strains because the gene that encodes the NRPS enzyme VabF is inactivated by the RS1 insertion sequence (278). Interestingly, this insertion sequence was originally described in the pJM1 plasmid, which contains the anguibactin gene cluster and removal of RS1 from *vabF* reactivates vanchrobactin production (107, 278). It has been proposed that *vabF* could have been inactivated because anguibactin is a better iron chelator than vanchrobactin and natural selection consequently forced the loss of the vanchrobactin (228, 275). One possible explanation as to why only strains from the O1 serotype contain the pJM plasmid is because the LPS O side-chain present in this serotype is needed for the stability of anguibactin outer membrane receptor FatA and that strains from other serotype do not possess LPS that can stabilize FatA (279).

Despite not being able to produce baumannoferrin, ATCC 19606^T can utilize this siderophore to grow under iron-limiting conditions. Uptake of baumannoferrin could be attributed to the putative siderophore receptor that is coded for by ORF8, which is supported by the RT-PCR data that indicated that the coding sequence is transcribed in ATCC 19606^T. This resembles observation regarding the O1 serotype of *V. anguillarum.* Despite not being able to produce vanchrobactin, *V. anguillarum* 775 was experimentally proven to be able to utilize this siderophore for growth under iron-chelated conditions (280-282). The uptake of this siderophore was mediated by the outer membrane receptor, FtvA, which is encoded by a gene located within the vanchrobactin cluster (277, 281).

In contrast to *V. anguillarum*, there are numerous reports of pathogens that produce more than one siderophore, including *E. coli*, *P. aeruginosa*, *Staphylococcus aureus*, and *Bacillus anthracis* (58). As previously stated, both the acinetobactin and the baumannoferrin gene clusters were identified in the genomes of almost fifty different *A. baumannii* clinical isolates that were examined, suggesting that these siderophore clusters could be found ubiquitously in this pathogen (151). The fact that both of these siderophore-mediated iron acquisition systems can be found in the majority of isolates has led to a working model (Fig. 21), which depicts an *A. baumannii* strain that produces both acinetobactin and baumannoferrin to acquire iron. In this

model, baumannoferrin is secreted from the cytoplasm by the MFS efflux pump encoded by ORF3 and then transported back into the cell by the predicted product from ORF8, which encodes an outer membrane receptor. Figure 21 also illustrates that some components needed for utilization and secretion of this siderophore have not been identified within the baumannoferrin gene cluster, and might be carried out by hypothetical proteins encoded within this locus. ORF10 and ORF11, which have similarity to a transmembrane helix and an ABC transporter permease, respectively, which might be components of a cognate transport system needed to transport ferric-baumannoferrin from the periplasmic space to the cytoplasm. There also could be other components, like a membrane fusion protein (MFP) and an outer membrane channel (OMC), that are needed to facilitate the secretion of baumannoferrin from the cytoplasm to the extracellular milieu. These components could interact with the product of ORF3, constituting a one-step secretion pathway, or the ORF3 product could secrete baumannoferrin into the periplasm in a two-step secretion pathway. Future experiments are needed to identify and characterize these other components.

Future studies are needed to survey which *A. baumannii* strains produce the hydroxamate siderophore and whether there are strains which can produce both acinetobactin and baumannoferrin. The identification of a strain that produces both siderophores would allow for examination of the role each siderophore has in the virulence of this nosocomial pathogen. One siderophore could be employed at a different growth stage or at different times during the infection process. An example of siderophore being produced at different growth phases is seen with achromobactin and chrysobactin. When grown under iron-limiting conditions, *Dickeya dadantii* will first produce achromobactin before chrysobactin, and as time progresses, this bacterium increases production of chrysobactin and decreases achromobactin synthesis (258). It was speculated that achromobactin was produced first as a preventive system to help cells cope with the transient loss of iron until chrysobactin could be produced (258).

Siderophores have been implicated in allowing pathogens to cause infection in certain tissues in the human host, as in *K. pneumoniae.* Normally this pathogen produces enterobactin, but it can also produce other siderophores, such aerobactin and yersiniabactin (267, 283). Those strains that produce both enterobactin and yersiniabactin are isolated at a greater frequency in

Figure 21. Proposed model for acinetobactin- and baumannoferrin-mediated iron acquisition in *A. baumannii*. This model depicts an *A. baumannii* strain that produces both siderophores as indicated by the grey and brown triangles, which represent acinetobactin and baumannoferrin, respectively. In this model, acinetobactin is secreted by BarA/B, but other secretion systems could be involved in export (red arrow). BarA/B can transport acinetobactin by either a one-step (blue arrow) or a two-step (orange arrow) secretion pathway. Baumannoferrin is secreted by ORF3 and can also be secreted by either a one-step (purple arrow) or a two-step (pink arrow) pathway. Ferric-acinetobactin and ferric-baumannoferrin are transported back into the cell by the outer membrane receptors, BauA and ORF8. Both siderophores are transported from the periplasmic space into the cell by their cognate ABC transport system, which in the case of baumannoferrin has yet to be determined.

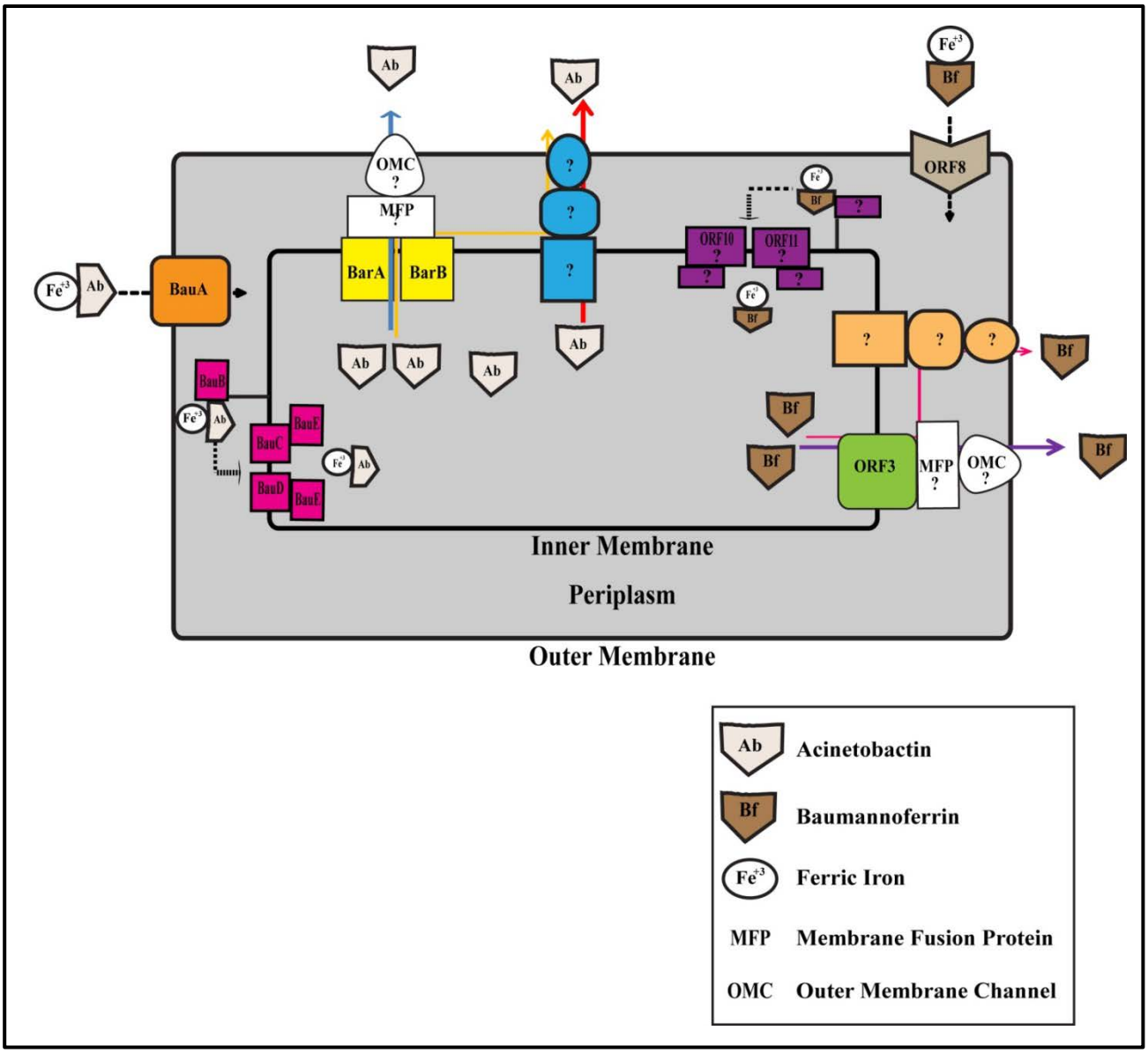
Ab
Ab
Fe+3
Bf
OMC
?
MFP
?
BarA
BarB
?
?
?
ORF8
Fe+3
Bf
?
ORF10
?
?
ORF11
?
?
Fe+3
Bf
Fe+3
Ab
BauA
Ab
Ab
Ab
Ab
?
?
?
Bf
BauB
Fe+3
Ab
BauC
BauE
Fe+3
Ab
BauD
BauE
Bf
Bf
ORF3
MFP
?
OMC
?
Bf
Inner Membrane
Periplasm
Outer Membrane
Ab
Acinetobactin
Bf
Baumannoferrin
Fe+3
Ferric Iron
MFP
Membrane Fusion Protein
OMC
Outer Membrane Channel

lung infections than those that only produce enterobactin (267). Yersiniabactin is an important virulence factor in pulmonary infections because of the high concentration of the innate immune protein lipocalin-2 (Lcn2) (267, 283). Lcn2 sequesters enterobactin preventing it from binding iron, but yersiniabactin is not sequestered by this host protein, allowing for acquisition of iron, which promotes respiratory tract infections (267, 283).

The role of BarA and BarB in acinetobactin secretion

This dissertation also examined how acinetobactin is secreted. Knowledge of how apo-siderophores are secreted from the cells is still lacking, which is surprising considering how much work has been involved in understanding the components of siderophore-mediated iron acquisition. Research from these studies has led to a greater understanding of the biosynthesis and uptake of siderophores but has done very little to describe the cell machinery involved in the secretion of siderophores from the cytoplasm. The known machinery involved in the export of siderophores represents members of both the major facilitator superfamily (MFS) and the ATP-binding cassette (ABC) transporter family. To both characterize how acinetobactin is secreted and to expand the knowledge of the export machinery involved in siderophore secretion, we examined the two genes, *barA* and *barB*, which are located within the acinetobactin locus and code for putative ABC transporters.

In silico analysis of BarA/B from ATCC 19606^T revealed that both of these proteins contain a permease domain that is tethered to an ABC domain, which has the hallmark Walker motifs present in ABC transporters, as well as the characteristic domain architecture of bacterial ABC exporters with fused ATPase and permease components (191). Disruption of the *barA/B* genes of ATCC 19606^T resulted in a decreased growth phenotype under iron-chelated conditions and contributed to a 40% reduction in the amount of acinetobactin secreted by this mutant. The inability of the 3213 *barA/B* mutant to export this siderophore efficiently also contributed to a reduced virulence phenotype in *ex vivo* and *in vivo* models. However, the fact that this mutant secretes some acinetobactin makes it more virulent than the s1 isogenic derivative, which does not secrete mature acinetobactin.

Since acinetobactin and anguibactin are structurally related to one another and there is high similarity between BarA and ORF14 (46.8% identity) and BarB and ORF15 (49.6 % identity), we did not anticipate the results obtained by HPLC analysis, which showed that the

3213 *barA/B* mutant had a reduction and not a complete abrogation of secreted acinetobactin. We expected the *barA/barB* mutant to have a similar phenotype to what was seen with the disruption of ORF14 in the anguibactin system of *V. anguillarum* 775, in which the ORF14 isogenic derivative showed a complete abolishment of anguibactin production (170). This reduction in the amount of acinetobactin secretion was also in contrast to previous research described by other investigators, who demonstrated that mutations in the ABC transporters needed for the secretion of pyoverdine (105) and salmochelin (106) led to a sharp decrease or complete loss of siderophore secretion. Acinetobactin might be exported by an alternative secretion system that involves one of the many efflux pumps that are present in this pathogen (195, 196). *A. baumannii* contains numerous exporters that belong to the ABC, MFS, RND, and MATE superfamilies (195). Some of these transporters are responsible for the efflux of antibiotics from the cell, which contributes to the lack of success of many therapeutic agents in treating *A. baumannii* infections (195). Because efflux systems are highly prevalent in *A. baumannii*, it is possible that acinetobactin is being secreted by non-specific export systems, such as those associated with antibiotic resistance.

Participation of multidrug efflux pumps as alternative transport systems for siderophore secretion has also been suggested as an explanation for the reduction in the amount of enterobactin and vibrioferrin secreted by the EntS-deficient *E. coli* strain and the PvsC-deficient *V. parahaemolyticus* (93, 95). The investigators who examined these siderophore exporters suggested that proteins from the RND superfamily might be responsible for the secretion of these siderophores to prevent deleterious effects caused by an intracellular accumulation of enterobactin or vibrioferrin (93, 95). Because *A. baumannii* contains a large number of RND transporters involved in export (195, 227), these transporters could be responsible for the efflux of acinetobactin into the extracellular milieu by the BarA/B deficient ATCC 19606^T 3213 strain. RND exporters have been shown to transport a very broad range of substrates including antibiotics, detergents, dyes, and siderophores (197, 284, 285). RND transporters that could be involved in the secretion of acinetobactin are AdeABC, AdeFGH, and AdeIJK efflux pumps, which are present in ATCC 19606^T and provide intrinsic antibiotic resistance (195, 197).

Our results showed a reduction in and not a loss of secreted acinetobactin in the absence of *barA/B*, leading us to propose that an alternative transport system is involved in secretion of this siderophore. This alternative secretion system, depicted in Fig. 21 in blue, could be one of

the many exporters that *A. baumannii* possesses, such as the RND exporters mentioned previously. To give credence to this claim, preliminary analysis of random insertion mutants generated by Emily Ohneck using the EZ::TN <R6K*γori*/KAN-2> tnp transposome system on the *A. baumannii* M2 strain revealed that an AdeK mutant had a growth defect on LB agar supplemented with increasing concentration of DIP. AdeK is the outer membrane factor of the AdeIJK RND efflux pump (200). Future studies are needed to determine whether a mutation in AdeK results in a similar phenotype in ATCC 19606^{T}.

The secretion of acinetobactin might depend upon BarA/B interacting with an MFP and an OMC to form a complex that traverses the cell envelope. These proteins are not encoded by genes located within the acinetobactin gene cluster. This complex could be involved in a one-step secretion pathway that directly exports acinetobactin from the cytoplasm to the extracellular milieu, as illustrated in Fig. 21. This figure also illustrates the possibility that BarA/B does not form a secretion system complex and that efflux occurs by a two-step secretion pathway, in which acinetobactin is exported to the periplasmic space by BarA/B, and then another transport system secretes acinetobactin into the extracellular milieu. A two-step secretion pathway has been experimentally demonstrated for the transport of pyoverdine in *P. aeruginosa* PAO1, in which the ABC transporter PvdE is needed for the secretion of pyoverdine to the periplasmic space, which is then exported from the cell by the efflux pump, PvdRT-OpmQ (105, 110). In our study, multiple attempts to generate an antibody against both BarA/B to be used to determine if these ABC transporters interact with other proteins failed because overexpression of these two proteins could not be achieved and consequently the interactions among these two ABC transporters with other proteins could not be determined. One possible reason that we could never overexpress these proteins is that overexpression of integral membrane proteins can be toxic to the cell, thus resulting in low yields of target proteins (286). Future attempts might employ a cell-free system (287) to produce high yields of BarA/B for generation of antibodies to determine if these two ABC transporters interact with other proteins to form a one-step secretion pathway.

In this work, we characterized components of the acinetobactin-mediated system that were not yet studied or identified and determined their roles not only in iron acquisition but also in virulence. We also determined the chemical nature of the uncharacterized siderophore produced by the AYE clinical isolate, which we called baumannoferrin, and proposed a structure

for this siderophore based on *in silico* examination of genes predicted to be involved in synthesis of this siderophore. The gene cluster responsible for the production of baumannoferrin, which was identified by comparative genomic studies, marks the fourth siderophore-mediated system found in this nosocomial pathogen. Two of these gene clusters, the DHBA-based siderophore found in 8399 and fimsbactin found in ATCC 17978, have been infrequently reported in the sequenced genomes of *A. baumannii*. In contrast, the acinetobactin- and baumannoferrin-mediated systems are found in almost all examined clinical isolates (151). The fact that both these siderophore-mediated iron acquisition systems are found in the majority of isolates led to the working model shown in Fig. 21, which proposes a mechanism for *A. baumannii* strains to use both acinetobactin and baumannoferrin to acquire the iron that they need not only for cellular processes but also to cause a successful infection in the human host. This model also indicates multiple transporters that might be involved in acinetobactin secretion. The results obtained throughout the course of this work have provided data needed for a number of future experiments to further expand our understanding of how acinetobactin is secreted and to characterize components of the baumannoferrin-mediated system. A more comprehensive understanding of how this pathogen acquires iron using these siderophore-mediated systems has the potential to yield new targets for the development of therapeutic agents to combat *A. baumannii.*

References

1. **Peleg AY, de Breij A, Adams MD, Cerqueira GM, Mocali S, Galardini M, Nibbering PH, Earl AM, Ward DV, Paterson DL, Seifert H, Dijkshoorn L.** 2012. The success of *Acinetobacter* species; genetic, metabolic and virulence attributes. PLoS one **7:**e46984.
2. **Visca P, Seifert H, Towner KJ.** 2011. *Acinetobacter* infection--an emerging threat to human health. IUBMB Life **63:**1048-1054.
3. **Gennari M, Parini M, Volpon D, Serio M.** 1992. Isolation and characterization by conventional methods and genetic transformation of *Psychrobacter* and *Acinetobacter* from fresh and spoiled meat, milk and cheese. Int J Food Microbiol **15:**61-75.
4. **Berlau J, Aucken HM, Houang E, Pitt TL.** 1999. Isolation of *Acinetobacter* spp. including *A. baumannii* from vegetables: implications for hospital-acquired infections. J Hosp Infect **42:**201-204.
5. **Berlau J, Aucken H, Malnick H, Pitt T.** 1999. Distribution of *Acinetobacter* species on skin of healthy humans. Eur J Clin Microbiol Infect Dis **18:**179-183.
6. **Fournier PE, Richet H.** 2006. The epidemiology and control of *Acinetobacter* baumannii in health care facilities. Clin Infect Dis **42:**692-699.
7. **Peleg AY, Seifert H, Paterson DL.** 2008. *Acinetobacter baumannii*: emergence of a successful pathogen. Clin Microbiol Rev **21:**538-582.
8. **Bergogne-Berezin E, Towner KJ.** 1996. *Acinetobacter* spp. as nosocomial pathogens: microbiological, clinical, and epidemiological features. Clin. Microbiol. Rev. **9:**148-165.
9. **Zarrilli R, Crispino M, Bagattini M, Barretta E, Di Popolo A, Triassi M, Villari P.** 2004. Molecular epidemiology of sequential outbreaks of *Acinetobacter baumannii* in an intensive care unit shows the emergence of carbapenem resistance. J Clin Microbiol **42:**946-953.
10. **Perez F, Ponce-Terashima R, Adams MD, Bonomo RA.** 2011. Are we closing in on an "elusive enemy"? The current status of our battle with *Acinetobacter baumannii*. Virulence **2:**86-90.
11. **Ong CW, Lye DC, Khoo KL, Chua GS, Yeoh SF, Leo YS, Tambyah PA, Chua AC.** 2009. Severe community-acquired *Acinetobacter baumannii* pneumonia: an emerging highly lethal infectious disease in the Asia-Pacific. Respirology **14:**1200-1205.

12. **Sengstock DM, Thyagarajan R, Apalara J, Mira A, Chopra T, Kaye KS.** 2010. Multidrug-resistant *Acinetobacter baumannii*: an emerging pathogen among older adults in community hospitals and nursing homes. Clin Infect Dis **50:**1611-1616.
13. **Fagon JY, Chastre J, Hance AJ, Montravers P, Novara A, Gibert C.** 1993. Nosocomial pneumonia in ventilated patients: a cohort study evaluating attributable mortality and hospital stay. Am. J. Med. **94:**281-288.
14. **Daniels TL, Deppen S, Arbogast PG, Griffin MR, Schaffner W, Talbot TR.** 2008. Mortality rates associated with multidrug-resistant *Acinetobacter baumannii* infection in surgical intensive care units. Infect Control Hosp Epidemiol **29:**1080-1083.
15. **Kalin G, Alp E, Coskun R, Demiraslan H, Gundogan K, Doganay M.** 2012. Use of high-dose IV and aerosolized colistin for the treatment of multidrug-resistant *Acinetobacter baumannii* ventilator-associated pneumonia: do we really need this treatment? J Infect Chemother **18:**872-877.
16. **Tseng CC, Liu SF, Wang CC, Tu ML, Chung YH, Lin MC, Fang WF.** 2012. Impact of clinical severity index, infective pathogens, and initial empiric antibiotic use on hospital mortality in patients with ventilator-associated pneumonia. Am J Infect Control **40:**648-652.
17. **Blot S, Vandewoude K, Colardyn F.** 2003. Nosocomial bacteremia involving *Acinetobacter baumannii* in critically ill patients: a matched cohort study. Intensive Care Med **29:**471-475.
18. **Rodriguez Guardado A, Blanco A, Asensi V, Perez F, Rial JC, Pintado V, Bustillo E, Lantero M, Tenza E, Alvarez M, Maradona JA, Carton JA.** 2008. Multidrug-resistant *Acinetobacter* meningitis in neurosurgical patients with intraventricular catheters: assessment of different treatments. J Antimicrob Chemother **61:**908-913.
19. **Liu YM, Chi CY, Ho MW, Chen CM, Liao WC, Ho CM, Lin PC, Wang JH.** 2005. Microbiology and factors affecting mortality in necrotizing fasciitis. J Microbiol Immunol Infect **38:**430-435.
20. **Charnot-Katsikas A, Dorafshar AH, Aycock JK, David MZ, Weber SG, Frank KM.** 2009. Two cases of necrotizing fasciitis due to *Acinetobacter baumannii*. J Clin Microbiol **47:**258-263.

21. **Sebeny PJ, Riddle MS, Petersen K.** 2008. *Acinetobacter baumannii* skin and soft-tissue infection associated with war trauma. Clin Infect Dis **47:**444-449.
22. **Davis KA, Moran KA, McAllister CK, Gray PJ.** 2005. Multidrug-resistant *Acinetobacter* extremity infections in soldiers. Emerg Infect Dis **11:**1218-1224.
23. **O'Shea MK.** 2012. *Acinetobacter* in modern warfare. Int J Antimicrob Agents **39:**363-375.
24. **Scott P, Deye G, Srinivasan A, Murray C, Moran K, Hulten E, Fishbain J, Craft D, Riddell S, Lindler L, Mancuso J, Milstrey E, Bautista CT, Patel J, Ewell A, Hamilton T, Gaddy C, Tenney M, Christopher G, Petersen K, Endy T, Petruccelli B.** 2007. An outbreak of multidrug-resistant *Acinetobacter baumannii-calcoaceticus* complex infection in the US military health care system associated with military operations in Iraq. Clin Infect Dis **44:**1577-1584.
25. **Griffith ME, Gonzalez RS, Holcomb JB, Hospenthal DR, Wortmann GW, Murray CK.** 2008. Factors associated with recovery of *Acinetobacter baumannii* in a combat support hospital. Infect Control Hosp Epidemiol **29:**664-666.
26. **Yun HC, Murray CK, Roop SA, Hospenthal DR, Gourdine E, Dooley DP.** 2006. Bacteria recovered from patients admitted to a deployed U.S. military hospital in Baghdad, Iraq. Mil Med **171:**821-825.
27. **Bayuga S, Zeana C, Sahni J, Della-Latta P, el-Sadr W, Larson E.** 2002. Prevalence and antimicrobial patterns of *Acinetobacter baumannii* on hands and nares of hospital personnel and patients: the iceberg phenomenon again. Heart Lung **31:**382-390.
28. **Huang YC, Su LH, Wu TL, Leu HS, Hsieh WS, Chang TM, Lin TY.** 2002. Outbreak of *Acinetobacter baumannii* bacteremia in a neonatal intensive care unit: clinical implications and genotyping analysis. Pediatr Infect Dis J **21:**1105-1109.
29. **Wagenvoort JH, De Brauwer EI, Toenbreker HM, van der Linden CJ.** 2002. Epidemic *Acinetobacter baumannii* strain with MRSA-like behaviour carried by healthcare staff. Eur J Clin Microbiol Infect Dis **21:**326-327.
30. **Garnacho-Montero J, Ortiz-Leyba C, Fernandez-Hinojosa E, Aldabo-Pallas T, Cayuela A, Marquez-Vacaro JA, Garcia-Curiel A, Jimenez-Jimenez FJ.** 2005. *Acinetobacter baumannii* ventilator-associated pneumonia: epidemiological and clinical findings. Intensive Care Med **31:**649-655.

31. **Dijkshoorn L, Nemec A, Seifert H.** 2007. An increasing threat in hospitals: multidrug-resistant *Acinetobacter baumannii*. Nat Rev Microbiol **5:**939-951.
32. **Wisplinghoff H, Schmitt R, Wohrmann A, Stefanik D, Seifert H.** 2007. Resistance to disinfectants in epidemiologically defined clinical isolates of *Acinetobacter baumannii*. J Hosp Infect **66:**174-181.
33. **Jawad A, Seifert H, Snelling AM, Heritage J, Hawkey PM.** 1998. Survival of *Acinetobacter baumannii* on dry surfaces: comparison of outbreak and sporadic isolates. J Clin Microbiol **36:**1938-1941.
34. **Catalano M, Quelle LS, Jeric PE, Di Martino A, Maimone SM.** 1999. Survival of *Acinetobacter baumannii* on bed rails during an outbreak and during sporadic cases. J Hosp Infect **42:**27-35.
35. **Cerqueira GM, Peleg AY.** 2011. Insights into *Acinetobacter baumannii* pathogenicity. IUBMB Life **63:**1055-1060.
36. **Maragakis LL, Perl TM.** 2008. *Acinetobacter baumannii*: epidemiology, antimicrobial resistance, and treatment options. Clin Infect Dis **46:**1254-1263.
37. **Talbot GH, Bradley J, Edwards JE, Jr., Gilbert D, Scheld M, Bartlett JG.** 2006. Bad bugs need drugs: an update on the development pipeline from the Antimicrobial Availability Task Force of the Infectious Diseases Society of America. Clin Infect Dis **42:**657-668.
38. **Diancourt L, Passet V, Nemec A, Dijkshoorn L, Brisse S.** 2010. The population structure of *Acinetobacter baumannii*: expanding multiresistant clones from an ancestral susceptible genetic pool. PLoS one **5:**e10034.
39. **Higgins PG, Dammhayn C, Hackel M, Seifert H.** 2010. Global spread of carbapenem-resistant *Acinetobacter baumannii*. J Antimicrob Chemother **65:**233-238.
40. **Neely AN.** 2000. A survey of gram-negative bacteria survival on hospital fabrics and plastics. J Burn Care Rehabil **21:**523-527.
41. **Tomaras AP, Dorsey CW, Edelmann RE, Actis LA.** 2003. Attachment to and biofilm formation on abiotic surfaces by *Acinetobacter baumannii*: involvement of a novel chaperone-usher pili assembly system. Microbiology **149:**3473-3484.

42. **Lee JC, Koerten H, van den Broek P, Beekhuizen H, Wolterbeek R, van den Barselaar M, van der Reijden T, van der Meer J, van de Gevel J, Dijkshoorn L.** 2006. Adherence of *Acinetobacter baumannii* strains to human bronchial epithelial cells. Res Microbiol **157:**360-366.

43. **Lee HW, Koh YM, Kim J, Lee JC, Lee YC, Seol SY, Cho DT.** 2008. Capacity of multidrug-resistant clinical isolates of *Acinetobacter baumannii* to form biofilm and adhere to epithelial cell surfaces. Clin Microbiol Infect **14:**49-54.

44. **Gaddy JA, Tomaras AP, Actis LA.** 2009. The *Acinetobacter baumannii* 19606 OmpA Protein Plays a Role in Biofilm Formation on Abiotic Surfaces and the Interaction of This Pathogen with Eukaryotic Cells. Infect Immun **77:**3150-3160.

45. **de Breij A, Gaddy J, van der Meer J, Koning R, Koster A, van den Broek P, Actis L, Nibbering P, Dijkshoorn L.** 2009. CsuA/BABCDE-dependent pili are not involved in the adherence of *Acinetobacter baumannii* ATCC19606^{T} to human airway epithelial cells and their inflammatory response. Res Microbiol **160:**213-218.

46. **Lee JS, Kim JW, Choi CH, Lee WK, Chung HY, Lee JC.** 2008. Anti-tumor activity of *Acinetobacter baumannii* outer membrane protein A on dendritic cell-based immunotherapy against murine melanoma. J Microbiol **46:**221-227.

47. **Choi CH, Lee JS, Lee YC, Park TI, Lee JC.** 2008. *Acinetobacter baumannii* invades epithelial cells and outer membrane protein A mediates interactions with epithelial cells. BMC Microbiol **8:**216.

48. **Choi CH, Lee EY, Lee YC, Park TI, Kim HJ, Hyun SH, Kim SA, Lee SK, Lee JC.** 2005. Outer membrane protein 38 of *Acinetobacter baumannii* localizes to the mitochondria and induces apoptosis of epithelial cells. Cell Microbiol **7:**1127-1138.

49. **Kim SW, Choi CH, Moon DC, Jin JS, Lee JH, Shin JH, Kim JM, Lee YC, Seol SY, Cho DT, Lee JC.** 2009. Serum resistance of *Acinetobacter baumannii* through the binding of factor H to outer membrane proteins. FEMS Microbiol Lett **301:**224-231.

50. **Russo TA, Luke NR, Beanan JM, Olson R, Sauberan SL, MacDonald U, Schultz LW, Umland TC, Campagnari AA.** 2010. The K1 capsular polysaccharide of *Acinetobacter baumannii* strain 307-0294 is a major virulence factor. Infect Immun **78:**3993-4000.

51. **Dorsey CW, Tomaras AP, Connerly PL, Tolmasky ME, Crosa JH, Actis LA.** 2004. The siderophore-mediated iron acquisition systems of *Acinetobacter baumannii* ATCC 19606 and *Vibrio anguillarum* 775 are structurally and functionally related. Microbiology **150:**3657-3667.

52. **Mihara K, Tanabe T, Yamakawa Y, Funahashi T, Nakao H, Narimatsu S, Yamamoto S.** 2004. Identification and transcriptional organization of a gene cluster involved in biosynthesis and transport of acinetobactin, a siderophore produced by *Acinetobacter baumannii* ATCC 19606^{T}. Microbiology **150:**2587-2597.

53. **Zimbler DL, Penwell WF, Gaddy JA, Menke SM, Tomaras AP, Connerly PL, Actis LA.** 2009. Iron acquisition functions expressed by the human pathogen *Acinetobacter baumannii*. Biometals **22:**23-32.

54. **Posey JE, Gherardini FC.** 2000. Lack of a role for iron in the Lyme disease pathogen. Science **288:**1651-1653.

55. **Schaible UE, Kaufmann SH.** 2004. Iron and microbial infection. Nat Rev Microbiol **2:**946-953.

56. **Weinberg ED.** 1997. The *Lactobacillus* anomaly: total iron abstinence. Perspect Biol Med **40:**578-583.

57. **Krewulak KD, Vogel HJ.** 2008. Structural biology of bacterial iron uptake. Biochim Biophys Acta **1778:**1781-1804.

58. **Crosa JH, Mey AR, Payne SM.** 2004. Iron transport in bacteria. ASM Press, Washington, D.C.

59. **Andrews SC, Robinson AK, Rodriguez-Quinones F.** 2003. Bacterial iron homeostasis. FEMS Microbiol Rev **27:**215-237.

60. **Stintzi A, Barnes C, Xu J, Raymond KN.** 2000. Microbial iron transport via a siderophore shuttle: a membrane ion transport paradigm. Proc Natl Acad Sci U S A **97:**10691-10696.

61. **Bullen JJ, Rogers HJ, Spalding PB, Ward CG.** 2006. Natural resistance, iron and infection: a challenge for clinical medicine. J Med Microbiol **55:**251-258.

62. **Rohmer L, Hocquet D, Miller SI.** 2011. Are pathogenic bacteria just looking for food? Metabolism and microbial pathogenesis. Trends Microbiol **19:**341-348.

63. **Johnson EE, Wessling-Resnick M.** 2012. Iron metabolism and the innate immune response to infection. Microbes Infect **14:**207-216.
64. **Weinberg ED.** 2009. Iron availability and infection. Biochim Biophys Acta **1790:**600-605.
65. **Doherty CP.** 2007. Host-pathogen interactions: the role of iron. J Nutr **137:**1341-1344.
66. **Skaar EP.** 2010. The battle for iron between bacterial pathogens and their vertebrate hosts. PLoS Pathog **6:**e1000949.
67. **Touati D.** 2000. Iron and oxidative stress in bacteria. Arch Biochem Biophys **373:**1-6.
68. **Chu BC, Garcia-Herrero A, Johanson TH, Krewulak KD, Lau CK, Peacock RS, Slavinskaya Z, Vogel HJ.** 2010. Siderophore uptake in bacteria and the battle for iron with the host; a bird's eye view. Biometals **23:**601-611.
69. **Ganz T.** 2009. Iron in innate immunity: starve the invaders. Curr Opin Immunol **21:**63-67.
70. **Nemeth E, Tuttle MS, Powelson J, Vaughn MB, Donovan A, Ward DM, Ganz T, Kaplan J.** 2004. Hepcidin regulates cellular iron efflux by binding to ferroportin and inducing its internalization. Science **306:**2090-2093.
71. **Nemeth E, Rivera S, Gabayan V, Keller C, Taudorf S, Pedersen BK, Ganz T.** 2004. IL-6 mediates hypoferremia of inflammation by inducing the synthesis of the iron regulatory hormone hepcidin. J Clin Invest **113:**1271-1276.
72. **Mickelsen A, Sparling PF.** 1981. Ability of *Neisseria gonorrhoeae*, *Neisseria meningitidis*, and commensal *Neisseria* species to obtain iron from transferrin and iron compounds. Infect. Immun. **33:**555-564.
73. **Simonson C, Brener D, De Voe IW.** 1982. Expression of a high-affinity mechanism for acquisition of transferrin iron by *Neisseria meningitidis*. Infect. Immun. **36:**107-113.
74. **Schryvers AB.** 1988. Characterization of the human transferrin and lactoferrin receptors in *Haemophilus influenzae*. Mol Microbiol **2:**467-472.
75. **Wandersman C, Delepelaire P.** 2004. Bacterial iron sources: from siderophores to hemophores. Annu Rev Microbiol **58:**611-647.
76. **Wandersman C, Stojiljkovic I.** 2000. Bacterial heme sources: the role of heme, hemoprotein receptors and hemophores. Curr Opin Microbiol **3:**215-220.

77. **Loeb MR.** 1995. Ferrochelatase activity and protoporphyrin IX utilization in *Haemophilus influenzae*. J Bacteriol **177:**3613-3615.

78. **Stull TL.** 1987. Protein sources of heme for *Haemophilus influenzae*. Infect Immun **55:**148-153.

79. **Henderson DP, Payne SM.** 1994. Characterization of the *Vibrio cholerae* outer membrane heme transport protein HutA: sequence of the gene, regulation of expression, and homology to the family of TonB-dependent proteins. J Bacteriol **176:**3269-3277.

80. **Arnoux P, Haser R, Izadi N, Lecroisey A, Delepierre M, Wandersman C, Czjzek M.** 1999. The crystal structure of HasA, a hemophore secreted by *Serratia marcescens*. Nat Struct Biol **6:**516-520.

81. **Rossi MS, Fetherston JD, Letoffe S, Carniel E, Perry RD, Ghigo JM.** 2001. Identification and characterization of the hemophore-dependent heme acquisition system of *Yersinia pestis*. Infect Immun **69:**6707-6717.

82. **Crosa JH, Walsh CT.** 2002. Genetics and assembly line enzymology of siderophore biosynthesis in bacteria. Microbiol Mol Biol Rev **66:**223-249.

83. **Saha R, Saha N, Donofrio RS, Bestervelt LL.** 2012. Microbial siderophores: a mini review. J Basic Microbiol.

84. **Boukhalfa H, Crumbliss AL.** 2002. Chemical aspects of siderophore mediated iron transport. Biometals **15:**325-339.

85. **Neilands JB.** 1995. Siderophores: structure and function of microbial iron transport compounds. J Biol Chem **270:**26723-26726.

86. **Barry SM, Challis GL.** 2009. Recent advances in siderophore biosynthesis. Curr Opin Chem Biol **13:**205-215.

87. **Challis GL.** 2005. A widely distributed bacterial pathway for siderophore biosynthesis independent of nonribosomal peptide synthetases. Chembiochem **6:**601-611.

88. **Miethke M, Marahiel MA.** 2007. Siderophore-based iron acquisition and pathogen control. Microbiol Mol Biol Rev **71:**413-451.

89. **Lambalot RH, Gehring AM, Flugel RS, Zuber P, LaCelle M, Marahiel MA, Reid R, Khosla C, Walsh CT.** 1996. A new enzyme superfamily - the phosphopantetheinyl transferases. Chem Biol **3:**923-936.

90. **Saidijam M, Benedetti G, Ren Q, Xu Z, Hoyle CJ, Palmer SL, Ward A, Bettaney KE, Szakonyi G, Meuller J, Morrison S, Pos MK, Butaye P, Walravens K, Langton K, Herbert RB, Skurray RA, Paulsen IT, O'Reilly J, Rutherford NG, Brown MH, Bill RM, Henderson PJ.** 2006. Microbial drug efflux proteins of the major facilitator superfamily. Curr Drug Targets **7:**793-811.

91. **Saier MH, Jr., Beatty JT, Goffeau A, Harley KT, Heijne WH, Huang SC, Jack DL, Jahn PS, Lew K, Liu J, Pao SS, Paulsen IT, Tseng TT, Virk PS.** 1999. The major facilitator superfamily. J Mol Microbiol Biotechnol **1:**257-279.

92. **Law CJ, Maloney PC, Wang DN.** 2008. Ins and outs of major facilitator superfamily antiporters. Annu Rev Microbiol **62:**289-305.

93. **Furrer JL, Sanders DN, Hook-Barnard IG, McIntosh MA.** 2002. Export of the siderophore enterobactin in *Escherichia coli*: involvement of a 43 kDa membrane exporter. Mol Microbiol **44:**1225-1234.

94. **Page WJ, Kwon E, Cornish AS, Tindale AE.** 2003. The *csbX* gene of *Azotobacter vinelandii* encodes an MFS efflux pump required for catecholate siderophore export. FEMS Microbiol Lett **228:**211-216.

95. **Tanabe T, Nakao H, Kuroda T, Tsuchiya T, Yamamoto S.** 2006. Involvement of the *Vibrio parahaemolyticus pvsC* gene in export of the siderophore vibrioferrin. Microbiol Immunol **50:**871-876.

96. **Brickman TJ, McIntosh MA.** 1992. Overexpression and purification of ferric enterobactin esterase from *Escherichia coli*. Demonstration of enzymatic hydrolysis of enterobactin and its iron complex. J Biol Chem **267:**12350-12355.

97. **Bleuel C, Grosse C, Taudte N, Scherer J, Wesenberg D, Krauss GJ, Nies DH, Grass G.** 2005. TolC is involved in enterobactin efflux across the outer membrane of *Escherichia coli*. J Bacteriol **187:**6701-6707.

98. **Biemans-Oldehinkel E, Doeven MK, Poolman B.** 2006. ABC transporter architecture and regulatory roles of accessory domains. FEBS Lett **580:**1023-1035.

99. **Locher KP, Lee AT, Rees DC.** 2002. The *E. coli* BtuCD structure: a framework for ABC transporter architecture and mechanism. Science **296:**1091-1098.

100. **Heddle J, Scott DJ, Unzai S, Park SY, Tame JR.** 2003. Crystal structures of the liganded and unliganded nickel-binding protein NikA from *Escherichia coli*. J Biol Chem **278:**50322-50329.

101. **Navarro C, Wu LF, Mandrand-Berthelot MA.** 1993. The *nik* operon of *Escherichia coli* encodes a periplasmic binding-protein-dependent transport system for nickel. Mol Microbiol **9:**1181-1191.

102. **Cruz-Ramos H, Cook GM, Wu G, Cleeter MW, Poole RK.** 2004. Membrane topology and mutational analysis of *Escherichia coli* CydDC, an ABC-type cysteine exporter required for cytochrome assembly. Microbiology **150:**3415-3427.

103. **Poole RK, Hatch L, Cleeter MW, Gibson F, Cox GB, Wu G.** 1993. Cytochrome bd biosynthesis in *Escherichia coli:* the sequences of the *cydC* and *cydD* genes suggest that they encode the components of an ABC membrane transporter. Mol Microbiol **10:**421-430.

104. **Polissi A, Georgopoulos C.** 1996. Mutational analysis and properties of the *msbA* gene of *Escherichia coli,* coding for an essential ABC family transporter. Mol Microbiol **20:**1221-1233.

105. **Yeterian E, Martin LW, Guillon L, Journet L, Lamont IL, Schalk IJ.** 2010. Synthesis of the siderophore pyoverdine in *Pseudomonas aeruginosa* involves a periplasmic maturation. Amino Acids **38:**1447-1459.

106. **Crouch ML, Castor M, Karlinsey JE, Kalhorn T, Fang FC.** 2008. Biosynthesis and IroC-dependent export of the siderophore salmochelin are essential for virulence of *Salmonella enterica* serovar Typhimurium. Mol Microbiol **67:**971-983.

107. **Di Lorenzo M, Stork M, Tolmasky ME, Actis LA, Farrell D, Welch TJ, Crosa LM, Wertheimer AM, Chen Q, Salinas P, Waldbeser L, Crosa JH.** 2003. Complete sequence of virulence plasmid pJM1 from the marine fish pathogen *Vibrio anguillarum* strain 775. J. Bacteriol. **185:**5822-5830.

108. **Zhu WM, Arceneaux JEL, Beggs ML, Byers BR, Eisenach KD, Lundrigan MD.** 1998. Exochelin genes in *Mycobacterium smegmatis*: identification of an ABC transporter and two non-ribosomal peptide synthetase genes. Mol Microbiol **29:**629-639.

109. **McMorran BJ, Merriman ME, Rombel IT, Lamont IL.** 1996. Characterisation of the *pvdE* gene which is required for pyoverdine synthesis in *Pseudomonas aeruginosa.* Gene **176:**55-59.

110. **Hannauer M, Yeterian E, Martin LW, Lamont IL, Schalk IJ.** 2010. An efflux pump is involved in secretion of newly synthesized siderophore by *Pseudomonas aeruginosa*. FEBS Lett **584:**4751-4755.

111. **Imperi F, Tiburzi F, Visca P.** 2009. Molecular basis of pyoverdine siderophore recycling in *Pseudomonas aeruginosa*. Proc Natl Acad Sci U S A **106:**20440-20445.

112. **Ferguson AD, Breed J, Diederichs K, Welte W, Coulton JW.** 1998. An internal affinity-tag for purification and crystallization of the siderophore receptor FhuA, integral outer membrane protein from *Escherichia coli* K-12. Protein Sci **7:**1636-1638.

113. **Buchanan SK, Smith BS, Venkatramani L, Xia D, Esser L, Palnitkar M, Chakraborty R, van der Helm D, Deisenhofer J.** 1999. Crystal structure of the outer membrane active transporter FepA from *Escherichia coli*. Nat Struct Biol **6:**56-63.

114. **Cobessi D, Celia H, Folschweiller N, Schalk IJ, Abdallah MA, Pattus F.** 2005. The crystal structure of the pyoverdine outer membrane receptor FpvA from *Pseudomonas aeruginosa* at 3.6 angstroms resolution. J Mol Biol **347:**121-134.

115. **Cobessi D, Celia H, Pattus F.** 2004. Crystallization and X-ray diffraction analyses of the outer membrane pyochelin receptor FptA from *Pseudomonas aeruginosa*. Acta Crystallogr D Biol Crystallogr **60:**1919-1921.

116. **Ferguson AD, Chakraborty R, Smith BS, Esser L, van der Helm D, Deisenhofer J.** 2002. Structural basis of gating by the outer membrane transporter FecA. Science **295:**1715-1719.

117. **Chakraborty R, Lemke EA, Cao Z, Klebba PE, van der Helm D.** 2003. Identification and mutational studies of conserved amino acids in the outer membrane receptor protein, FepA, which affect transport but not binding of ferric-enterobactin in *Escherichia coli*. Biometals **16:**507-518.

118. **Ferguson AD, Braun V, Fiedler HP, Coulton JW, Diederichs K, Welte W.** 2000. Crystal structure of the antibiotic albomycin in complex with the outer membrane transporter FhuA. Protein Sci **9:**956-963.

119. **Postle K, Larsen RA.** 2007. TonB-dependent energy transduction between outer and cytoplasmic membranes. Biometals **20:**453-465.

120. **Noinaj N, Guillier M, Barnard TJ, Buchanan SK.** 2010. TonB-dependent transporters: regulation, structure, and function. Annu Rev Microbiol **64:**43-60.

121. **Clarke TE, Ku SY, Dougan DR, Vogel HJ, Tari LW.** 2000. The structure of the ferric siderophore binding protein FhuD complexed with gallichrome. Nat Struct Biol **7:**287-291.

122. **Halle F, Meyer JM.** 1992. Iron release from ferrisiderophores. A multi-step mechanism involving a NADH/FMN oxidoreductase and a chemical reduction by FMNH2. Eur J Biochem **209:**621-627.

123. **Zhu M, Valdebenito M, Winkelmann G, Hantke K.** 2005. Functions of the siderophore esterases IroD and IroE in iron-salmochelin utilization. Microbiology **151:**2363-2372.

124. **Lin H, Fischbach MA, Liu DR, Walsh CT.** 2005. In vitro characterization of salmochelin and enterobactin trilactone hydrolases IroD, IroE, and Fes. J Am Chem Soc **127:**11075-11084.

125. **Miethke M, Klotz O, Linne U, May JJ, Beckering CL, Marahiel MA.** 2006. Ferri-bacillibactin uptake and hydrolysis in *Bacillus subtilis*. Mol Microbiol **61:**1413-1427.

126. **Enz S, Mahren S, Stroeher UH, Braun V.** 2000. Surface signaling in ferric citrate transport gene induction: interaction of the FecA, FecR, and FecI regulatory proteins. J Bacteriol **182:**637-646.

127. **Braun V, Mahren S, Ogierman M.** 2003. Regulation of the FecI-type ECF sigma factor by transmembrane signalling. Curr Opin Microbiol **6:**173-180.

128. **Hollander A, Mercante AD, Shafer WM, Cornelissen CN.** 2011. The iron-repressed, AraC-like regulator MpeR activates expression of *fetA* in *Neisseria gonorrhoeae*. Infect Immun **79:**4764-4776.

129. **Anderson MT, Armstrong SK.** 2004. The BfeR regulator mediates enterobactin-inducible expression of *Bordetella enterobactin* utilization genes. J Bacteriol **186:**7302-7311.

130. **Masse E, Vanderpool CK, Gottesman S.** 2005. Effect of RyhB small RNA on global iron use in *Escherichia coli*. J Bacteriol **187:**6962-6971.

131. **Wee S, Neilands J, Bittner M, Hemming B, Haymore B, Seetharam R.** 1988. Expression, isolation, and properties of Fur (ferric uptake regulation) protein of *Escherichia coli* K-2. Biol. Metals **1:**62-68.

132. **Carpenter BM, Whitmire JM, Merrell DS.** 2009. This is not your mother's repressor: the complex role of fur in pathogenesis. Infect Immun **77:**2590-2601.

133. **Bagg A, Neilands JB.** 1987. Ferric uptake regulation protein acts as a repressor, employing iron (II) as a cofactor to bind the operator of an iron transport operon in *Escherichia coli*. Biochemistry **26:**5471-5477.

134. **Hantke K.** 1981. Regulation of ferric iron transport in *Escherichia coli* K12: isolation of a constitutive mutant. Mol Gen Genet **182:**288-292.

135. **Rombel IT, McMorran BJ, Lamont IL.** 1995. Identification of a DNA sequence motif required for expression of iron-regulated genes in pseudomonads. Mol Gen Genet **246:**519-528.

136. **Baichoo N, Helmann JD.** 2002. Recognition of DNA by Fur: a reinterpretation of the Fur box consensus sequence. J Bacteriol **184:**5826-5832.

137. **Lavrrar JL, McIntosh MA.** 2003. Architecture of a fur binding site: a comparative analysis. J Bacteriol **185:**2194-2202.

138. **McHugh JP, Rodriguez-Quinones F, Abdul-Tehrani H, Svistunenko DA, Poole RK, Cooper CE, Andrews SC.** 2003. Global iron-dependent gene regulation in *Escherichia coli*. A new mechanism for iron homeostasis. J Biol Chem **278:**29478-29486.

139. **Escolar L, Perez-Martin J, de Lorenzo V.** 1999. Opening the iron box: transcriptional metalloregulation by the Fur protein. J Bacteriol **181:**6223-6229.

140. **Foster JW, Hall HK.** 1992. Effect of *Salmonella typhimurium* ferric uptake regulator (fur) mutations on iron- and pH-regulated protein synthesis. J Bacteriol **174:**4317-4323.

141. **Mollmann U, Heinisch L, Bauernfeind A, Kohler T, Ankel-Fuchs D.** 2009. Siderophores as drug delivery agents: application of the "Trojan Horse" strategy. Biometals **22:**615-624.

142. **Xu YP, Miller MJ.** 1998. Total syntheses of mycobactin analogues as potent antimycobacterial agents using a minimal protecting group strategy. J Org Chem **63:**4314-4322.

143. **McPherson CJ, Aschenbrenner LM, Lacey BM, Fahnoe KC, Lemmon MM, Finegan SM, Tadakamalla B, O'Donnell JP, Mueller JP, Tomaras AP.** 2012. Clinically Relevant Gram-Negative Resistance Mechanisms Have No Effect on the Efficacy of MC-1, a Novel Siderophore-Conjugated Monocarbam. Antimicrob Agents Chemother **56:**6334-6342.

144. **Brown KA, Ratledge C.** 1975. The effect of p-aminosalicyclic acid on iron transport and assimilation in mycobacteria. Biochim Biophys Acta **385:**207-220.

145. **May JJ, Kessler N, Marahiel MA, Stubbs MT.** 2002. Crystal structure of DhbE, an archetype for aryl acid activating domains of modular nonribosomal peptide synthetases. Proc Natl Acad Sci U S A **99:**12120-12125.

146. **Miethke M, Bisseret P, Beckering CL, Vignard D, Eustache J, Marahiel MA.** 2006. Inhibition of aryl acid adenylation domains involved in bacterial siderophore synthesis. Febs J **273:**409-419.

147. **Ferreras JA, Ryu JS, Di Lello F, Tan DS, Quadri LE.** 2005. Small-molecule inhibition of siderophore biosynthesis in *Mycobacterium tuberculosis* and *Yersinia pestis*. Nat Chem Biol **1:**29-32.

148. **Dorsey CW, Beglin MS, Actis LA.** 2003. Detection and analysis of iron uptake components expressed by *Acinetobacter baumannii* clinical isolates. J. Clin. Microbiol. **41:**4188-4193.

149. **Dorsey CW, Tolmasky ME, Crosa JH, Actis LA.** 2003. Genetic organization of an *Acinetobacter baumannii* chromosomal region harbouring genes related to siderophore biosynthesis and transport. Microbiology **149:**1227-1238.

150. **Eijkelkamp BA, Hassan KA, Paulsen IT, Brown MH.** 2011. Investigation of the human pathogen *Acinetobacter baumannii* under iron limiting conditions. BMC Genomics **12:**126.

151. **Antunes LC, Imperi F, Towner KJ, Visca P.** 2011. Genome-assisted identification of putative iron-utilization genes in *Acinetobacter baumannii* and their distribution among a genotypically diverse collection of clinical isolates. Res Microbiol **162:**279-284.

152. **Piechaud M, Second L.** 1951. Studies of 26 strains of *Moraxella Iwoffi*. Ann Inst Pasteur (Paris) **80:**97-99.

153. **Smith MG, Gianoulis TA, Pukatzki S, Mekalanos JJ, Ornston LN, Gerstein M, Snyder M.** 2007. New insights into *Acinetobacter baumannii* pathogenesis revealed by high-density pyrosequencing and transposon mutagenesis. Genes Dev **21:**601-614.

154. **Proschak A, Lubuta P, Grun P, Lohr F, Wilharm G, De Berardinis V, Bode HB.** 2013. Structure and Biosynthesis of Fimsbactins A-F, Siderophores from *Acinetobacter baumannii* and *Acinetobacter baylyi*. Chembiochem **14:**633-638.

155. **Antunes LC, Imperi F, Carattoli A, Visca P.** 2011. Deciphering the multifactorial nature of *Acinetobacter baumannii* pathogenicity. PLoS one **6:**e22674.

156. **Proschak A, Lubuta P, Grun P, Lohr F, Wilharm G, De Berardinis V, Bode HB.** 2013. Structure and Biosynthesis of Fimsbactins A-F, Siderophores from *Acinetobacter baumannii* and *Acinetobacter baylyi*. Chembiochem.

157. **Yamamoto S, Okujo N, Sakakibara Y.** 1994. Isolation and structure elucidation of acinetobactin, a novel siderophore from *Acinetobacter baumannii*. Arch Microbiol **162:**249-254.

158. **Jalal M, Hossain D, van der Helm J, Sanders-Loerh J, Actis LA, Crosa JH.** 1989. Structure of anguibactin, a unique plasmid-related bacterial siderophore from the fish pathogen *Vibrio anguillarum*. J. Am. Chem. Soc. **111:**292-296.

159. **Nahlik M, Brickman T, Ozenberg B, McIntosh M.** 1989. Nucleotide sequence and transcriptional organization of the *Escherichia coli* enterobactin biosynthesis cistrons *entB* and *entA*. J. Bacteriol. **171:**784-790.

160. **Butterton JR, Choi MH, Watnick PI, Carroll PA, Calderwood SB.** 2000. *Vibrio cholerae* VibF is required for vibriobactin synthesis and is a member of the family of nonribosomal peptide synthetases. J. Bacteriol. **182:**1731-1738.

161. **Nwugo CC, Gaddy JA, Zimbler DL, Actis LA.** 2011. Deciphering the iron response in *Acinetobacter baumannii*: A proteomics approach. J Proteomics **74:**44-58.

162. **Cuiv PO, Clarke P, O'Connell M.** 2006. Identification and characterization of an iron-regulated gene, *chtA*, required for the utilization of the xenosiderophores aerobactin, rhizobactin 1021 and schizokinen by *Pseudomonas aeruginosa*. Microbiology **152:**945-954.

163. **Funahashi T, Tanabe T, Mihara K, Miyamoto K, Tsujibo H, Yamamoto S.** 2012. Identification and characterization of an outer membrane receptor gene in *Acinetobacter baumannii* required for utilization of desferricoprogen, rhodotorulic acid, and desferrioxamine B as xenosiderophores. Biol Pharm Bull **35:**753-760.

164. **Butterton JR, Calderwood SB.** 1994. Identification, cloning, and sequencing of a gene required for ferric vibriobactin utilization by *Vibrio cholerae*. J Bacteriol **176:**5631-5638.

165. **Gaddy JA, Arivett BA, McConnell MJ, Lopez-Rojas R, Pachon J, Actis LA.** 2012. Role of acinetobactin-mediated iron acquisition functions in the interaction of *Acinetobacter baumannii* strain ATCC 19606^{T} with human lung epithelial cells, Galleria mellonella caterpillars, and mice. Infect Immun **80:**1015-1024.

166. **Towner KJ.** 2009. *Acinetobacter*: an old friend, but a new enemy. J Hosp Infect **73:**355-363.

167. **Joly-Guillou ML.** 2005. Clinical impact and pathogenicity of *Acinetobacter*. Clin Microbiol Infect **11:**868-873.

168. **Oppenheimer SJ.** 2001. Iron and its relation to immunity and infectious disease. J Nutr **131:**616S-633S; discussion 633S-635S.

169. **Farhana A, Kumar S, Rathore SS, Ghosh PC, Ehtesham NZ, Tyagi AK, Hasnain SE.** 2008. Mechanistic insights into a novel exporter-importer system of *Mycobacterium tuberculosis* unravel its role in trafficking of iron. PLoS one **3:**e2087.

170. **Tolmasky ME, Actis LA, Crosa JH.** 1988. Genetic analysis of the iron uptake region of the *Vibrio anguillarum* plasmid pJM1: molecular cloning of genetic determinants encoding a novel *trans* activator of siderophore biosynthesis. J. Bacteriol. **170:**1913-1919.

171. **Yamamoto S, Okujo N, Sakakibara Y.** 1994. Isolation and structure elucidation of acinetobactin, a novel siderophore from *Acinetobacter baumanii*. Arch. Microbiol. **162:**249-252.

172. **Sambrook J, Russell DW.** 2001. Molecular Cloning. A Laboratory Manual, 3rd ed. Cold Spring Harbor Laboratory Press, Cold Spring Harbor, N. Y.

173. **Hoang TT, Karkhoff-Schweizer RR, Kutchma AJ, Schweizer HP.** 1998. A broad-host-range Flp-FRT recombination system for site-specific excision of chromosomally-located DNA sequences: application for isolation of unmarked *Pseudomonas aeruginosa* mutants. Gene **212:**77-86.

174. **Leong SA, Ditta GS, Helinski DR.** 1982. Heme biosynthesis in *Rhizobium*: Identification of a cloned gene coding for delta-aminolevulininc acid synthetase from *Rhizobium meliloti*. J. Biol. Chem. **257:**8724-8730.

175. **Miller J.** 1972. Experiments in molecular genetics. Cold Spring Harbor Laboratory, Cold spring Harbor, N.Y.

176. **Meade HM, Long SR, Ruvkum GB, Brown SE, Ausubel FM.** 1982. Physical and genetic characterization of symbiotic and auxotrophic mutants *Rhizobium meliloti* induced by transposon Tn5 mutagenesis. J. Bacteriol. **149:**114-122.

177. **Barcak JG, Chandler MS, Redfield RJ, Tomb JF.** 1991. Genetic systems in *Haemophilus influenzae*. Methods Emzymol. **204:**321-432.

178. **Tusnady GE, Simon I.** 2001. The HMMTOP transmembrane topology prediction server. Bioinformatics **17:**849-850.

179. **Moller S, Croning MD, Apweiler R.** 2001. Evaluation of methods for the prediction of membrane spanning regions. Bioinformatics **17:**646-653.

180. **Spyropoulos IC, Liakopoulos TD, Bagos PG, Hamodrakas SJ.** 2004. TMRPres2D: high quality visual representation of transmembrane protein models. Bioinformatics **20:**3258-3260.

181. **Hulo N, Bairoch A, Bulliard V, Cerutti L, De Castro E, Langendijk-Genevaux PS, Pagni M, Sigrist CJ.** 2006. The PROSITE database. Nucleic Acids Res **34:**D227-230.

182. **Finn RD, Mistry J, Schuster-Bockler B, Griffiths-Jones S, Hollich V, Lassmann T, Moxon S, Marshall M, Khanna A, Durbin R, Eddy SR, Sonnhammer EL, Bateman A.** 2006. Pfam: clans, web tools and services. Nucleic Acids Res **34:**D247-251.

183. **Marchler-Bauer A, Lu S, Anderson JB, Chitsaz F, Derbyshire MK, DeWeese-Scott C, Fong JH, Geer LY, Geer RC, Gonzales NR, Gwadz M, Hurwitz DI, Jackson JD, Ke Z, Lanczycki CJ, Lu F, Marchler GH, Mullokandov M, Omelchenko MV, Robertson CL, Song JS, Thanki N, Yamashita RA, Zhang D, Zhang N, Zheng C, Bryant SH.** 2011. CDD: a Conserved Domain Database for the functional annotation of proteins. Nucleic Acids Res **39:**D225-229.

184. **Altschul SF, Gish W, Miller W, Myers EW, Lipman DJ.** 1990. Basic local alignment search tool. J Mol Biol **215:**403-410.

185. **Arnow L.** 1937. Colorimetric determination of the components of 3,4-dihydroxyphenylalanine-tyrosine mixtures. J. Biol. Chem. **118:**531-537.

186. **Penwell WF, Arivett BA, Actis LA.** 2012. The *Acinetobacter baumannii entA* Gene Located Outside the Acinetobactin Cluster Is Critical for Siderophore Production, Iron Acquisition and Virulence. PLoS one **7:**e36493.

187. **Lieber M, Smith B, Szakal A, Nelson-Rees W, Todaro G.** 1976. A continuous tumor-cell line from a human lung carcinoma with properties of type II alveolar epithelial cells. Int J Cancer **17:**62-70.

188. **Zimbler DL, Park TM, Arivett BA, Penwell WF, Greer SM, Woodruff TM, Tierney DL, Actis LA.** 2012. Stress Response and Virulence Functions of the *A. baumannii* NfuA Fe-S Scaffold Protein. J Bacteriol.

189. **Peleg AY, Jara S, Monga D, Eliopoulos GM, Moellering RC, Jr., Mylonakis E.** 2009. *Galleria mellonella* as a model system to study *Acinetobacter baumannii* pathogenesis and therapeutics. Antimicrob Agents Chemother **53:**2605-2609.

190. **Kaplan EL, Meier P.** 1958. Nonparametric estimation from incomplete data. J. Amer. Statist. Assn. **53:**457-481.

191. **Hollenstein K, Dawson RJ, Locher KP.** 2007. Structure and mechanism of ABC transporter proteins. Curr Opin Struct Biol **17:**412-418.

192. **Walker JE, Saraste M, Runswick MJ, Gay NJ.** 1982. Distantly related sequences in the alpha- and beta-subunits of ATP synthase, myosin, kinases and other ATP-requiring enzymes and a common nucleotide binding fold. Embo J **1:**945-951.

193. **Pedersen K, Tiainen T, Larsen JL.** 1995. Antibiotic resistance of *Vibrio anguillarum*, in relation to serovar and plasmid contents. Acta Vet Scand **36:**55-64.

194. **Vila J, Marti S, Sanchez-Cespedes J.** 2007. Porins, efflux pumps and multidrug resistance in *Acinetobacter baumannii*. J Antimicrob Chemother **59:**1210-1215.

195. **Coyne S, Courvalin P, Perichon B.** 2011. Efflux-mediated antibiotic resistance in *Acinetobacter* spp. Antimicrob Agents Chemother **55:**947-953.

196. **Iacono M, Villa L, Fortini D, Bordoni R, Imperi F, Bonnal RJ, Sicheritz-Ponten T, De Bellis G, Visca P, Cassone A, Carattoli A.** 2008. Whole-genome pyrosequencing of an epidemic multidrug-resistant *Acinetobacter baumannii* strain belonging to the European clone II group. Antimicrob Agents Chemother **52:**2616-2625.

197. **Fernando D, Kumar A.** 2012. Growth phase-dependent expression of RND efflux pump- and outer membrane porin-encoding genes in *Acinetobacter baumannii* ATCC 19606. J Antimicrob Chemother **67:**569-572.

198. **Magnet S, Courvalin P, Lambert T.** 2001. Resistance-nodulation-cell division-type efflux pump involved in aminoglycoside resistance in *Acinetobacter baumannii* strain BM4454. Antimicrob Agents Chemother **45:**3375-3380.

199. **Coyne S, Rosenfeld N, Lambert T, Courvalin P, Perichon B.** 2010. Overexpression of resistance-nodulation-cell division pump AdeFGH confers multidrug resistance in *Acinetobacter baumannii*. Antimicrob Agents Chemother **54:**4389-4393.

200. **Damier-Piolle L, Magnet S, Bremont S, Lambert T, Courvalin P.** 2008. AdeIJK, a resistance-nodulation-cell division pump effluxing multiple antibiotics in *Acinetobacter baumannii*. Antimicrob Agents Chemother **52:**557-562.

201. **Hassan KA, Brzoska AJ, Wilson NL, Eijkelkamp BA, Brown MH, Paulsen IT.** 2011. Roles of DHA2 family transporters in drug resistance and iron homeostasis in *Acinetobacter* spp. J Mol Microbiol Biotechnol **20:**116-124.

202. **Franza T, Mahe B, Expert D.** 2005. *Erwinia chrysanthemi* requires a second iron transport route dependent of the siderophore achromobactin for extracellular growth and plant infection. Mol Microbiol **55:**261-275.

203. **Nichol H, Law JH, Winzerling JJ.** 2002. Iron metabolism in insects. Annu Rev Entomol **47:**535-559.

204. **Nikaido H.** 1996. Multidrug efflux pumps of gram-negative bacteria. J Bacteriol **178:**5853-5859.

205. **Anstey NM, Currie BJ, Withnall KM.** 1991. Community-acquired *Acinetobacte*r pneumonia in the northern territory of Australia. Clin. Infect. Dis. **14:**83-91.

206. **Dijkshoorn L, Nemec A, Seifert H.** 2007. An increasing threat in hospitals: multidrug-resistant *Acinetobacter baumannii*. Nat Rev Microbiol **5:**939-951.

207. **CDC.** 2004. *Acinetobacter baumannii* infections among patients at military medcal facilities treating U.S. service members, 2002-2004. MMWR **53:**1063-1066.

208. **Crichton R.** 2009. Iron metabolism. From molecular mechanisms to clinical consequences, Third ed. John Wiley & Sons Ltd., West Sussex, United Kingdom.

209. **Weinberg ED.** 2009. Iron availability and infection. Biochim Biophys Acta **1790:**600-605.

210. **Wandersman C, Delepelaire P.** 2004. Bacterial iron sources: from siderophores to hemophores. Annu Rev Microbiol **58:**611-647.

211. **Echenique JR, Arienti H, Tolmasky ME, Read R, Staneloni J, Crosa JH, Actis LA.** 1992. Characterization of a high-affinity iron transport system in *Acinetobacter baumannii*. J. Bacteriol. **174:**7670-7679.

212. **Antunes LC, Imperi F, Towner KJ, Visca P.** 2011. Genome-assisted identification of putative iron-utilization genes in *Acinetobacter baumannii* and their distribution among a genotypically diverse collection of clinical isolates. Res Microbiol **162:**279-284.

213. **Earhart CF.** 1996. Uptake and metabolism of iron and molybdenum., p. 1075-1090. *In* Neidhardt, F. C. (ed.), *Escherichia coli* and *Salmonella*. Cellular and Molecular Biology., Second edition ed, vol. 1. American Society for Microbiology, Washington, DC.

214. **Walsh CT, Liu J, Rusnak F, Sakaitani M.** 1990. Molecular studieson enzymes in chorismate metabolism and enterobactin biosynthetic pathway. Chem. Rev. **90:**1105-1129.

215. **Feinberg AP, Vogelstein B.** 1983. A technique for radiolabeling DNA restriction endonuclease fragments to high specific activity. Anal. Biochem. **132:**6-13.

216. **Vallenet D, Nordmann P, Barbe V, Poirel L, Mangenot S, Bataille E, Dossat C, Gas S, Kreimeyer A, Lenoble P, Oztas S, Poulain J, Segurens B, Robert C, Abergel C, Claverie JM, Raoult D, Medigue C, Weissenbach J, Cruveiller S.** 2008. Comparative analysis of *Acinetobacters*: three genomes for three lifestyles. PLoS ONE **3:**e1805.

217. **Murray NE, Brammar WJ, Murray K.** 1977. Lambdoid phages that simplify the recovery of *in vitro* recombinants. Mol. Gen. Genet. **150:**53-61.

218. **Staab JF, Earhart CF.** 1990. EntG activity of *Escherichia coli* enterobactin synthetase. J Bacteriol **172:**6403-6410.

219. **Pollack JR, Ames BN, Neilands JB.** 1970. Iron transport in *Salmonella typhimurium*: mutants blocked in the biosynthesis of enterobactin. J. Bacteriol. **104:**635-639.

220. **Knauf VC, Nester EW.** 1982. Wide host range cloning vectors: a cosmid clone bank of an *Agrobacterium* Ti plasmid. Plasmid **8:**45-54.

221. **Hunger M, Schmucker R, Kishan V, Hillen W.** 1990. Analysis and nucelotide sequence of an origin of DNA replication in *Acinetobacter calcoaceticus* and its use for *Escherichia coli* shuttle plasmids. Gene **87:**45-51.

222. **Yanisch-Perron C, Vieira J, Messing J.** 1985. Improved M13phage cloning vectorsand host strains: nucleotide sequence of the M13mp18 and pUC19 vectors. Gene **33:**103-109.

223. **Altschul SF, Madden TL, Schäffer AA, Zhang J, Zhang Z, Miller W, Lipman DJ.** 1997. Gapped BLAST and PSI-BLAST: a new generation of protein database search programs. Nucleic Acids Res. **25:**3389-3402.

224. **Dorsey CW, Tomaras AP, Actis LA.** 2002. Genetic and phenotypic analysis of *Acinetobacter baumannii* insertion derivatives generated with a Transposome system. Appl. Environ. Microbiol. **68:**6353-6360.

225. **Schwyn B, Neilands JB.** 1987. Universal chemical asssay for the detection and determination of siderophores. Anal. Biochem. **160:**47-56.

226. **Adams MD, Goglin K, Molyneaux N, Hujer KM, Lavender H, Jamison JJ, MacDonald IJ, Martin KM, Russo T, Campagnari AA, Hujer AM, Bonomo RA, Gill SR.** 2008. Comparative genome sequence analysis of multidrug-resistant *Acinetobacter baumannii*. J Bacteriol **190:**8053-8064.

227. **Iacono M, Villa L, Fortini D, Bordoni R, Imperi F, Bonnal RJ, Sicheritz-Ponten T, De Bellis G, Visca P, Cassone A, Carattoli A.** 2008. Whole-genome pyrosequencing of an epidemic multidrug-resistant *Acinetobacter baumannii* strain belonging to the European clone II group. Antimicrob Agents Chemother **52:**2616-2625.

228. **Alice AF, Lopez CS, Crosa JH.** 2005. Plasmid- and chromosome-encoded redundant and specific functions are involved in biosynthesis of the siderophore anguibactin in *Vibrio anguillarum* 775: a case of chance and necessity? J Bacteriol **187:**2209-2214.

229. **Naka H, Lopez CS, Crosa JH.** 2008. Reactivation of the vanchrobactin siderophore system of *Vibrio anguillarum* by removal of a chromosomal insertion sequence originated in plasmid pJM1 encoding the anguibactin siderophore system. Environ Microbiol **10:**265-277.

230. **Snitkin ES, Zelazny AM, Montero CI, Stock F, Mijares L, Murray PR, Segre JA.** 2011. Genome-wide recombination drives diversification of epidemic strains of *Acinetobacter baumannii*. Proc Natl Acad Sci USA **108:**13758-13763.

231. **Naka H, Crosa JH.** 2012. Identification and characterization of a novel outer membrane protein receptor FetA for ferric enterobactin transport in *Vibrio anguillarum* 775 (pJM1). Biometals **25:**125-133.

232. **Zhou Z, Lai JR, Walsh CT.** 2007. Directed evolution of aryl carrier proteins in the enterobactin synthetase. Proc Natl Acad Sci U S A **104:**11621-11626.

233. **Di Lorenzo M, Stork M, Crosa JH.** Genetic and biochemical analyses of chromosome and plasmid gene homologues encoding ICL and ArCP domains in *Vibrio anguillarum* strain 775. Biometals **24:**629-643.

234. **Drake EJ, Nicolai DA, Gulick AM.** 2006. Structure of the EntB multidomain nonribosomal peptide synthetase and functional analysis of its interaction with the EntE adenylation domain. Chem Biol **13:**409-419.

235. **Barbe V, Vallenet D, Fonknechten N, Kreimeyer A, Oztas S, Labarre L, Cruveiller S, Robert C, Duprat S, Wincker P, Ornston LN, Weissenbach J, Marliere P, Cohen GN, Medigue C.** 2004. Unique features revealed by the genome sequence of *Acinetobacter* sp. ADP1, a versatile and naturally transformation competent bacterium. Nucleic Acids Res **32:**5766-5779.

236. **Kavanagh K, Reeves EP.** 2004. Exploiting the potential of insects for in vivo pathogenicity testing of microbial pathogens. FEMS Microbiol Rev **28:**101-112.

237. **Bellaire BH, Elzer PH, Baldwin CL, Roop RM, 2nd.** 2003. Production of the siderophore 2,3-dihydroxybenzoic acid is required for wild-type growth of *Brucella abortus* in the presence of erythritol under low-iron conditions in vitro. Infect Immun **71:**2927-2932.

238. **Parent MA, Bellaire BH, Murphy EA, Roop RM, 2nd, Elzer PH, Baldwin CL.** 2002. *Brucella abortus* siderophore 2,3-dihydroxybenzoic acid (DHBA) facilitates intracellular survival of the bacteria. Microb Pathog **32:**239-248.

239. **Caza M, Lepine F, Dozois CM.** 2011. Secretion, but not overall synthesis, of catecholate siderophores contributes to virulence of extraintestinal pathogenic Escherichia coli. Mol Microbiol **80:**266-282.

240. **Cendrowski S, MacArthur W, Hanna P.** 2004. *Bacillus anthracis* requires siderophore biosynthesis for growth in macrophages and mouse virulence. Mol Microbiol **51:**407-417.

241. **Falagas ME, Rafailidis PI.** 2007. Attributable mortality of *Acinetobacter baumannii*: no longer a controversial issue. Crit Care **11:**134.

242. **Garcia-Quintanilla M, Pulido MR, Lopez-Rojas R, Pachon J, McConnell MJ.** 2013. Emerging therapies for multidrug resistant *Acinetobacter baumannii*. Trends Microbiol.

243. **Falagas ME, Rafailidis PI.** 2007. Attributable mortality of *Acinetobacter baumannii*: no longer a controversial issue. Crit Care **11:**134.

244. **Fournier PE, Vallenet D, Barbe V, Audic S, Ogata H, Poirel L, Richet H, Robert C, Mangenot S, Abergel C, Nordmann P, Weissenbach J, Raoult D, Claverie JM.** 2006. Comparative genomics of multidrug resistance in *Acinetobacter baumannii*. PLoS Genet **2:**e7.

245. **Sahl JW, Gillece JD, Schupp JM, Waddell VG, Driebe EM, Engelthaler DM, Keim P.** 2013. Evolution of a pathogen: a comparative genomics analysis identifies a genetic pathway to pathogenesis in acinetobacter. PLoS one **8:**e54287.

246. **Okujo N, Sakakibara Y, Yoshida T, Yamamoto S.** 1994. Structure of acinetoferrin, a new citrate-based dihydroxamate siderophore from *Acinetobacter haemolyticus*. Biometals **7:**170-176.

247. **Payne SM.** 1994. Detection, isolation, and characterization of siderophores. Methods Enzymol **235:**329-344.

248. **Atkin CL, Neilands JB, Phaff HJ.** 1970. Rhodotorulic acid from species of *Leucosporidium, Rhodosporidium, Rhodotorula, Sporidiobolus, and Sporobolomyces*, and a new alanine-containing ferrichrome from *Cryptococcus melibiosum*. J Bacteriol **103:**722-733.

249. **Sigrist CJ, Cerutti L, de Castro E, Langendijk-Genevaux PS, Bulliard V, Bairoch A, Hulo N.** 2010. PROSITE, a protein domain database for functional characterization and annotation. Nucleic Acids Res **38:**D161-166.

250. **Funahashi T, Tanabe, T., Maki, J., Miyamoto, K., Tsujibo, H. and Yamamoto, S.** 2013. Identification and characterization of a cluster of genes involved in biosynthesis and transport of acinetoferrin, a siderophore produced by *Acinetobacter haemolyticus* ATCC 17906T. Microbiology **doi:10.1099/mic.0.065177-0**.

251. **Berti AD, Thomas MG.** 2009. Analysis of achromobactin biosynthesis by *Pseudomonas syringae* pv. syringae B728a. J Bacteriol **191:**4594-4604.

252. **Muller K, Matzanke BF, Schunemann V, Trautwein AX, Hantke K.** 1998. FhuF, an iron-regulated protein of *Escherichia coli* with a new type of [2Fe-2S] center. Eur J Biochem **258:**1001-1008.

253. **Loper JE, Ishimaru CA, Carnegie SR, Vanavichit A.** 1993. Cloning and Characterization of Aerobactin Biosynthesis Genes of the Biological Control Agent *Enterobacter cloacae*. Appl Environ Microbiol **59:**4189-4197.

254. **Gibson F, Magrath DI.** 1969. The isolation and characterization of a hydroxamic acid (aerobactin) formed by *Aerobacter aerogenes* 62-I. Biochim Biophys Acta **192:**175-184.

255. **Lynch D, O'Brien J, Welch T, Clarke P, Cuiv PO, Crosa JH, O'Connell M.** 2001. Genetic organization of the region encoding regulation, biosynthesis, and transport of rhizobactin 1021, a siderophore produced by *Sinorhizobium meliloti*. J Bacteriol **183:**2576-2585.

256. **Tanabe T, Funahashi T, Nakao H, Miyoshi S, Shinoda S, Yamamoto S.** 2003. Identification and characterization of genes required for biosynthesis and transport of the siderophore vibrioferrin in *Vibrio parahaemolyticus*. J Bacteriol **185:**6938-6949.

257. **Owen JG, Ackerley DF.** 2011. Characterization of pyoverdine and achromobactin in *Pseudomonas syringae* pv. phaseolicola 1448a. BMC Microbiol **11:**218.

258. **Franza T, Mahe B, Expert D.** 2005. *Erwinia chrysanthemi* requires a second iron transport route dependent of the siderophore achromobactin for extracellular growth and plant infection. Mol Microbiol **55:**261-275.

259. **Ikai H, Yamamoto S.** 1996. Sequence analysis of the gene encoding a novel L-2,4-diaminobutyrate decarboxylase of *Acinetobacter baumannii*: similarity to the group II amino acid decarboxylases. Arch Microbiol **166:**128-131.

260. **Ikai H, Yamamoto S.** 1997. Identification and analysis of a gene encoding L-2,4-diaminobutyrate:2-ketoglutarate 4-aminotransferase involved in the 1,3-diaminopropane production pathway in *Acinetobacter baumannii*. J Bacteriol **179:**5118-5125.

261. **Skiebe E, de Berardinis V, Morczinek P, Kerrinnes T, Faber F, Lepka D, Hammer B, Zimmermann O, Ziesing S, Wichelhaus TA, Hunfeld KP, Borgmann S, Grobner S, Higgins PG, Seifert H, Busse HJ, Witte W, Pfeifer Y, Wilharm G.** 2012. Surface-associated motility, a common trait of clinical isolates of *Acinetobacter baumannii*, depends on 1,3-diaminopropane. Int J Med Microbiol **302:**117-128.

262. **de Lorenzo V, Neilands JB.** 1986. Characterization of *iucA* and *iucC* genes of the aerobactin system of plasmid ColV-K30 in *Escherichia coli*. J Bacteriol **167:**350-355.

263. **Oves-Costales D, Kadi N, Challis GL.** 2009. The long-overlooked enzymology of a nonribosomal peptide synthetase-independent pathway for virulence-conferring siderophore biosynthesis. Chem Commun (Camb)**:**6530-6541.

264. **Cheung J, Beasley FC, Liu S, Lajoie GA, Heinrichs DE.** 2009. Molecular characterization of staphyloferrin B biosynthesis in *Staphylococcus aureus*. Mol Microbiol **74:**594-608.

265. **Forman S, Nagiec MJ, Abney J, Perry RD, Fetherston JD.** 2007. Analysis of the aerobactin and ferric hydroxamate uptake systems of *Yersinia pestis*. Microbiology **153:**2332-2341.

266. **Brickman TJ, Armstrong SK.** 1996. The ornithine decarboxylase gene odc is required for alcaligin siderophore biosynthesis in *Bordetella* spp.: putrescine is a precursor of alcaligin. J Bacteriol **178:**54-60.

267. **El Fertas-Aossani R, Messai, Y, Alouache S, Bakour R**. 2012. Virulence profile and antibiotic susceptibility patterns of *Klebsiella pneumoniae* strains isolated from different clinical specimens. Pathol Biol 12.

268. **Zhou Z, Lai JR, Walsh CT.** 2007. Directed evolution of aryl carrier proteins in the enterobactin synthetase. Proc Natl Acad Sci U S A **104:**11621-11626.

269. **Laird AJ, Ribbons DW, Woodrow GC, Young IG.** 1980. Bacteriophage Mu-mediated gene transposition and in vitro cloning of the enterochelin gene cluster of *Escherichia coli*. Gene **11:**347-357.

270. **Snitkin ES, Zelazny AM, Montero CI, Stock F, Mijares L, Murray PR, Segre JA.** 2011. Genome-wide recombination drives diversification of epidemic strains of *Acinetobacter baumannii*. Proc Natl Acad Sci U S A **108:**13758-13763.

271. **Imperi F, Antunes LC, Blom J, Villa L, Iacono M, Visca P, Carattoli A.** 2011. The genomics of *Acinetobacter baumannii*: insights into genome plasticity, antimicrobial resistance and pathogenicity. IUBMB life **63:**1068-1074.

272. **Parent MA, Bellaire BH, Murphy EA, Roop RM, 2nd, Elzer PH, Baldwin CL.** 2002. *Brucella abortus* siderophore 2,3-dihydroxybenzoic acid (DHBA) facilitates intracellular survival of the bacteria. Microb Pathog **32:**239-248.

273. **Chipperfield JR, Ratledge C.** 2000. Salicylic acid is not a bacterial siderophore: a theoretical study. Biometals : an international journal on the role of metal ions in biology, biochemistry, and medicine **13:**165-168.

274. **Burrell M, Hanfrey CC, Kinch LN, Elliott KA, Michael AJ.** 2012. Evolution of a novel lysine decarboxylase in siderophore biosynthesis. Molecular Microbiology **86:**485-499.

275. **Lemos ML, Balado M, Osorio CR.** 2010. Anguibactin- versus vanchrobactin-mediated iron uptake in *Vibrio anguillarum*: evolution and ecology of a fish pathogen. Environmental microbiology reports **2:**19-26.

276. **Stork M, Di Lorenzo M, Welch TJ, Crosa LM, Crosa JH.** 2002. Plasmid-mediated iron uptake and virulence in *Vibrio anguillarum*. Plasmid **48:**222-228.

277. **Balado M, Osorio CR, Lemos ML.** 2006. A gene cluster involved in the biosynthesis of vanchrobactin, a chromosome-encoded siderophore produced by *Vibrio anguillarum*. Microbiology **152:**3517-3528.

278. **Naka H, Lopez CS, Crosa JH.** 2008. Reactivation of the vanchrobactin siderophore system of *Vibrio anguillarum* by removal of a chromosomal insertion sequence originated in plasmid pJM1 encoding the anguibactin siderophore system. Environ Microbiol **10:**265-277.

279. **Welch TJ, Crosa JH.** 2005. Novel role of the lipopolysaccharide O1 side chain in ferric siderophore transport and virulence of *Vibrio anguillarum.* Infection and immunity **73:**5864-5872.

280. **Naka H, Crosa JH.** 2012. Identification and characterization of a novel outer membrane protein receptor FetA for ferric enterobactin transport in *Vibrio anguillarum* 775 (pJM1). Biometals **25:**125-133.

281. **Balado M, Osorio CR, Lemos ML.** 2009. FvtA is the receptor for the siderophore vanchrobactin in *Vibrio anguillarum*: utility as a route of entry for vanchrobactin analogues. Applied and environmental microbiology **75:**2775-2783.

282. **Soengas RG, Larrosa M, Balado M, Rodriguez J, Lemos ML, Jimenez C.** 2008. Synthesis and biological activity of analogues of vanchrobactin, a siderophore from *Vibrio anguillarum* serotype O2. Organic & biomolecular chemistry **6:**1278-1287.

283. **Lawlor MS, O'Connor C, Miller VL.** 2007. Yersiniabactin is a virulence factor for *Klebsiella pneumoniae* during pulmonary infection. Infection and immunity **75:**1463-1472.

284. **Nikaido H, Takatsuka Y.** 2009. Mechanisms of RND multidrug efflux pumps. Biochimica et biophysica acta **1794:**769-781.

285. **Wells RM, Jones., C. M., Xi, Z. Speer, A., Danilchanka., O., Doornbos, K. S., Sun, P., Wu, F., Tian, C., and Niederweis, M.** 2013. Discovery of a Siderophore Export System Essential for Virulence of *Mycobacterium tuberculosis*. PLoS pathogens **9**.

286. **Gubellini F, Verdon G, Karpowich NK, Luff JD, Boel G, Gauthier N, Handelman SK, Ades SE, Hunt JF.** 2011. Physiological response to membrane protein overexpression in *E. coli.* Mol Cell Proteomics **10:**M111 007930.

287. **Katzen F, Chang G, Kudlicki W.** 2005. The past, present and future of cell-free protein synthesis. Trends in biotechnology **23:**150-156.